relative to the M-frame at problem start. Earth parallax will be given by the mean Earth-Moon distance. Similarly, during Earth training exercises, the Moon is fixed to the Celestial Sphere based on its right ascension and declination relative to the E-frame. Obviously, motion of a pasted Moon or Earth across the star field cannot be simulated. However, this should have no influence on LEM-astronaut training.

c. Solar Effects - As the Sun enters the field of view, the cathode ray tube light intensity is increased This has the effect of washing out the star field. The control parameter of interest is angle $\gamma_{pq}^{\odot}$ measured from the optical line-of-sight, to the Sun's vector direction. Angle $\gamma_{pq}^{\odot}$ is computed as follows: Define the Sun's position in the optical axes system:

$$\bar{r}_{pq}^{\odot} = 1_{ij_{pq_n}} \bar{r}_{n/\odot} \qquad \text{(J-30)}$$

Vector $\bar{r}_{n/\odot}$ denotes the Sun's position relative to the E or M-frame. Vector $\bar{r}_{E/\odot}$ is generated by the Ephemeris (E-30), whereas $\bar{r}_{M/\odot}$ is:

$$\bar{r}_{M/\odot} = \bar{r}_{E/\odot} - \bar{r}_{E/M} \qquad \text{(J-31)}$$

The angle subtended by the sun is:

$$\cos \gamma_{pq}^{\odot} = \frac{\bar{r}_{pq}^{\odot} \cdot \hat{k}_{pq}}{\left|\bar{r}_{n/\odot}\right|} = \frac{Z_{pq}^{\odot}}{r_{n/\odot}} \qquad \text{(J-32)}$$

$$0 \leq \gamma_{pq}^{\odot} \leq \pi$$

Normal lighting conditions exist whenever the sun is outside of the field of view ($\gamma_{pq}^{\odot} > \gamma_{pq_{max}}^{\odot}$) whereas, maximum lighting conditions exist when the Sun is within the field of view (see logic J-33).

3. Mission Effects Projector (MEP)

a. Location of LEM with Respect to Film Strip Reference. - The MEP provides continual lunar or geographic terrain displays to the astronauts at altitudes above approximately 1200 feet. Pre-selected terrain swaths are recorded on film strips and displayed by a TV image generator. Each film strip is scaled for five altitude ranges. As the altitude ($h_{M/L}$; G-30) diminishes or increases beyond prescribed limits, the film strip views are dissolved into the next.

The film strip is positioned with respect to the projection apparatus, based on the location of the vehicle's subsatellite point relative to the film strip centerline (Figure 16). It is assumed that all film strips represent great circle swaths around the central body. If the nominal training mission orbits are equatorial, then the film centerline will correspond to the nominal orbit trace projected on the central body. For this case, film strip drive coordinates are given by the vehicle's selenographic longitude and latitude (G-12) or geographic latitude and longitude.

If, however, the nominal orbits are inclined to the equator, then the projected orbit trace will not correspond to the film strip centerline. This results because the orbit trace on a rotating central body cannot be represented by a great circle path. For this case, the subsatellite point may be located by angles Θ_f and δ_f. This point must fall within the confines of the film strip. Note that (Figure 16):

i. Θ_f is measured from the film strip ascending node, along the film strip centerline to the projection of the LEM radius vector onto the film strip plane. For an equatorial orbit Θ_f would be measured from the X_s or X_G axis and correspond exactly to $\lambda_{S/L}$ or $\lambda_{G/L}$.

ii. δ_f represents the declination relative to the film strip plane and is measured positive northward. Whenever equatorial orbits are considered, δ_f reduces to latitude.

Angles Θ_f and δ_f, for the general case, are ascertained below:

Let any desired, terrain swath (film strip) be specified by a right ascension of the ascending node (Ω_f) and an inclination (i_f). Film strip axes, X_f, Y_f and Z_f are related to the reference central body axes as follows:

$$\begin{bmatrix} \hat{i}_f \\ \hat{j}_f \\ \hat{k}_f \end{bmatrix} = \begin{bmatrix} \cos \Omega_f & \sin \Omega_f & 0 \\ -\sin \Omega_f \cos i_f & \cos i_f \cos \Omega_f & \sin i_f \\ \sin \Omega_f \sin i_f & -\sin i_f \cos \Omega_f & \cos i_f \end{bmatrix} \begin{bmatrix} \hat{i}_Q \\ \hat{j}_Q \\ \hat{k}_Q \end{bmatrix} \qquad (J-4)$$

$$Q = S \text{ or } G$$

Equatorial direct orbits are specified by $\Omega_f = i_f = 0$, while equatorial retrograde orbits (LEM) are specified by $\Omega_f = 0$, $i_f = \pi$. This means that $\hat{r}_f = \hat{r}_Q$.

The LEM radius vector in terms of selenographic (lunar mission) and geographic (Earth mission) coordinates is required. The former is known (A-22); the latter is computed as follows:

$$\begin{bmatrix} X_G \\ Y_G \\ Z_G \end{bmatrix} = \begin{bmatrix} \text{Cos GHA} & \text{Sin GHA} & 0 \\ -\text{Sin GHA} & \text{Cos GHA} & 0 \\ 0 & 0 & 1 \end{bmatrix} \begin{bmatrix} X_{E/L} \\ Y_{E/L} \\ Z_{E/L} \end{bmatrix} \qquad \text{(J-49)}$$

It was recommended earlier that relative motion equations, based on two-body CSM motion, be used to compute $\bar{r}_{E/L}$ during independent LMS Earth mission modes. Consequently, nodal regression due to the Earth's oblateness is not accounted for whenever this mode is activated. Accordingly, after a complete circuit around the Earth, the astronaut would view a geographic scene that corresponds to the change in the Earth's angular position only. The real world scene would correspond to a view from a slightly different spacial position due to the orbit plane regression relative to inertial space. This "true scene" can be synthesized (first order only) by altering the Earth's true rotation rate. For example, replace GHA in (D-60) by (GHA - $\dot{\Omega}$ t) where $\dot{\Omega}$ is given by equation (H-22).

Drive angle θ_f depends on the projection of $\bar{r}_{Q/L}$ onto the film strip reference plane. Call this projection $\hat{P}$, where:

$$\hat{P} = \hat{k}_f \times \frac{\left[\bar{r}_{Q/L} \times \hat{k}_f\right]}{r_{n/L} \text{ Sin } \delta_f} \qquad \text{(j-5)}$$

Now:

$$\text{Tan } \theta_f = \frac{\hat{P} \cdot \hat{j}_f}{\hat{P} \cdot \hat{i}_f} \qquad \text{(J-40)}$$

and:

$$\text{Sin } \delta_f = \hat{P} \cdot \hat{k}_f \qquad \text{(J-40)}$$

$$-\frac{\pi}{2} \leq \delta_f \leq \frac{\pi}{2}$$

Equations (J-40) reduce to longitude and latitude whenever equatorial orbits are considered.

b. Angular Drives For MEP Optics.- Film strip terrain information is transmitted to a TV vidicon camera through a series of mirrors, lenses and prisms (reference 37). The optical equipment is positioned by three angular drive signals $\psi_{pq}{}^*$, $\sigma_{pq}{}^*$ and $\phi_{pq}{}^*$. Physically, these angles relate the optical axes systems to a local terrain coordinate system (X_T, Y_T, Z_T), as shown in Figure 16. This system was derived on the following basis:

i. $\hat{i}_T$ is directed along the local radius vector.

ii. $\hat{j}_T$ lies in the local horizon plane and is parallel to the plane formed by the strip centerline.

iii. $\hat{k}_T = \hat{i}_T \times \hat{j}_T$.

Let all MEP drive angles be zero. For this condition the relation between the optical axes $\hat{r}_{pq}$ and the terrain axes $\hat{r}_T$ is:

$$\hat{X}_{pq} = \hat{Z}_T$$

$$\hat{Y}_{pq} = \hat{Y}_T$$

$$\hat{Z}_{pq} = -\hat{X}_T$$

To obtain any arbitrary orientation between $\hat{r}_{pq}$ and $\hat{r}_T$ rotate first about $-\hat{X}_T$ through azimuth angle $\psi_{pq}{}^*$. Note that $\psi_{pq}{}^*$ is always measured in the LEM local horizon plane. Next, rotate about the new $\hat{Y}_T$ axis so formed through an elevation angle $\sigma_{pq}{}^*$. Angles $\psi_{pq}{}^*$ and $\sigma_{pq}{}^*$ position the optical line-of-sight axis to the landmark being sighted. Last, rotate about the optical line-of-sight through roll angle $\phi_{pq}{}^*$. The correspondence between r_{pq} and r_T is:

$$\begin{bmatrix} X_{pq} \\ Y_{pq} \\ Z_{pq} \end{bmatrix} = \begin{bmatrix} \text{Cos}\,\phi_{pq}^*\,\text{Sin}\,\sigma_{pq}^* & \begin{matrix}\text{Cos}\,\phi_{pq}^*\,\text{Cos}\,\sigma_{pq}^*\,\text{Sin}\,\psi_{pq}^* \\ +\text{Sin}\,\phi_{pq}^*\,\text{Cos}\,\psi_{pq}^*\end{matrix} & \begin{matrix}\text{Cos}\,\phi_{pq}^*\,\text{Cos}\,\sigma_{pq}^*\,\text{Cos}\,\psi_{pq}^* \\ -\text{Sin}\,\phi_{pq}^*\,\text{Sin}\,\psi_{pq}^*\end{matrix} \\ -\text{Sin}\,\phi_{pq}^*\,\text{Sin}\,\sigma_{pq}^* & \begin{matrix}-\text{Sin}\,\phi_{pq}^*\,\text{Cos}\,\sigma_{pq}^*\,\text{Sin}\,\psi_{pq}^* \\ +\text{Cos}\,\phi_{pq}^*\,\text{Cos}\,\psi_{pq}^*\end{matrix} & \begin{matrix}-\text{Sin}\,\phi_{pq}^*\,\text{Cos}\,\sigma_{pq}^*\,\text{Cos}\,\psi_{pq}^* \\ -\text{Cos}\,\phi_{pq}^*\,\text{Sin}\,\psi_{pq}^*\end{matrix} \\ -\text{Cos}\,\sigma_{pq}^* & \text{Sin}\,\sigma_{pq}^*\,\text{Sin}\,\psi_{pq}^* & \text{Sin}\,\sigma_{pq}^*\,\text{Cos}\,\psi_{pq}^* \end{bmatrix} \begin{bmatrix} X_T \\ Y_T \\ Z_T \end{bmatrix}$$

(j-6)

or:

$$\hat{r}_{pq} = M(\psi^*_{pq}, \sigma^*_{pq}, \phi^*_{pq})\,\hat{r}_T \qquad \text{(j-6)}$$

The matrix elements given by (j-6) are known from previously generated data. For example, the optical axes orientation relative to the selenographic (lunar mission) or geographic (Earth mission) coordinate system is specified by:

$$\hat{r}_{pq} = {l^T_{ij}}_{pq}\; a^T_{jk}\; \hat{r}_s \quad \text{(lunar)}$$

$$\hat{r}_{pq} = {l^T_{ij}}_{pq}\; f^T_{jk}\; \hat{r}_G \quad \text{(terrestrial)} \qquad \text{(j-7)}$$

From (j-4), the constant relation between $\hat{r}_Q$ and the film strip axes system is:

$$\hat{r}_f = M(\Omega_f, i_f)\,\hat{r}_Q \qquad \text{(j-4)}$$

Finally, equations (J-40) provide the link between $\hat{r}_T$ and $\hat{r}_f$:

$$\begin{bmatrix} X_T \\ Y_T \\ Z_T \end{bmatrix} = \begin{bmatrix} \text{Cos }\theta_f \text{ Cos }\delta_f & \text{Cos }\delta_f \text{ Sin }\theta_f & \text{Sin }\delta_f \\ -\text{Sin }\theta_f & \text{Cos }\theta_f & 0 \\ -\text{Sin }\delta_f \text{ Cos }\theta_f & -\text{Sin }\delta_f \text{ Sin }\theta_f & \text{Cos }\delta_f \end{bmatrix} \begin{bmatrix} X_f \\ Y_f \\ Z_f \end{bmatrix} \qquad \text{(j-8)}$$

or:

$$\hat{r}_T = M(\theta_f, \delta_f)\,\hat{r}_f \qquad \text{(j-8)}$$

Combining equations j-7, j-4 and j-8 gives the desired transformation:

$$\hat{r}_{pq} = l_{ki}{}^T\; a'_{ji}{}^T\; M_{ih}{}^T(\Omega_f, i_f)\; M_{hg}{}^T(\theta_f, \delta_f)\,\hat{r}_T \qquad \text{(J-46)}$$

or equivalently:

$$\hat{r}_{pq} = \left[M_{gh}(\theta_f, \delta_f)\; M_{hi}(\Omega_f, i_f)\; a'_{ij}\; l_{ik}\right]^T \hat{r}_T \qquad \text{(J-46)}$$

Whereupon:

$$\hat{r}_{pq} = \nu_{gk}\,\hat{r}_T \qquad \text{(J-46)}$$

Angles $\psi_{pq}*$, $\sigma_{pq}*$ and $\phi_{pq}*$ can now be found by comparing elements of v_{mi} and M ($\psi_{pq}*$, $\sigma_{pq}*$, $\phi_{pq}*$). The solution is similar to the Celestial Sphere drives and is given by equations (J-41).

Equations (J-42) present gimbal lock logic. This logic ensures a true view of the Earth or Moon limb whenever the astronaut sights along the local horizon ($\sigma_{pq}* = \frac{\pi}{2}$).

4. Landing and Ascent Image Generator (L/A).

a. Drive Coordinates. - The L&A model is referenced to the same coordinate system as the MEP film (paragraph 3). Given a set of selenographic coordinates $(X,Y,Z)_s$ for a particular landing site, the parameters $\delta_{LA\,o}$ and θ_{LAo} can be derived via (J-40). Making this the L&A reference point, the drive coordinates can then be derived:

$$Y_{LA} = K_o\ (\theta_f\ -\ \theta_{LAo}) \qquad \text{(J-51)}$$

$$Z_{LA} = K_o\ (\delta_f\ - \delta_{LAo}$$

where K_o is a constant to convert Y_{LA} and Z_{LA} into feet.

b. Angular Drives for L/A Optics. - The MEP optical head is identical to the L/A optical head. Hence, angles $\psi_{wq}*$, $\sigma_{wq}*$ and $\phi_{wq}*$ serve a dual purpose.

A single (L/A) optical head is used to present the landing site image in either the left window (q=l) or the right window (q = r), at the instructor's discretion.

c. Altitude Drive for the L&A Optical Head. - An altitude signal must be generated to drive a focusing circuit included in the optical head. It is intended to measure the altitude from the design eye to the lunar surface. A first order correction ($\theta \approx 0^o$) is given by:

$$X_{LA} = h_{M/L} + (\alpha_{DE}\ -\ \alpha_{CG}) \qquad \text{(J-52)}$$

5. Rendezvous and Docking Simulator.

a. General. - Rendezvous and docking simulation displays depend on the distance between vehicles. Whenever the LEM-CSM range exceeds 14,000 feet, CSM motion is depicted by a blinking light whose intensity varies with distance. Between 14,000 and 8,000 feet, the CSM is represented by an illuminated model. During these phases, the rendezvous table carriage (see Figure 18) remains parked at a maximum distance from the $\frac{1}{80}$ scale CSM model. From 8000 to 530 feet, the table carriage is activated. CSM rotational motion is simulated by a two gimbal, $\frac{1}{80}$ scale model. As the relative distance closes to 530 feet, a three gimbal $\frac{1}{20}$ CSM docking model is employed. Switching occurs by the removal of a dissolve mirror and reversing the carriage motion.

Drive signals must be generated to:

i. Position the CSM in the LEM window.

ii. Define the relative orientation of the CSM as seen by the astronauts.

iii. Provide the correct CSM solar illumination during all mission phases.

Each item is discussed below.

b. Reference Table Coordinates. -In order to synthesize true vehicle motions, it is necessary to establish a rendezvous table reference coordinate system. Let this coordinate system be defined by unit directions ρ_1, ρ_2, ρ_3 (Figure 18). Let ρ_1 be normal to the relative distance table and direct ρ_3 parallel to the carriage motion toward the $\frac{1}{20}$ CSM scale model. Optical compensation ensures that ρ_3 is properly directed when the $\frac{1}{80}$ scale model becomes active. Neglecting parallax, the true line-of-sight vector $\bar{\rho}*$ is always directed along ρ_3. The basic problem is to define the true vehicle motion in table-top coordinates.

c. Optical Head Drives for Left and Right Window Viewing. An optical head is fixed to the movable carriage. This head represents the LEM vehicle and is used to position the CSM in the LEM windows. The optical head consists of a post and trunnion and has two degrees of angular freedom relative to the non-rotating table-top axes. Fixed to the horizontal trunnion are two cameras positioned on either side of the post. These cameras have the same orientation with respect to the post and trunnion as the LEM window axes have with respect to the body axes. Thus, correspondence between the camera axes and the actual LEM vehicle axes, with respect to the relative range vector $\bar{\rho}*$, is achieved by a rotation about the post ($\hat{\rho}_1$) through angle ϕ_{LS}, followed by a rotation about the new trunnion axis through Θ_{LS}. The relation between the LEM body axes and the table axes is therefore:

$$\begin{bmatrix} \rho_{X_B} \\ \rho_{Y_B} \\ \rho_{Z_B} \end{bmatrix} = \begin{bmatrix} \text{Cos } \Theta_{LS} & \text{Sin } \Theta_{LS} \text{ Sin } \phi_{LS} & -\text{Sin } \Theta_{LS} \text{ Cos } \phi_{LS} \\ 0 & \text{Cos } \phi_{LS} & \text{Sin } \phi_{LS} \\ \text{Sin } \Theta_{LS} & -\text{Cos } \Theta_{LS} \text{ Sin } \phi_{LS} & \text{Cos } \Theta_{LS} \text{ Cos } \phi_{LS} \end{bmatrix} \begin{bmatrix} \rho_1 \\ \rho_2 \\ \rho_3 \end{bmatrix} \qquad \text{(J-63)}$$

or:

$$\bar{\rho}_B = q_{ij} \; \rho_{Table} \qquad \text{(J-63)}$$

Vector $\bar{\rho}_B$, given by subset equation F-23, defines the distance measured from LEM CG to CSM CG. Optical parallax corrections may become important as the relative distance diminishes. For this reason, vector $\bar{\rho}$ * is redefined. Let $\bar{\rho}'_B$ be measured from the camera origin (Figure 18) to the CSM pivot point which is assumed to correspond to a nominal CSM CG. Hence:

$$\bar{\rho}'_B = \bar{\rho}_B - \bar{\rho}_{DE} \; ; \quad \rho'_{LS} = |\bar{\rho}'_B| \qquad \text{(J-64a)}$$

Drive angles ϕ_{LS} and Θ_{LS} are derived from expression (J-63) as follows. First replace $\bar{\rho}_B$ by $\bar{\rho}_B'$. Since the line-of-sight vector $\bar{\rho}'_B$ must lie along ρ_3, the components of $\bar{\rho}_B'$ measured in table axes are $\rho_1 = 0$, $\rho_2 = 0$, $\rho_3 = \rho'_{LS}$. Equations (J-63) can therefore be written as:

$$\begin{aligned} \rho'_{X_B} &= -\rho'_{LS} \text{ Sin } \Theta_{LS} \text{ Cos } \phi_{LS} \\ \rho'_{Y_B} &= \rho'_{LS} \text{ Sin } \phi_{LS} \\ \rho'_{Z_B} &= \rho'_{LS} \text{ Cos } \Theta_{LS} \text{ Cos } \phi_{LS} \end{aligned} \qquad \text{(j-10)}$$

Equations (j-9) are manipulated to give:

$$\text{Tan } \theta_{LS} = \frac{-\rho'_{X_B}}{\rho'_{Z_B}}$$

$$\text{Tan } \phi_{LS} = \frac{\rho'_{Y_B}}{\rho'_{Z_B} \text{ Cos } \theta_{LS} - \rho'_{X_B} \text{ Sin } \theta_{LS}} \qquad \text{(J-64)}$$

d. Optical Head Drives for Telescope and Overhead Window Viewing. The Rendezvous and Docking simulator is designed such that the trunnion-fixed right camera generates a CSM image whenever the telescope modes are activated. Similarly, the trunnion-fixed left camera is employed to simulate CSM motion in the overhead window.

Consider telescope viewing. Recall that the right camera is fixed to the optical head or equivalently, the LEM body axes. The problem, therefore, is to define a new body axes (and associated optical head drive angles $\theta_{LS_{Tq}}$ and $\phi_{LS_{Tq}}$) that has the same orientation with respect to the telescope axes as the original body axes has to the right window axes. This is accomplished by rotating about the telescope Y_{Tq} axes through θ'_{Wr}, followed by a rotation ϕ'_{Wr} about the new X'_{Tq} axis, followed by a raster rotation ψ'_{Wr} about the new Z'_{Tq} axis. The correspondence between the new body axes and the telescope axes reduces to:

$$\rho_{B_{Tq}} = h'_{ij_{wr}} \, \bar{r}_{Tq} \qquad \text{(J-72)}$$

If rotations θ'_{wr}, ϕ'_{wr} and ψ'_{wr} were equal to $-\theta_{wr}$, $-\phi_{wr}$ and zero respectively, then frame $\rho_{B_{rq}}$ would bear the same relation to $\bar{r}_{Tq}$ as $\bar{r}_B$ has to $\bar{r}_{wr}$. Hardware constraints, however, require that the optical axes relative to the CRT be shifted by angles $\theta_{\epsilon\, Tq}$ and $\phi_{\epsilon\, Tq}$ when viewing is switched from the right window to the telescope mode. Furthermore, during the switch from window to telescope viewing, a raster rotation or change in scanning is necessary in order that the vidicon cover the complete field of view. These items are compensated for geometrically by defining the elements of $h'_{ij_{wr}}$ as:

$$\phi'_{wr} = -\phi_{wr} + \phi_{\epsilon_{Tq}}$$

$$\theta'_{wr} = -\theta_{wr} + \theta_{E_{Tq}} \qquad (J\text{-}74)$$

$$\psi'_{wr} = \psi ras_{Tq}$$

Relative distance components measured in the new body axes must be found. This is accomplished by eliminating $\bar{r}_{Tq}$ in (J-72). As shown previously:

$$\bar{r}_{Tq} = h_{ij_{Tq}} \rho'_B \qquad (j\text{-}70)$$

Hence:

$$\bar{\bar{\ }}_{B_{Tq}} = h'_{ij_{wr}} \, h_{jk_{Tq}} \rho'_B \qquad (J\text{-}70a)$$

The relative distance vector $\bar{\rho}_{B_{Tq}}$ that must lie along $\hat{\rho}_3$. Accordingly, optical head drive angles for telescope viewing are derived based on the same reasoning described in Subsection 5c above. The results are:

$$\text{Tan } \theta_{LS_{Tq}} = \frac{-\rho_{X_{Tq}}}{\rho_{Z_{Tq}}}$$

$$\text{Tan } \phi_{LS_{Tq}} = \frac{\rho_{Y_{Tq}}}{\rho_{Z_{Tq}} \text{ Cos } \theta_{LS_{Tq}} - \rho_{X_{Tq}} \text{ Sin } \theta_{LS_{Tq}}} \qquad (J\text{-}71a)$$

Optical head drive angles for overhead window viewing are derived in a similar manner as above. Exceptions are that the right window subscript is replaced by the left window subscript and the telescope axes are replaced by the overhead window axes.

e. Camera Switch Logic. Two cameras are used for three telescopes, two front windows and overhead window viewing modes. Combinations of simultaneous telescope, front window or overhead window CSM viewing is impossible. No drawback results with regard to telescope viewing since, the telescope and window view cones do not intersect. In addition, when the relative distance is less than 530 feet, the telescopes are inoperative, consequently, the CSM cannot overlap the telescope and front window view cones. During docking the CSM can be seen in the overhead and front windows simultaneously. This configuration, however, cannot be simulated.

As the CSM enters a particular view cone, it is proposed to automatically compute the corresponding post and trunnion drive angles. To determine whether the CSM can be seen, approximate the field of view about each optical axis line-of-sight by a cone angle Λ^*_{pq}. If the CSM-CG is within this cone angle, then the appropriate post and trunnion drives are activated.

The optical line-of-sight is $\hat{Z}_{pq}$. The CSM position referenced to the design eye is ρ'_B. Accordingly, the cone angle made by $\hat{Z}_{pq}$ and ρ'_B is:

$$\cos \Lambda_{pq} = \frac{\bar{\rho}'_B \bullet \hat{Z}_{pq}}{\rho'_{LS}} \qquad \text{(J-75)}$$

$$0 \leq \Lambda_{pq} \leq \pi$$

Angle Λ_{pq} is compared to allowable angle Λ_{pq}^*, in loop (J-73), to ascertain which set of equations (J-71a, or J-71b, or J-64) should be used to compute the post and trunnion drive angles.

f. CSM Orientation. - The foregoing subsections define the CSM position in the LEM windows. It is now required to determine the CSM orientation. Two CSM models are used for this purpose (Figure 18). Consider the three gimbal, $\frac{1}{20}$ scale, CSM docking model. Locate the table-top reference coordinate system at the CSM pivot point (Figure 18). Let all gimbal angles be zero. This forces the CSM body axes $\hat{X}_{B/C}$ to lie along $\hat{\rho}_3$, $\hat{Y}_{B/C}$ to lie along $\hat{\rho}_2$ and $Z_{B/C}$ to lie along negative $\hat{\rho}_1$. Rotate first about the negative outer gimbal axis ($-\hat{\rho}_1$) through $(\psi_G)_{CSM}$, then about the middle gimbal axis through $(\theta_G)_{CSM}$, and last about the inner gimbal axis through $(\phi_G)_{CSM}$ to obtain an arbitrary CSM orientation relative to the reference table axes. The table axes is related to the CSM body axes by the following gimbal angle transformation:

8/65

$$\begin{bmatrix} \hat{X}_{B/C} \\ \hat{Y}_{B/C} \\ \hat{Z}_{B/C} \end{bmatrix} = \begin{bmatrix} \mathrm{Sin}(\theta_G)_{CSM} & \mathrm{Cos}(\theta_G)_{CSM}\,\mathrm{Sin}(\phi_G)_{CSM} & \mathrm{Cos}(\theta_G)_{CSM}\,\mathrm{Cos}(\psi_G)_{CSM} \\ -\mathrm{Sin}(\phi_G)_{CSM}\,\mathrm{Cos}\,(\theta_G)_{CSM} & \begin{matrix}\mathrm{Sin}(\psi_G)_{CSM}\,\mathrm{Sin}(\theta_G)_{CSM}\,\mathrm{Sin}(\phi_G)_{CSM} \\ +\mathrm{Cos}(\phi_G)_{CSM}\,\mathrm{Cos}(\quad_G)_{CSM}\end{matrix} & \begin{matrix}\mathrm{Cos}(\psi_G)_{CSM}\,\mathrm{Sin}(\theta_G)_{CSM}\,\mathrm{Sin}(\phi_G)_{CSM} \\ -\mathrm{Sin}(\psi_G)_{CSM}\,\mathrm{Cos}(\phi_G)_{CSM}\end{matrix} \\ -\mathrm{Cos}(\phi_G)_{CSM}\,\mathrm{Cos}(\theta_G)_{CSM} & \begin{matrix}\mathrm{Sin}(\psi_G)_{CSM}\,\mathrm{Sin}(\theta_G)_{CSM}\,\mathrm{Cos}(\phi_G)_{CSM} \\ -\mathrm{Sin}(\phi_G)_{CSM}\,\mathrm{Cos}(\quad_G)_{CSM}\end{matrix} & \begin{matrix}\mathrm{Sin}(\theta_G)_{CSM}\,\mathrm{Cos}(\phi_G)_{CSM}\,\mathrm{Cos}(\psi_G)_{CSM} \\ +\mathrm{Sin}(\phi_G)_{CSM}\,\mathrm{Sin}(\psi_G)_{CSM}\end{matrix} \end{bmatrix} \begin{bmatrix} \hat{\rho}_1 \\ \hat{\rho}_2 \\ \hat{\rho}_3 \end{bmatrix} \qquad \text{(J-11)}$$

As before, another transformation must be found that relates $\hat{r}_{B/C}$ to $\hat{\rho}_{TABLE}$ based on known, real world, variables.

Matrix operator (J-63; q_{ij}) relates the LEM body axes to the table axes. The LEM body axes relative to the Inertial Reference axes is known (D-40). Combining gives:

$$\hat{r}_n = \left[g_{ij}^T \quad q_{jk}\right] \hat{\rho}_{TABLE} \qquad \text{(j-12)}$$

The CSM is oriented to the same stable member coordinate reference as the LEM. CSM ordered rotations are specified by ψ_c about Z_n followed by θ_c about Y'_n, followed by ϕ_c about X'_n (reference 38). During integrated operation the angles (ψ_c, θ_c, ϕ_c) or direction cosine elements are supplied by the AMS. During independent operation, the instructor will control the CSM attitude (J-62a). In any event:

$$\hat{r}_{B/C} = (g_{ij})_c \quad \hat{r}_n \qquad \text{(J-62)}$$

Combining (J-62) and (j-11) gives:

$$\hat{r}_{B/C} = \left[(g_{ik})_c \quad g^T_{kl} \quad q_{lj}\right] \hat{\rho}_{TABLE} \qquad \text{(J-61)}$$

or:

$$\bar{r}_{B/C} = \left[P_{ij}\right] \bar{\rho}_{TABLE} \qquad \text{(J-61)}$$

Gimbal angles $(\psi_G)_{CSM}$, $(\theta_G)_{CSM}$ and $(\phi_G)_{CSM}$ are found by comparing known elements of matrix P_{ij} with matrix elements of (j-11). The final result is given in (J-60).

Matrix P_{ij} must be modified whenever the telescope or overhead window viewing mode is activated This modification is required because matrix q_{ij} (J-63) relates the ficticious body axes $\bar{\rho}_{B_{Tq}}$ or $\bar{\rho}_{B_{wa}}$ to the table axes. For telescope viewing, the LEM body axes is reintroduced as follows:

$$\hat{\rho}_{B_{Tq}} = q_{ij} \quad \hat{\rho}_{TABLE} \qquad \text{(J-63)}$$

But:

$$\hat{\rho}_{B_{rq}} = (h'_{ij_{wr}}) \; (h_{jk_{rq}}) \quad \hat{r}_{B/L} \qquad \text{(J-70a)}$$

Therefore:

$$\hat{r}_{B/L} = (h^T_{ij_{rq}}) \; (h'^T_{jk_{wr}}) \; q_{kl} \quad \hat{\rho}_{TABLE} \qquad \text{(j-13)}$$

Following through gives:

$$P_{ij} = (g_{ik})_c \, (g^T_{kl}) \, (h_{lm_{fq}})^T (h'_{mn_{wr}})^T \, (q_{n_j}) \qquad \text{(J-61)}$$

for the telescope, and:

$$P_{ij} = (g_{ik})_c \, (g_{kl})^T \, (h_{lm_{wa}})^T \, (h'_{mn_{wl}})^T \, (q_{nj}) \qquad \text{(J-61)}$$

for the overhead window.

When the relative distance exceeds 530 feet, the two gimbal, $\frac{1}{80}$ CSM scale model is employed. For this regime the lunar gimbal angle $(\phi_G)_{CSM}$ is not computed.

g. CSM Solar Illumination. The solar illumination sub-assembly for both CSM models consists of fixed banks of lights arranged in rings and surrounding each model (Figures 18 and 19). CSM solar illumination is simulated by selective switching of the light bank quadrants. The lighting array is fixed to the table. Each bank of lights extend over an angle range given by $\gamma^{\odot}_n - \gamma^{\odot}_{n-1}$ measured in the $\hat{\rho}_1 - \hat{\rho}_2$ table reference plane (Figure 19). The problem of light selection, therefore, reduces to ascertaining the Sun's direction in table coordinates.

The Sun's coordinates measured relative to the Earth or Moon are computed in the Ephemeris subsection. The orientation of the CSM is also known relative to the M or E-frame. Consequently, the Sun's coordinates in CSM body axes are:

$$\hat{r}^{\odot}_{B/C} = (g_{ij})_c \, \hat{r}_{n/\odot} \qquad \text{(J-85)}$$

But, matrix P_{ij} (J-61) relates the CSM body frame to the table top frame. Accordingly, the Sun's direction relative to the table is:

$$\hat{\rho}^{\odot} = P^T_{ij} \, \hat{r}^{\odot}_{B/C} \qquad \text{(J-84)}$$

Angles $\sigma^{\odot}$ and $\gamma^{\odot}$ are used to control the lights. Angle $\sigma^{\odot}$ defines the central angle between the Sun's direction and ρ_3, while $\gamma^{\odot}$ locates the Sun's projection in the plane of the lamps (Figure 19). Hence:

$$\cos \sigma^{\odot} = \hat{\rho}_3 \cdot \hat{\rho}^{\odot} = \rho^{\odot}_3 \qquad \text{(J-82)}$$

$$0 \leq \sigma^{\odot} \leq \pi$$

and: $$\operatorname{Tan} \gamma = \frac{\rho^{\odot}_{2}}{\rho^{\odot}_{1}} \qquad \text{(J-83)}$$

Refer to Figure 19. When the Sun lies in region A ($\sigma^{\odot} \leq \sigma^{\odot}_{Min}$), the LEM, CSM and Sun are nearly aligned. The CSM as seen from the LEM is not illuminated. All lamps are turned off. When the Sun lies in region B, ($\sigma^{\odot} \geq \pi - \sigma^{\odot}_{Max}$), rhw CSM as seen from the LEM is fully illuminated. All lamps are turned on. A servo driven by the angle $\gamma^{\odot}$ will illuminate the particular bank of lights required to simulate the sun's direction.

h. CSM or LEM In Shadow. - If the CSM lies in the Moon (lunar mission) or Earth shadow (Earth mission), then all lamps are turned off. A shadow cylinder is generated by assuming the Sun is at infinity (see sketch).

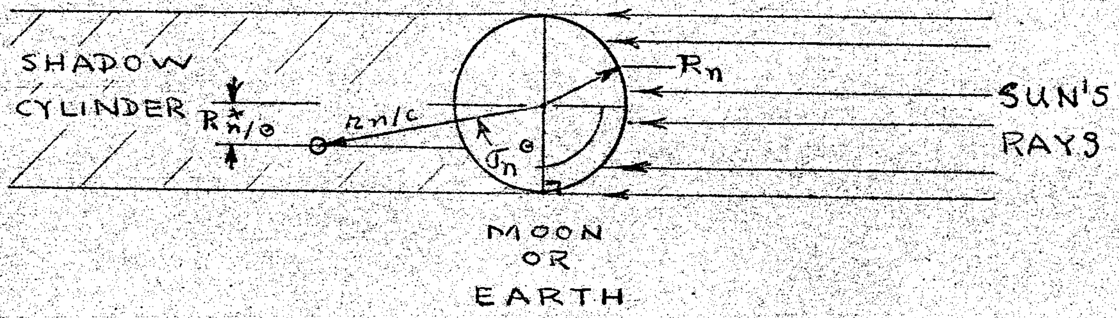

The CSM is in sunlight whenever the CSM radius vector, projected on a plane normal to the Sun's direction ($R^*_{n/\odot}$), is greater than the central body radius (R_n). In equation form this gives:

$$R^*_{n/\odot} = r_{n/c} \operatorname{Sin} \sigma^{\odot}_{n}$$

Where:

$$\operatorname{Cos} \sigma^{\odot}_{n} = \frac{\bar{r}_{n/\odot} \cdot \bar{r}_{n/c}}{r_{n/\odot} \; r_{n/c}} \qquad \text{(J-87)}$$

$$0 \leq \sigma^{\odot}_{n} \leq \pi$$

As shown in the sketch, if $R^*_{n/\odot} < R_n$ but $0 \leq \sigma^{\odot}_{n} \leq \frac{\pi}{2}$, the CSM is illuminated (Logic J-86).

i. Shadow Generation. - One of the required cues is the shadow of the LEM on the lunar surface. In order to generate the LEM shadow use is made of the Rendezvous and Docking System. The CSM will be viewed by the R&D probe as if it were the LEM's shadow, and its signal will be used to blank out the appropriate portion of the L&A scene.

In order to correctly drive the R&D probe, the position of the LEM shadow is computed and transformed into probe coordinates.

Given the sum azimuth angle $\psi^{\odot}$ and elevation angle $\theta^{\odot}$ the L&A terrain frame $(\hat{X}_T, \hat{Y}_T, \hat{Z}_T)$ and the altitude of the LEM above the model datum $(h_{M/L})$, the shadow position may be derived (see figure 11).

$$X_{LAS} = h_{M/L}$$

$$Y_{LAS} = \frac{X_{LAS} \cos \psi^{\odot}}{\tan \theta^{\odot}} \qquad \text{(J-90)}$$

$$Z_{LAS} = \frac{X_{LAS} \sin \psi^{\odot}}{\tan \theta^{\odot}}$$

and converting into the body frame:

$$\begin{bmatrix} \rho_{XLA} \\ \rho_{YLA} \\ \rho_{ZLA} \end{bmatrix} = \sqrt{gk} \begin{bmatrix} X_{LAS} \\ Y_{LAS} \\ Z_{LAS} \end{bmatrix} \qquad \text{(J-91)}$$

The parameters $\hat{\rho}_{LA}$ are then treated identically to any other value of $\hat{\rho}_B$ in equation set J-64 to derive the post and trunnion camera drives.

The CSM model drives will be held fixed at $(\psi_G)_{CSM} = 90^{\circ}$, $(\theta_G)_{CSM}$ $(\phi_G)_{CSM} = -90^{\circ}$.

1200H-1

LED-440-3
True Motion Equations
Part II, Section 1-3

IV. References

1. GAEC: "Design Control Specification For LEM Mission Simulator", LSP-440-43100A, 16 January 1964.

2. Beck, H.D.: "IMCC and AMS Mathematical Model, Compatibility Requirements", NASA, MSC, 8 November 1963.

3. Tross, C.: "Lunar Vehicle Orbit Determination", ARS Journal, April 1962.

4. Pinkham, G.; Sobierajski, F.: "Astrodynamics of Lunar Satellites: Part II - Lunar Orbit Stability", Grumman Research Report RE-170, November 1964.

5. Pulgrano, L.; Howe, E.: "Analysis of the Interaction of Propellant Sloshing in the LEM Ascent Stage With Attitude Control System, Including the Effects of Vertical Slosh Forces", LMO-500-230, 8 December 1964.

6. Pulgrano, L.; Howe, R.: "Mechanical Model Representations for LEM Ascent and Descent Stage Propellant Sloshing", LMO-500-168, 8 April 1964.

7. Pulgrano, L.: "A Mathematical Representation of Main Propellant Sloshing For Use In the Full Mission Engineering Simulator", LMO-500-169, 31 March 1964.

8. See Appendix I in Enclosure 1.

9. Pantason, P.: "Simulation of Ascent Stage FITH (Fire-In-The Hole) Force and Moment Staging Forces", AVO #LAV 500-87, March 1965.

10. Not Used.

11. Not Used

12. Battin, R. H.: "Astronautical Guidance", McGraw-Hill Publishing Company, 1964.

13. Not Used

14. Not Used

15. Not Used

16. Sterne, T. E.: "An Introduction to Celestial Mechanics", Interscience Publishers, Inc., 1960.

17. Not Used

18. Not Used

19. Not Used

20. Not Used

21. Not Used

22. Pantason, P.: "LEM Staging Dynamics For Abort During the Lunar Powered Descent Phase, "LMO-500-213, 30 January 1965.

23. Greene, J.P.: "The Use of Quaternions in FMES", LMO-510-248, 21 August 1964.

24. Greene, J.P.: "Quaternions", LMO-570-260, 12 October, 1964.

25. Shapiro, M.: "LMS Math Model - Notes On Attitude Simulation Utilizing Either Quaternion Rate Equations or Direction Cosine Rate Equations-Third Progress Report," LMO-500-207, 1 August 1964.

26. Robinson, A.C.: "On The Use of Quaternions In Simulation of Rigid-Body Motion", WADC Technical Report 58-17, December 1958.

27. Goldstein, H.: "Classical Mechanics", Addison-Wesley Publishing Company, 1959.

28. Eichler, J.: "A Method To Force Orthogonality of the Quaternion-Derived Attitude Matrix," LMO-500-216, 5 October 1964.

29. "Explanatory Supplement to the Astronomical Ephemeris and the American Ephemeris and Nautical Almanac," Her Majesty's Stationery Office, 1961.

30. Hutchinson, R.C.: "Inertial Orientation of the Moon," MIT-IL-R-335, October, 1962.

31. Linderifelser, W.A.: "Definition of Coincidence of LEM Vehicle Axes and Inertial Reference Frame At Lunar Landing Site", LMO-300-99, 27 March 1964.

32. Sears, N.E.; Trageser, M.B.; Woodbury, R.B.: "Primary G & N System Lunar Orbit Operations", MIT R-446, Volume I of II, April 1964.

33. Peabody, P.R.; Scott, J.F.; Orozco, E.G.: "Users' Descriptions of JPL Ephemeris Tapes," TR No. 32-580, March 2, 1964.

34. Not Used

200K

35. Green, J.: "GAEC Recommended Changes to LSP-370-2A," LMO-370-168, 22 April 1964.

36. Pulgrano, L.: "An Alternate Mathematical Representation of Propellant Sloshing For Use in the LEM Simulators," LMO-500-198, 9 July 1964.

37. Project 545-556: "LEM-EVDE Design Report, "Farrand Optical Company, 8 January 1965.

38. Woycechowsky, B.J.: "Apollo Mission Simulator - Equations of Motion, "General Precision ER-488, 15 June 1963.

39. Howe, R. E.: "Planar Analysis of Propellant Sloshing Interactions With the LEM Descent Stage Flight Control System," LMO-500-256, 15 March 1965.

40. Not Used

TRUE MOTION EQUATIONS

Part II   LMS Data

Section 1. Equations of Motions

4. Intersystem Requirements

   a. Boolean Assignments

   b. Continuous Data

   Not available at this time.

LED-440-3
True Motion Equations
Part II, Section 1-4
SUBSYSTEM: Equations of Motion

a. BOOLEAN INTERSYSTEM ASSIGNMENT

SHEET 1 OF 1

ENGINEER: M. Fischtal

FROM		TO			
BOOLEAN NO.	ORIGIN (PANEL, BLOCK BOX, etc.)	SUBSYSTEM	DESTINATION (PANEL, BLOCK, BOX, etc.)	IDENTIFICATION	FUNCTION
B_{1115}	J - 86	ECS, Radar, Instr., Comm, RCS			LEM vehicle is in sunlight
B_{1116}	J - 86	EVDE	AUX Cont		CSM is in sunlight
B_{1117}		Not used.			
B_{1118}		Communications			LEM CSM LOS communications possible
B_{1119}	H - 34	Not used.			
B_{1120}	J80-4	EVDE	AUX Cont		Frontal Illumination
B_{1121}		"	" "		$\rho_{LS} \leq 8000$ Ft.
B_{1122}	J33	" , ECS	EVDE		CRT washout RW
B_{1123}	J33	" , "	"		CRT washout LW
B_{1124}	"	" , "	"		CRT washout Ovhd W
B_{1125}	"	"	"		CRT washout Tel.
B_{1126}	J35	"	"		Sun shafting enable Left
B_{1127}	J35	"	"		Sun shafting enable Rt
B_{1128}	J35	"	"		Sun shafting enable Ovhd

1777

DATE 11/65

b. CONTINUOUS INTERSYSTEM DATA

SUBSYSTEM: Equations of Motion (Sheets A thru J)

SHEET 1 OF 1

ENGINEER: M. Fischthal

FROM		TO			
SYMBOL	ORIGIN (PANEL, BLOCK BOX, etc.)	SUBSYSTEM	DESTINATION (PANEL, BLOCK BOX, etc.)	IDENTIFICATION	FUNCTION
E_{LS}	F - 20	Rendezvous Radar			LEM to CSM LOS elevation angle
A_{LS}	F - 21	"			LEM to CSM LOS azimuth angle
P_{LS}	F - 10	"			LOS range to CSM
$\dot{P}_{LS}$	F - 10	"			LOS range rate to CSM
Y_{LM}	G - 50	Lunar Landmass Simulator			LEM Sub-sattelite point
Z_{LM}	G - 50	" " "			" " " "
ψ_{LM}	G - 60	" " "			Scan azimuth angle
$h_{M/L}$	G - 30	" " "			Vehicle altitude
θ_C	H - 40	Communications			Elevation angle of Earth WRT LEM
ϕ_C	H - 42	"			Azimuth " " " " "
F_{XB}	A - 81	Propulsion			Total external forces along LEM X-body axis
p,q,r	C - 11	SCS, IMU (PGNCS)			Vehicle angular rates
$\dot{p},\dot{q},\dot{r}$	C - 11	IMU (PGNCS)			Vehicle angular acceleration
m_L	I - 10	" " and Propulsion			Total LEM Mass
F_{XB}, F_{YB}, F_{ZB}	A - 81	" "			Total External forces along body axis
V_{CB}	I - 20	" "			Position of LEM GG
R_4'	G - 46	Landing Radar			Slant range along altitude beam
D_{S1}, D_{S2}, D_{S3}	G - 40	" "			Doppler velocities

TRUE MOTION EQUATIONS

Part II LMS DATA

Section 2. Primary Guidance and Navigation

1. Symbol Definition. - The symbols that follow pertain to the IMU, LGC, and AOT subsystem equations. Those symbols appearing on sheets L through R of the PGN equations, but not in the symbol list that follows can be found in the equations of Motion Symbol List for sheets A through J.

TRUE MOTION EQUATIONS

Part II LMS Data

Section 2. Primary Guidance and Navigation

1. Symbol Definition
2. Equations
3. Equation Documentation
4. Intersystem Requirements
    a. Boolean Assignments
    b. Continuous Data

LMS SYMBOL DEFINITIONS

LED-440-3
True Motion Equation
Part II, Section 2-1
Primary Guidance and Navigation

Date 2/65

SYMBOL	DEFINITION	UNITS	RANGE	IN/OUT INTERNAL	REMARKS
a_{ij}	Transformation matrix from inertial M frame to selenographic S frame.				
a_V $V = L, C$	Semi Major Axis of LEM or CSM Orbit.				
$a_T(0)$	Desired thrust acceleration at initiation of powered descent visibility phase (this parameter is used to predetermine the desired Phase 1 powered flight end conditions).				
a_{T_x}, a_{T_y}, a_{T_z}	Desired thrust acceleration components along IMU directions.				
a_x, a_y, a_z	Acceleration to be gained (Hohmann descent insertion).				
a_ξ , a_η , a_ζ	Desired thrust acceleration components along local vertical, local horizon and local normal directions.				

LMS SYMBOL DEFINITIONS

LED-440-3
Part II, Section 2-1
True motion Equations
Primary Guidance & Navigation

Date 11/65

SYMBOL	DEFINITION	UNITS	RANGE	REMARKS
a'_ν, b'_ν, c'_ν	Direction cosine of star 1 relative to platform axes.		± 1	$\nu = f, c$
$a''_\nu, b''_\nu, c''_\nu$	Direction cosine of star 2 relative to platform axes.		± 1	

FORM G54A REV 1 6-64 GRUMMAN AIRCRAFT ENGINEERING CORPORATION TABULATION FORM

LMS SYMBOL DEFINITIONS

LED-440-3
True Motion Equation
Part II, Section 2-1
Primary Guidance and Navigation (Cont)

Date 2/65

SYMBOL	DEFINITION	UNITS	RANGE	IN/OUT INTERNAL	REMARKS
$\hat{A}$	Estimate of azimuth angle measurement				
$A_{IMU/RR}$	Rendezvous radar azimuth angle measurement resolved into the IMU frame	$ft/_{sec^2}$	0-12		
$A_{X/B}$, $A_{Y/B}$, $A_{Z/B}$	Non-gravity accelerations along body axes	$ft/_{sec^2}$	0-12		
$A_{X/IMU}$, $A_{Y/IMU}$, $A_{Z/IMU}$	Non-gravity accelerations along actual IMU axes				
A_{TL}	Rendezvous radar azimuth angle measurement relative to the body axes	$ft/_{sec^2}$	$\pm$ 0.5		
$\Delta A_{X/IMU}$, $\Delta A_{Y/IMU}$ $\Delta A_{Z/IMU}$	Acceleration errors due to imperfect accelerometers	$ft/_{sec^2}$	0-12		
$A_{X/acc}$, $A_{Y/acc}$, $A_{Z/acc}$	Total non-gravity acceleration read by the accelerometers				
$\bar{b}_{\rho}$, $\bar{b}_{\dot{\rho}}$, $\bar{b}_E$, $\bar{b}_A$	Geometry vector having components equal to the partial derivatives of the estimated 1) line of sight (cont.) measurement, 2) line of sight rate	ON	PAGE 1208		

LMS SYMBOL DEFINITIONS

LED-440-3
Part II, Section 2-1
True Motion Equation
Primary Guidance & Navigation

Date 11/65

SYMBOL	DEFINITION	UNITS	RANGE	REMARKS
B_5	Boolean issued when IMU temperature exceeds allowable value; $\Delta T = \pm 5°F$			
B_{12}	Boolean value of 1 when $\Delta Vx/acc \geq Kx_1$ or $\Delta Vx/acc \geq Kx_2$			
B_{13}	Boolean value of 1 when $\Delta Vy/acc \geq Ky_1$ or $\Delta Vy/acc \geq Ky_2$			
B_{14}	Boolean value of 1 when $\Delta Vz/acc \geq Kz_1$ or $\Delta Vz/acc \geq Kz_2$			
B_{18}	PIPA fail, Boolean equals one			

FORM G54A REV I 6-64

GRUMMAN AIRCRAFT ENGINEERING CORPORATION

TABULATION FORM

1207B

LMS SYMBOL DEFINITIONS

LED-440-3
Part II, Section 2-1
True Motion Equations
Primary Guidance & Navigation

Date 11/65

SYMBOL	DEFINITION	UNITS	RANGE	REMARKS
B_{51}	MG - CDU FAIL			
B_{52}	IG - CDU FAIL			
B_{53}	OG - CDU FAIL			
B_{60}	CDU(ISS) FAIL			

1785

LMS SYMBOL DEFINITIONS

LED-440-3
Part II, Section 2-1. True Motion Equation
Primary Guidance and Navigation Less Radar (PSA)

Date 8/65

SYMBOL	DEFINITION	UNITS	RANGE	REMARKS
* B_{300}	3.2 KPPS displaced 90 electrical deg (0°, 90°, 180° & 270°) and used as a timing and phase control for 3.2 KC 28 V IRIG & PIPA supply.	-	Boolean value of "1" denotes presence of signal.	
* B_{301}	3.2 KC feedback from IMU to 3.2 KC 28 V PIPA & IRIG supply used for amplitude control	-	"	
* B_{302}	25.6 KPPS synchronizing signal used in the generation of -28 VDC.	-	"	
* B_{303}	800 PPS (at 0 and π phase) used in generation of 28 V 800 CPS 1% regulation supply.	-	"	
		-	"	
		-	"	
				* For Future Use.

LMS SYMBOL DEFINITIONS

LED-440-3
Part II, Section 2-1 True Motion Equations
Primary Guidance and Navigation Less Radar (PSA)

Date 8/65

SYMBOL	DEFINITION	UNITS	RANGE	REMARKS
B_{320}	28 V @ 3.2 KC 1% regulation IRIG and PIPA reference and Gimbal Servo Amp. Ref.	-	Boolean value of "1" denotes presence of signal	where: $B_{320}=B_{300}B_{301}B_{323}$
B_{321}	28 V @ 800 CPS	-	"	where: $B_{321}=B_{303}B_{323}$
B_{322}	-28 VDC	-	"	where: $B_{322}=B_{323}B_{302}$
B_{323}	+28 VDC (Operate)	-	"	$B_{323}=B_{584}$ (IMU OPR PWR AVAIL)
B_{324}	+28 VDC (Standby)	-	"	$B_{324}=B_{581}$ (IMU STANDBY PWR AVAIL)
B_{325}	28V @ 800 CPS common to 0° phase of two phase supply	-	"	where: $B_{325}=B_{321}B_{323}$
B_{326}	28V @ 800 CPS common to 90° phase of two phase supply	-	"	where: $B_{326} = B_{325}B_{323}$

209E

LMS SYMBOL DEFINITIONS

LED-440-3
Part II, Section 2.1 Primary Guidance & Navigation
Primary Guidance and Navigation Less Radar - IMU

Date 5/65

SYMBOL	DEFINITION	UNITS	RANGE	IN/OUT INTERNAL	REMARKS
B_{328}	$\begin{cases} 1 \text{ if } \lvert e_y \rvert \geq 5.5 \text{ v rms} \\ 0 \text{ Otherwise} \end{cases}$	—	—	Int	Servo error too large
B_{329}	$\begin{cases} 1 \text{ if } \lvert e_m \rvert \geq 5.5 \text{ v rms} \\ 0 \text{ Otherwise} \end{cases}$	—	—	Int	Servo error too large
B_{327}	$\begin{cases} 1 \text{ if } \lvert e_o \rvert \geq 5.5 \text{ v rms} \\ 0 \text{ Otherwise} \end{cases}$	—	—	Int	Servo error too large
		—	—		
B_{330}	$B_{328} + B_{329} + B_{327} + \overline{B}_{320} + \overline{B_{325} B_{326}}$	—	—	Int	IMU Fail Descrete to LGC (L-10a)
		—	—		

LMS SYMBOL DEFINITIONS

LED-440-3
Part II, Section 2-1 Equations
True Motion
Primary Guidance & Navigation

Date 11/65

SYMBOL	DEFINITION	UNITS	RANGE	REMARKS
B_{335}	COARSE ALIGN ENABLE Boolean			
B_{336}	IMU Cage Discrete			
B_{399}	FINE ALIGN ENABLE			
B_{406}, B_{407}, B_{408}	Boolean for failing $\Delta V_x/acc$, $\Delta V_y/acc$, $\Delta V_z/acc$ increment between $i-1$ & i computer cycle.			L-21
B_{409}, B_{410}, B_{411}	Boolean for partially degrading $\Delta V_x/acc$, $\Delta V_y/acc$, $\Delta V_z/acc$ increment.			L-21
B_{412}, B_{413}, B_{414}	Boolean for Zeroing Accelerometer outputs during Coast Phases (See L-20)			

LMS SYMBOL DEFINITIONS

LED-440-3
True Motion Equation
Part II, Section 2-1
Primary Guidance and Navigation

Date 2/65

SYMBOL	DEFINITION	UNITS	RANGE	IN/OUT INTERNAL	REMARKS
(cont.) FROM PAGE 1267	measurement, 3) elevation angle measurement and 4) azimuth angle measurement.				
$b_{X/R}$, $b_{Z/R}$	Non-gravity accelerations required for Hohmann descent initiation				
b_{ij}	Transformation matrix from true IMU coordinates to local vertical, local horizon coordinates				
c	Chord length for Lambert's Routine				
C_1, C_2, C_3 C_4, C_5, C_6	Guidance constants required to shape the powered descent and ascent trajectory				
" , C_{ij}	Transformation matrix from inertial M or E frame to the desired platform axes				
C_X, C_Y, C_Z	Accelerometer bias errors	ft/sec^2			Input Constants
C_{1X}, C_{1Y}, C_{1Z}	Accelerometer first order scale factor error	$\left(\frac{ft/sec^2}{ft/sec^2}\right)$			Input Constants

12088A

LMS SYMBOL DEFINITIONS

LED-440-3
Part II, Section 2-1
True Motion Equation
Primary Guidance & Navigation

Date 11/65

SYMBOL	DEFINITION	UNITS	RANGE	REMARKS
C_{xt}, C_{yt}, C_{zt}	PIPA coefficient expressing PIPA offset in ft/sec^2 per unit temperature offset from nominal.			

1209

LMS SYMBOL DEFINITIONS

LED-440-2
True Motion Equation
Part II, Section 2-1
Primary Guidance and Navigation

Date 2/65

SYMBOL	DEFINITION	UNITS	RANGE	IN/OUT INTERNAL	REMARKS
C_{2X}, C_{2Y}, C_{2Z}	Accelerometer second order scale factor error	$\left(\frac{K\ ft/sec^2}{1\ ft/sec^2}\right)$			Input Constants
C_{iX}, C_{iY}, C_{iZ} $i = 3, 5$	Accelerometer cross coupling zero bias sensitivity coefficients				
C_{iX}, C_{iY}, C_{iZ} $i = 4, 6$	Accelerometer cross coupling scale factor sensitivity coefficients				
C_v, C_{h1}, C_{h2}	Landing Radar weighting factor constants	ft	-		$C_v = 15000$ $C_{h2} = 25000$ $C_{h1} = 20000$
d_{ij}	Transformation matrix from desired platform axes to LEM body axes				
d'_{ij}	Transformation matrix from indicated platform axes to LEM body axes		± 1		Computed L-17
d_{LS}	Line of sight distance from LEM to hover point				
d_o	Days measured from Jan 1.0 1950 to epoch or problem start				

1792

Date 2/65

SYMBOL	DEFINITION	UNITS	RANGE	IN/OUT INTERNAL	REMARKS
e_c	CSM eccentricity				
$\hat{E}$	Estimate of elevation angle measurement				
$E_{IMU/RR}$	Rendezvous radar elevation angle measurement resolved into IMU frame				
E_{TL}	Rendezvous radar elevation angle measurement relative to the body axes				
$E(t_o)$, $\hat{E}(t)$ $E'(t)$	Initial value, best estimate and extrapolated value of the covariance matrix				
$\hat{E}_1(t), \hat{E}_2(t)$	Rectification of covariance matrix after processing first and second measurements				
E_{CO}, E_{LO}, $E_{C_{BO}}$, E_I	CSM eccentric anomaly measured at CSM epoch, LEM lift-off, LEM burnout and LEM-CSM intercept respectively				
f_{SEP}, f_{HOH}, f_{PF}	Central angles measured from platform axis to initiation of separation maneuver, Hohmann transfer and powered descent				5/65

1793

210A

IMS SYMBOL DEFINITIONS

LED-440-3
Part II, Section 2-1
True Motion Equations
Primary Guidance & Navigation

Date 11/65

SYMBOL	DEFINITION	UNITS	RANGE	REMARKS
e_y, e_o, e_m	Simulated Servo Error Signals (inner, outer, & middle respectively) driving Gimbal Servo			
	Amplifier in actual system.			

LMS SYMBOL DEFINITIONS

LED-440-3
True Motion Equation
Part II, Section 2-1
Primary Guidance and Navigation

Date 2/65

SYMBOL	DEFINITION	UNITS	RANGE	IN/OUT INTERNAL	REMARKS
$(f_{PF})_{MIN}$, $(f_{PF})_{MAX}$	Minimum and maximum central angles for initiating powered descent maneuver				
f	Central angle of LEM measured from x platform axis				
f, g	Kepler parameters for two body computations				
f_{CO}, f_{BO}	CSM true anomaly at epoch and central angle measured from CSM at epoch to CSM at LEM burnout				
$(f_{LO})_o$, f_{LO}	Central angle measured from CSM at epoch to the projection of the take-off site into the CSM plane at epoch ~~and at actual lift-off~~				
g_X, g_Y, g_Z	Spherical gravity components measured in platform coordinates				
$\overline{g}_{avg}$	Average gravity vector between present value, $\overline{g}$ and predicted end point value $\overline{g}(T_{GO})$				
g_E	Earth gravity constant				5/65

FORM G54A REV 1 6-64

GRUMMAN AIRCRAFT ENGINEERING CORPORATION

TABULATION FORM

1795

LMS SYMBOL DEFINITIONS

LED-440-3
True Motion Equation
Part II, Section 2-1
Primary Guidance and Navigation

Date 2/65

SYMBOL	DEFINITION	UNITS	RANGE	IN/OUT INTERNAL	REMARKS
G	Differential gravity matrix				
h_h, h_v	Altitudes used to activate landing radar weighting loop				
h_{LR}	Altitude defined by landing radar				
h_{HOV}	Desired hover altitude				
h_{BO}	Desired burnout altitude				
$\hat{h}_c$, $\hat{h}_L$	Specific angular momentum directions of 1) CSM orbit and 2) desired LEM ascent orbit for great circle steering				
$\hat{h}_D$	Desired LEM specific angular momentum direction				
$(h_{ij})_{Tq}$	Transformation matrix from LEM body axes to telescope optical axes ($q = 1$, r or a)				5/65

LMS SYMBOL DEFINITIONS

LED-440-3
Part II, Section 2-1
True motion Equations
Primary Guidance & Navigation

Date 11/65

SYMBOL	DEFINITION	UNITS	RANGE	REMARKS
h	Altitude from Lunar surface derived from inertial data.	ft	0- 60,000	For display purposes - L 14 a
$\dot{h}$	Altitude rate	ft/sec	± 500	" "
h^*_{ij}	Transformation between rotated reticle pattern and zero reference position (telescope axes)		± 1	

LMS SYMBOL DEFINITIONS

LED-440-3
True Motion Equation
Part II, Section 2-1
Primary Guidance and Navigation

Date 2/65

SYMBOL	DEFINITION	UNITS	RANGE	IN/OUT INTERNAL	REMARKS
H_R	Gyro rotor angular momentum.				
$\hat{i}_s, \hat{j}_s, \hat{k}_s$	Unit directions of selenographic S - frame.				
$\hat{i}_M, \hat{j}_M, \hat{k}_M$	Unit directions of inertial M - frame.				
$\hat{i}, \hat{j}, \hat{k}$	Unit directions of IMU frame.				
i_L, i_C	Inclination of LEM ascent orbit and CSM orbit relative to the equatorial M-frame.				
I	Identity matrix.				
I_{SP}	Specific impulse.				
K_F, K_R, K_S	AOT, fine align, reticle and spiral scale factors respectively.				5/65

1213A

LMS SYMBOL DEFINITIONS

LED-440-3
Part II, Section 2-1
True Motion Equations
Primary Guidance & Navigation

Date 11/65

SYMBOL	DEFINITION	UNITS	RANGE	REMARKS
K_{x1}, K_{Y1}, K_{Z1}	Upper limit of X, Y, Z PIPA velocity increment in a computer cycle. Any velocity increment exceeding these constants is a malfunction.			
K_{x2}, K_{Y2}, K_{Z2}	Lower limit of X, Y, Z PIPA velocity increment in a computer cycle. Any velocity increment below these constants is a malfunction.			
K_y, K_o, K_m	Inverse transform constants relating IMU Gimbal rate to Servo errors.			

LMS SYMBOL DEFINITIONS

LED-440-3
True Motion Equation
Part II, Section 2-1
Primary Guidance and Navigation

Date 2/65

SYMBOL	DEFINITION	UNITS	RANGE	IN/OUT INTERNAL	REMARKS
K_{ω}	Command angle gain factor (Hohmann descent initiation).				
m	Vehicle mass.				
$(m_{PF})_o$	Vehicle mass at start of powered descent.				
$\hat{N}_L$, $\hat{N}_C$	Unit vector denoting the direction of the ascending node of the desired LEM ascent plane (L) or the CSM plane (C).				
P	Precomputed ideal velocity parameter.				
$P(t_{n+1}, t_n)$	Transition matrix including bias terms.				
P_L	Latus rectum of LEM transfer orbit.				
r_D, $\dot{r}_D$	Desired radius and desired radius rate.				5/65

IMS SYMBOL DEFINITIONS

LED-440-3
Part II, Section 2-1
True Motion Equations
Primary Guidance & Navigation

Date 11/65

SYMBOL	DEFINITION	UNITS	RANGE	REMARKS
Q_{ij}	Transformation matrix from reference frame to actual LEM platform frame.			

1801

LMS SYMBOL DEFINITIONS

LED-440-3
True Motion Equation
Part II, Section 2-1
Primary Guidance and Navigation

Date 2/65

SYMBOL	DEFINITION	UNITS	RANGE	IN/OUT INTERNAL	REMARKS
$\bar{r}_{S/LO}$	Vector direction of the lift-off site in selenographic coordinates.				
$\bar{r}_{L/LO}$, $\bar{r}_{L/BO}$	Vector direction of LEM at lift-off and burn out.				
$r_{L/C}$	Line of sight measured from LEM to CSM.				
$\bar{r}_{C/I}$	CSM vector at intercept.				
$\bar{r}_D(T_{GO})$	Desired LEM radius vector projected ahead by T_{GO} seconds.				
$\hat{r}(T_{GO})$	Unit direction of LEM position projected ahead T_{GO} seconds.				
r_P	Pericynthion radius.				
$\bar{r}_{proj}$	Projection of LEM radius vector onto the original LEM transfer plane.				5/65

LMS SYMBOL DEFINITIONS

LED-440-3
Part II, Section 2-1
True Motion Equations
Primary Guidance & Navigation

Date 11/65

SYMBOL	DEFINITION	UNITS	RANGE	REMARKS
r	Scalar radius of current LEM position			
$\hat{r}_B$	LEM body axes coordinates			Unit vector
$\hat{r}_P$	Actual platform " "			" "
$\hat{r}_R$	Desired " " " "			" "
$\hat{r}'_{P/S}$	Unit direction of star 1 in platform coordinates.			" "
$\hat{r}''_{P/S}$	Unit direction of star 2 in platform coordinates			" "
$(\hat{r}^*_P)_i$	Unit direction normal to star			Unit vector $i = X_T, Y_T$
$\hat{r}_{Tq}$	Telescope coordinate axes			Unit vector $q = \ell, r,$ or a

LMS SYMBOL DEFINITIONS

LED-440-3
True Motion Equation
Part II, Section 2-1
Primary Guidance and Navigation

Date 2/65

SYMBOL	DEFINITION	UNITS	RANGE	IN/OUT INTERNAL	REMARKS
$\dot{\bar{R}}_{M/S}$	Linear velocity vector of take-off site with respect to the inertial M frames.				
R_M	Radius of spherical moon.				
R_M^*	Local radius of moon based on landing radar and IMU data.				
RA_{SK} $K = 1, 2$	Right Ascension of star.	deg or hours minutes & seconds	0-360 0-24		Input Constant
R_X, R_Y, R_Z	Fixed gyro drift rate.				
s	Perimeter of triangle formed by LEM transfer geometry (required for Lambert's equation).				
Δs	Distance traveled in zero g gravity field.				
S_{ij}, S_{ijv}^* $v = f, c$	Transformation matrix between: 1) desired platform axes and star coordinate frame and 2) indicated platform axes and star coordinate frame.		± 1		

217

LMS SYMBOL DEFINITIONS

LED-440-3
True Motion Equation
Part II, Section 2-1
Primary Guidance and Navigation

Date 2/65

1805

SYMBOL	DEFINITION	UNITS	RANGE	IN/OUT INTERNAL	REMARKS
$S_{ij_f}^{**}$, $S_{ij_c}^{**}$	Transformation matrix between indicated platform axes and desired platform axes (fine align mode and coarse align mode).		± 1		
$(S_{SS} - S_{ii})$	Direct compliance.				
S_{Si}, S_{iS}	Cross compliance.				
$S_{m,\ n}$	Anisoelastic coefficients which contribute to gyro drift.				
t_{ALIGN}	Time required for the gimbal torques or the gyro torques to align the platform.				
t_{BO}	Actual time measured from lift-off to burn out.				
t_{TR}	Time counted from initialization of terminal rendezvous loop.				
t_{cor}	Fixed time measured from burn out required for initiating midcourse velocity corrections.				
Δt_{LW}, Δt_{PW}	Direct ascent launch window and parking orbit launch window.				
Δt	Accelerometer sampling interval (used for least square fit of V_e and γ).				11/65

LMS SYMBOL DEFINITIONS

LED-440-3
Part II, Section 2-1
True Motion Equations
Primary Guidance & Navigation

Date 11/65

SYMBOL	DEFINITION	UNITS	RANGE	REMARKS
t_{321}	Time base initiated when B_{321} goes from 1 to 0.			
t_f	Time of IMU shut-down	sec		L-216
t_g	Time of glycol failure	sec		L-216

1806

LMS SYMBOL DEFINITIONS

LED-440-3
True Motion Equation
Part II, Section 2-1
Primary Guidance and Navigation

Date 2/65

SYMBOL	DEFINITION	UNITS	RANGE	IN/OUT INTERNAL	REMARKS
Δt_{BO}	Estimated LEM ascent burn time.				
$t_{C_{LO}}$, $t_{C_{BO}}$, $t_{C/I}$	Time measured from CSM at epoch to LEM lift-off, LEM burnout and LEM-CSM intercept.				
t_{ff}	LEM free flight time required to achieve LEM-CSM intercept as defined by Lambert's equation.				
t_m	Time required for LEM-CSM intercept based on minimum orbit energy transfer path.				
t_{VR}	LEM vertical rise time.				
t*	Time counted from problem start or CSM epoch. This parameter defines the platform orientation based on the nominal position of the desired landing site ~~at landing or the desired take-off~~ site at lift-off.				
T*	t* measured in Julian centuries.				

LMS SYMBOL DEFINITIONS

LED-440-3
True Motion Equation
Part II, Section 2-1
Primary Guidance and Navigation

Date 2/65

SYMBOL	DEFINITION	UNITS	RANGE	IN/OUT INTERNAL	REMARKS
T_I	Fixed time from LEM lift-off to intercept.				
T_{I_j} $j = 1, 2, 3$	Fixed time to intercept. This parameter is initialized just prior to each terminal rendezvous velocity correction.				
T^*_{GO}	Predetermined time to go for powered flight visibility phase.				
$\tilde{T}_{GO}$, $(T_{GO})_o$	Initial estimate of time to go.				
$(T_{GO})_{min}$	Time signal which stops iteration cycle and maintains constant vehicle attitude.				
T_{GO}	Time to go.				
T_E	Time signal for engine shut down in order to compensate for tail off effects.				
ΔT	Time to go increment for regula-falsi iteration technique.				5/65

1808

LMS SYMBOL DEFINITIONS

LED-440-3
Part II, Section 2-1
True Motion Equations
Primary Guidance & Navigation

Date 11/65

SYMBOL	DEFINITION	UNITS	RANGE	REMARKS
T_A	Accelerometer temperature	deg	0 - 150	L-216
T_G	Gyro temperature	deg	0 - 150	L-216

1220

1810

LED-440-3
True Motion Equation
Part II, Section 2-1
Primary Guidance and Navigation

LMS SYMBOL DEFINITIONS

Date : 2/65

SYMBOL	DEFINITION	UNITS	RANGE	IN/OUT INTERNAL	REMARKS
$T_{D_{MAX}}$, $T_{D_{MIN}}$	Maximum and minimum thrust (descent engine).				
U_{ij_η} $\eta = \alpha$ or β	Transformation matrix from telescope axes to indicated IMU axes computed at instant when star crosses the X_T or Y_T reticle axes.				
U, U'	CSM lead angle. Angle measured between the projection of the launch site into the plane of the CSM (at epoch and at lift-off) with the CSM at time of lift-off				
ΔU	Incremental lead angle required for launch window iteration.				
ΔU_{LW}	Incremental lead angle that defines the direct ascent launch window.				
ΔU_{PW}	Approximate incremental lead angle that defines the parking orbit launch window.				
$U'_{L/LO}$, $U_{L/LO}$	Argument of latitude of the projection of the take-off site vector into the CSM plane measured at epoch and at lift-off.				
$U_{L/BO}$	Argument of latitude of the LEM vehicle measured at burnout.				5/65

LMS SYMBOL DEFINITIONS

LED-440-3
Part II, Section 2-1
True Motion Equations
Primary Guidance & Navigation

Date 11/65

SYMBOL	DEFINITION	UNITS	RANGE	REMARKS
ν_{tx}, ν_{ty}, ν_{tz}	Gyro Drift. Drift per unit temperature from nominal.	°/hr/ 1° F		
ΔT_a	Temperature increment exceeding nominal IMU temperature.	°F	0-5	
$\Delta V_{X\epsilon}$, $\Delta V_{Y\epsilon}$, $\Delta V_{Z\epsilon}$	Imputted velocity error for partially failing $\Delta Vx/acc$, $\Delta Vy/acc$, $\Delta VZ/acc$ increment.			L-21

LMS SYMBOL DEFINITIONS

LED-440-3
True Motion Equation
Part II, Section 2-1
Primary Guidance and Navigation

Date 2/65

SYMBOL	DEFINITION	UNITS	RANGE	IN/OUT INTERNAL	REMARKS
U_X, U_Y, U_Z	Mass unbalance.				
U_{SX}, U_{XY}, U_{SZ}	Mass unbalance about spin axis.				
ν_{HOH}	Velocity increment which deactivates descent engine upon completion of Hohmann insertion maneuver.				
ν_{SEP}	Velocity increment which deactivates RCS jets at separation maneuver completion.				
$V_{X/acc}$, $V_{Y/acc}$, $V_{Z/acc}$	Non-gravity acceleration velocity components as read by the accelerometers.				
$\Delta V_{X/acc}$, $\Delta V_{Y/acc}$, $\Delta V_{Z/acc}$	Velocity increments sampled during each accelerometer cycle.				$\left\{ \Delta V_{x/acc} = \left[\int_{i-1}^{i} A_{x/acc}\,dt + \Delta V_{x\varepsilon} B409 \right]_{i-1}^{i} \right.$. Similiarly for $\Delta V_{y/acc}$ & $\Delta V_{z/acc}$. (See L-21)
V_e	Main engine exhaust velocity (either pre-loaded or defined by least square fit).				
$V_{e_{RCS}}$	Exhaust velocity corresponding to RCS jets.				
V	LEM scalar velocity.				

11/65

1812

LMS SYMBOL DEFINITIONS

LED-440-3
Part II, Section 2-1
True Motion Equations
Primary Guidance & Navigation

Date 11/65

SYMBOL	DEFINITION	UNITS	RANGE	REMARKS
μ_{ij}	Transformation matrix from rotated reticle axis to platform axis.		± 1	
μ_s	Central angle between stars 1, and 2.	rad	0 to π	
$\mu_{s\nu}$	Central angle between stars 1, and 2 based on fine or coarse align reading.	rad	0 to π	$\nu = f, c$
$(\nu_x, \nu_y, \nu_z)_k$	Direction cosine of star 1, or 2 relative to the desired platform axes.		± 1	$k = 1, 2$

FORM G54A REV I 6-64 GRUMMAN AIRCRAFT ENGINEERING CORPORATION TABULATION FORM

LMS SYMBOL DEFINITIONS

LED-440-3
Part II, Section 2-1
True Motion Equations
Primary Guidance & Navigation

Date 11/65

SYMBOL	DEFINITION	UNITS	RANGE	REMARKS
V_{FWD}	Fwd. Component of vehicle velocity referenced to horizontal coord's of a local coord system by the IMU YAW angle	ft/sec	± 200	
V_{LAT}	Lateral Component of vehicle velocity referenced to horizontal coord's of a local coord system by the IMU YAW angle.	ft/sec	± 200	
V_{XL}, V_{YL}, V_{ZL}	Inertial velocities transformed to a local coordinate system on moon's surface	ft/sec	± 200	

1814

LED-440-3
True Motion Equation
Part II, Section 2-1
Primary Guidance and Navigation

LMS SYMBOL DEFINITIONS

Date 2/65

SYMBOL	DEFINITION	UNITS	RANGE	IN/OUT INTERNAL	REMARKS
V_D	Desired velocity				
$\overline{V}_G$	Velocity to be gained vector				
V_{SEP}	Predetermined velocity to be gained for separation maneuver				
V_{RH}	Required velocity to ensure a desired pericynthion radius				
ΔV_M	Characteristics velocity required for midcourse corrections(Lambert output)				
ΔV_{TR}	Characteristic velocity required for terminal rendezvous correction (Lambert output)				
ΔV	Total characteristic velocity				
ΔV_2	Impulsive velocity required by LEM for rendezvous				5/65

1815

122

LMS SYMBOL DEFINITIONS

LED-440-3
True Motion Equation
Part II, Section 2-1
Primary Guidance and Navigation

Date 2/65

SYMBOL	DEFINITION	UNITS	RANGE	IN/OUT INTERNAL	REMARKS
$f(V_{L/BO})$	Characteristic velocity charged to gravity loss (stored function)				
W_h, W_v	Landing radar altitude and velocity weighting factors				
$\overline{W}_\gamma$, $\overline{W}_A$, $\overline{W}_E$	Weighting matrices for line of sight rate observation, azimuth angle observation and elevation angle observation				
$(x, y, z)_{IMU/RR}$	Transformation of radar measurements into IMU coordinates				
X, Y, Z	LEM position coordinates measured in the IMU frame and computed from the LGC equations of motion				
$\hat{X}$, $\hat{Y}$, $\hat{Z}$	Best estimate of LEM position coordinates (used to reinitialize equations of motion)				
$(X, Y, Z)_{L/C}$	Position coordinates of CSM with respect to LEM				
$X(T_{GO})$, $Y(T_{GO})$, $Z(T_{GO})$	Position coordinates of LEM projected ahead T_{GO} seconds				

1816

5/65

LMS SYMBOL DEFINITIONS

LED 440-3
True Motion Equation
Part II, Section 2-1
Primary Guidance and Navigation

Date 2/65

SYMBOL	DEFINITION	UNITS	RANGE	IN/OUT INTERNAL	REMARKS
$(X, Y, Z)_{D_1}$	Desired position coordinates at the end of phase I powered descent				
$(X,Y,Z)_{D_2}$	Desired position coordinates at the end of phase 2 powered descent (ideally hover condition)				
$(X, Y, Z)_{LR}$	Landing radar math model data resolved in LEM body axes				
$(X', Y', Z')_{LR}$	Landing radar math model data relative to IMU axes				
$(\dot{X},\dot{Y},\dot{Z})_G$	Velocity to be gained components				
$(\dot{X}, \dot{Y}, \dot{Z})_{LR_I}$	Landing radar velocity components resolved in the IMU frame and including the rotational velocity of the moon				
$(\dot{X}, \dot{Y}, \dot{Z})_{M/S}$	Velocity components of the moon, at the subsatellite position, relative to the inertial M frame				
$(\dot{X}, \dot{Y}, \dot{Z})_{L/I}$	Velocity components of LEM at intercept.				5/65

1817

LMS SYMBOL DEFINITIONS

LED-440-3
Part II, Section 2-1
True Motion Equations
Primary Guidance & Navigation

Date 11/65

SYMBOL	DEFINITION	UNITS	RANGE	REMARKS
X_T, Y_T	Plane of reticle pattern, components of telescope axes.			

FORM G54A REV I 6-64 GRUMMAN AIRCRAFT ENGINEERING CORPORATION TABULATION FORM

LMS SYMBOL DEFINITIONS

LED 440-3
True Motion Equation
Part II, Section 2-1
Primary Guidance and Navigation

Date 2/65

SYMBOL	DEFINITION	UNITS	RANGE	IN/OUT INTERNAL	REMARKS
$\dot{X}_W, \dot{Y}_W, \dot{Z}_W$	LEM velocity components based on weighting IMU data with landing radar data				
$(\Delta\dot{X}, \Delta\dot{Y}, \Delta\dot{Z})_2$	Impulsive velocity components required by LEM for rendezvous				
$Y^*, \dot{Y}^*$	Lateral excursion and velocity measured normal to desired ascent plane				
$Y_D^*, \dot{Y}_D^*$	Desired lateral excursion and velocity measured normal to desired ascent plane				
$(\bar{\alpha}, \bar{\beta}, \bar{\gamma})$	Distance from IMU-CG to instantaneous vehicle CG				
$(\alpha, \beta, \gamma)_{IMU}$	Distance from reference position to IMU-CG				
α	Denotes pilot mark when star crosses telescope X_T reticle				
α, β	Lambert variables				5/65

1819

LMS SYMBOL DEFINITIONS

LED 440-3
True Motion Equation
Part II, Section 2-1
Primary Guidance and Navigation

Date 2/65

SYMBOL	DEFINITION	UNITS	RANGE	IN/OUT INTERNAL	REMARKS
α^*	Angle between desired thrust direction and local horizon				
α_W	Angle between optical axis and line of sight direction to new landing site				
β	Denotes pilot mark where star cross telescope Y_T reticle				
$\beta_x, \beta_y, \beta_z$	Direction cosines between the line of sight direction and the body axes				
β_m	Lambert variable for minimum energy transfer orbit				
γ	Direction cosine of star measured by reticle rotation				
γ^*	Desired flight path angle measured from the local horizon to the velocity direction				
$\gamma_x, \gamma_y, \gamma_z$	Direction cosines between the line of sight vector and the platform axes				5/65

IMS SYMBOL DEFINITIONS

LED-440-3
True Motion Equation
Part II, Section 2-1
Primary Guidance and Navigation

Date 2/65

SYMBOL	DEFINITION	UNITS	RANGE	IN/OUT INTERNAL	REMARKS
$\gamma_{L/BO}$	Flight path angle at LEM burnout.				
δ	Direction cosine of star as determined by spiral rotation.				
δ_K $K = 1, 2$	Declination of star 1 or 2				
δ_T	Incremental thrust commands.				
δ_n	Tolerance parameter for Regula-Falsi iteration.				
$\delta_{\hat{X}}, \delta_{\hat{Y}}, \delta_{\hat{Z}}$ $\delta_{\hat{\dot{X}}}, \delta_{\hat{\dot{Y}}}, \delta_{\hat{\dot{Z}}}$	Best estimate of state vector deviation error.				
$\delta_{\xi}, \delta_{\dot{\xi}}, \delta_{A}, \delta_{E}$	Incremental error between measured data and estimated data.				
$\delta\xi_{BI}$, $\delta\xi_{BI}$ $\delta_{A_{BI}}$, $\delta_{E_{BI}}$	Bias estimates.				

LMS SYMBOL DEFINITIONS

LED-440-3
Part II, Section 2-1
True Motion Equations
Primary Guidance & Navigation

Date 11/65

SYMBOL	DEFINITION	UNITS	RANGE	REMARKS
$(\theta,\psi,\phi)_{CDU}$	Disturbing function for simulating CDU malfunctions	-	-	Simulation of following hardware malfunctions 1) cos $(\theta-\psi)$ loss 2) fine error too high 3) coarse error too high 4) Read counter failure 5) loss of 14VDC
$(\theta_1(t), \psi_1(t), \phi_1(t)$	Disturbing function for simulating gyro drift when gyro spin supply fails	-	-	L-13
$\theta_2(t), \psi_2(t), \phi_2(t)$	Disturbing function for simulating total loss of 3.2 KC reference voltage to Gimbal Servo Demod, PIPA & IRIG Ref.	-	-	L-13
$\theta_3(t), \psi_3(t), \phi_3(t)$	Disturbing function for simulating loss of 3.2 KC or 800 cps to Gimbal Servo Amp or coarse align amps respectively			L-13

1223

1822

LMS SYMBOL DEFINITIONS

LED-440-3
True Motion Equation
Part II, Section 2-1
Primary Guidance and Navigation

Date 2/65

SYMBOL	DEFINITION	UNITS	RANGE	IN/OUT INTERNAL	REMARKS
θ_{BO}	Central angle traversed by LEM during powered ascent.				
$\theta_{c_{pf}}$	Central angle traversed by CSM during LEM powered ascent.				
θ, ψ, ϕ	Platform gimbal angles with respect to MorE frame				
$\theta_{IMU}, \psi_{IMU}, \phi_{IMU}$	IMU gimbal angles.				
θ_c, ψ_c, ϕ_c	Command gimbal angles.				
θ_S	Final value of reticle rotation required for spiral to coincide with star	rad	0-2		Input via pilot mark.
θ_S^*	Angle measured along spiral from origin to position where star and spiral coincide	rad	0-2		

LMS SYMBOL DEFINITIONS

LED-440-3
True Motion Equation
Part II, Section 2 - 1
Primary Guidance and Navigation

Date 2/65

SYMBOL	DEFINITION	UNITS	RANGE	IN/OUT INTERNAL	REMARKS
θ_d, ψ_d, ϕ_d	Euler angles which relate the actual LEM platform frame to the reference frame.				
θ_e, ψ_e, ϕ_e	Gimbal angle errors used to activate RCS jets.				
$(\theta, \psi, \phi)_{e_c}$	Gimbal angle coarse align errors.	rad	$\pm$ 1/60		
$(\theta, \psi, \phi)_{e_f}$	Gimbal angle fine align errors.	rad	0 - 2π		
$(\dot{\theta}, \dot{\psi}, \dot{\phi})_{e_c}$	Coarse align gimbal angle accelerometers.	rad/sec			Input Constants
$(\Delta\theta, \Delta\psi, \Delta\phi)_{e_c}$	Coarse align error tolerance.	rad	$> 1^\circ$		" "
$(\Delta\theta, \Delta\psi, \Delta\phi)_{e_f}$	Fine align error tolerance	rad	$\overset{\frown}{100}$ sec		" "

FORM G54A REV. 6-54

LMS SYMBOL DEFINITIONS

LED-440-3
True Motion Equation
Part II, Section 2-1
Primary Guidance and Navigation

Date 2/65

SYMBOL	DEFINITION	UNITS	RANGE	IN/OUT INTERNAL	REMARKS
$(\theta, \psi, \phi)_{pq}$	Fixed angles between body axes and window (P = W) axes (q = l, r, a) & telescope (P=T) axes (q=l, r, a).				
λ	Transformation variable used to compute semi-major axis in Lambert's routine.				
λ^*	Desired angle between flight path direction and thrust axis.				
$\lambda_{S/L}$	Selenographic longitude of landing site on take-off site.				
$\lambda_{S}, \lambda_{Sf}, \lambda_{Sc}$	Angle between two stars subtended in M frame and in indicated IMU frame used for fine align and coarse align.				
μ_M	Gravitation constant of moon.				
$\hat{\xi}, \hat{\eta}, \hat{\zeta}$	Unit directions which describe the LEM local horizon, local vertical and local normal system.				
$\mathcal{S}_{RR}$	Rendezvous radar line of sight measurement.				5/65

LMS SYMBOL DEFINITIONS

LED-440-3
True Motion Equation
Part II, Section 2-1
Primary Guidance and Navigation

Date 2/65

SYMBOL	DEFINITION	UNITS	RANGE	IN/OUT INTERNAL	REMARKS
ρ_1, ρ_2, ρ_3	Line of sight distances required to initiate terminal velocity corrections.				
ρ_D	Desired line of sight rate.				
τ	Effective time constant that relates exhaust velocity to initial acceleration. Either a constant input or computed by least square fit.				
$\phi_{S/L}$	Selenographic latitude of landing or take-off site.				
ϕ_{ff}	LEM free flight central angle from descent positions to intercept.				
ϕ_X, ϕ_Y, ϕ_Z	Approximate IMU gimbal error angles.				
Φ_{ff}	CSM central angle measured from LEM burnout to intercept.				
$\Phi(t_{n+1}, t_n)$	Transition matrix between time t_n and t_{n+1}.				5/65

LMS SYMBOL DEFINITIONS

LED-440-3
True Motion Equation
Part II, Section 2-1
Primary Guidance and Navigation

Date 2/65

SYMBOL	DEFINITION	UNITS	RANGE	IN/OUT INTERNAL	REMARKS
Φ_{Bias}	Constant bias transition matrix.				
ψ_{GL}	Middle gimbal value which warns pilot of impending gimbal lock.				
ω_L, ω_C	Mean motion of LEM and CSM orbits.				
$\omega_{x_d}, \omega_{y_d}, \omega_{z_d}$	Platform drift rates.				
$\omega_{x_c}, \omega_{y_c}, \omega_{z_c}$	Command angle signals measured with respect to IMU axes.				
Ω_L, Ω_C	Right ascension of ascending node of LEM orbit and CSM orbit.				
$\frac{\Omega_X}{\Omega}, \frac{\Omega_Y}{\Omega}, \frac{\Omega_Z}{\Omega}$	Direction cosines of desired LEM rotation vector measured in IMU frame.				
					5/65

TRUE MOTION EQUATIONS

Part II LMS Data

Section 2. Primary Guidance and Navigation

2. Equations

a. Initial Conditions and Constants

b. Development

1233

TRUE MOTION EQUATIONS

Part II, LMS Data

Section 2. Primary Guidance and Navigation

2. Equations

a. Initial Conditions and Constants. See Enclosure 2.

1235

IML - LED-440-3 PART II. SECTION 2-2 TRUE MOTION EQUATIONS (CONT)

SHEET 1 OF 3

PLATFORM GIMBAL ANGLES

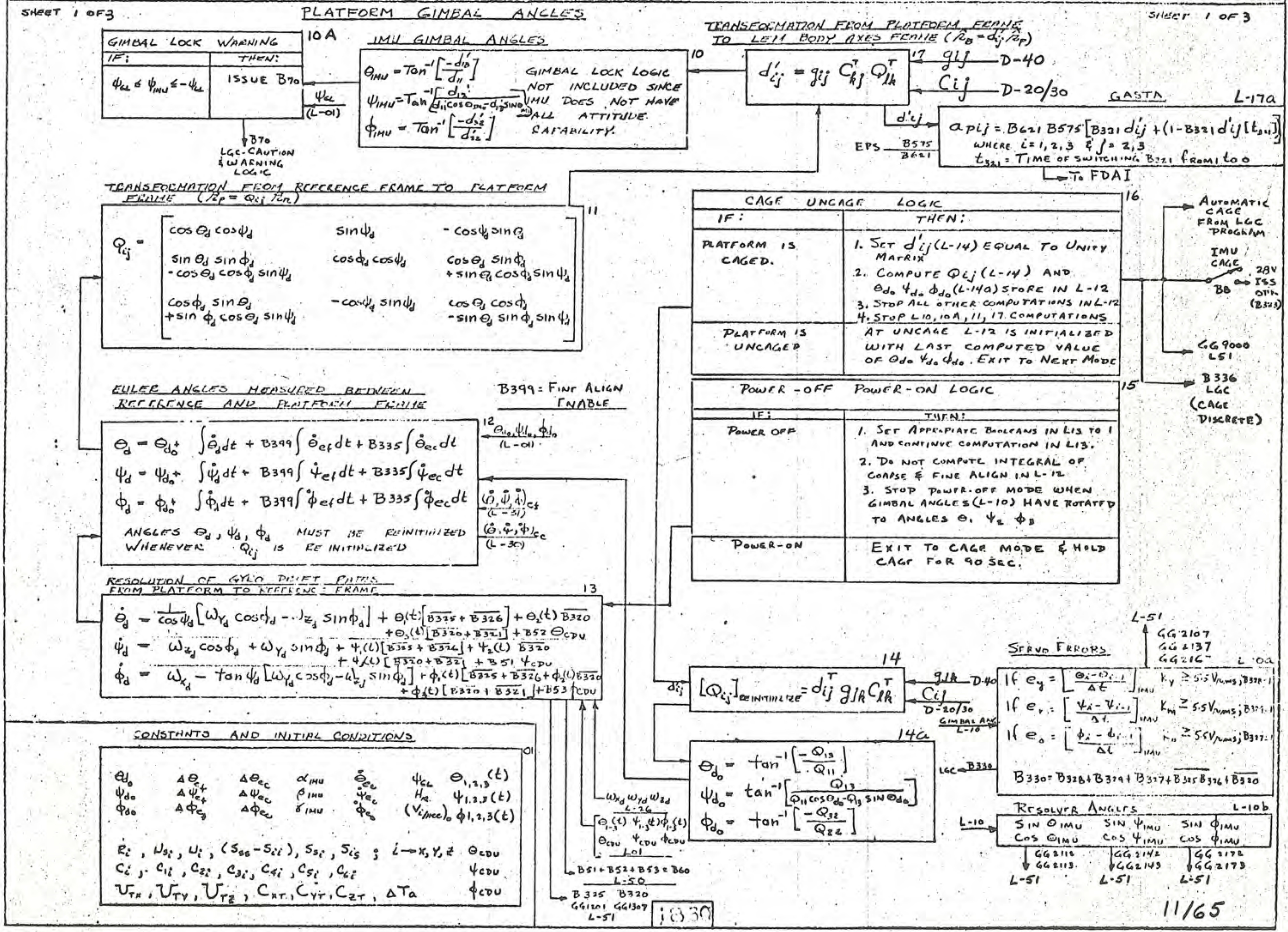

1830

11/65

12J6A

ACCELEROMETER OUTPUTS AND GYRO DRIFT

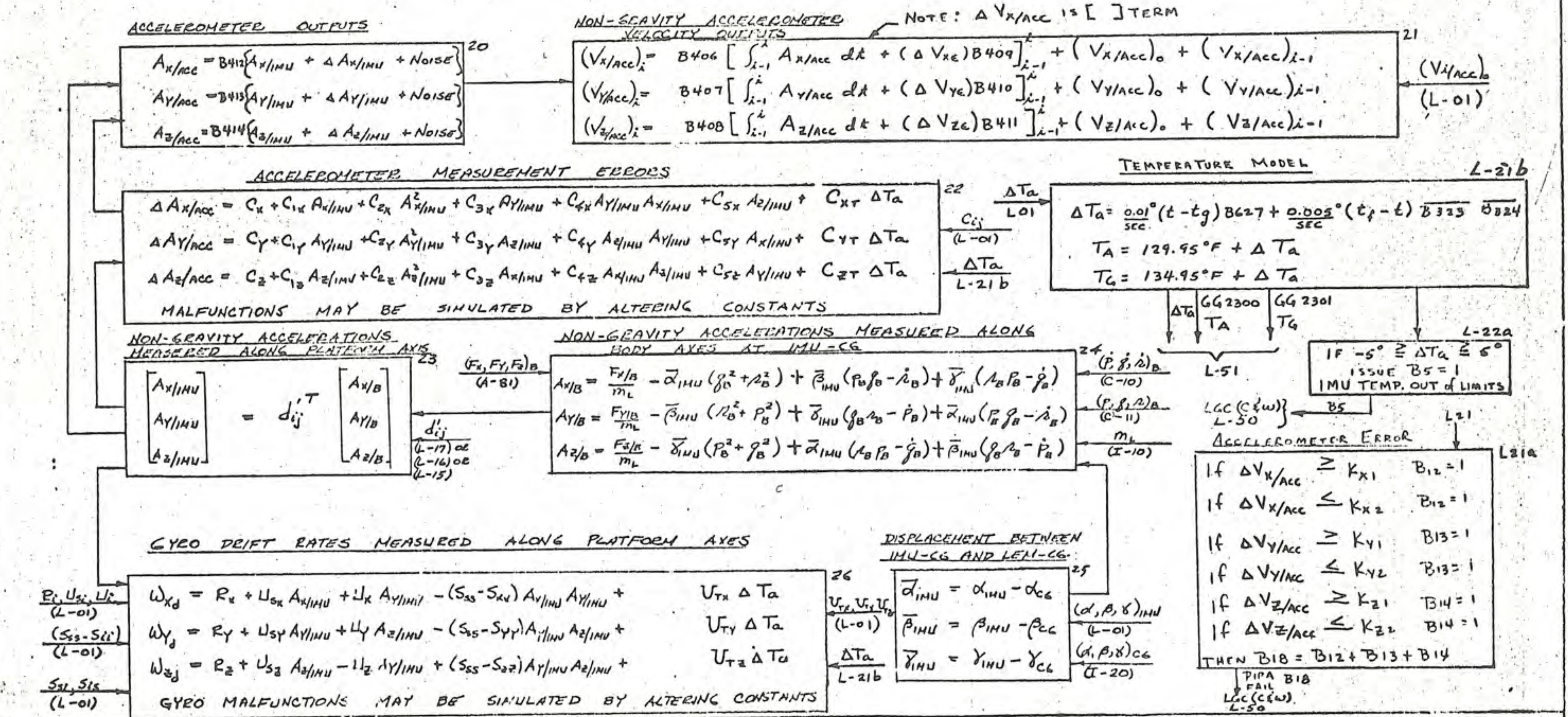

ACCELEROMETER OUTPUTS

20

$$A_{x/acc} = B412\{A_{x/IMU} + \Delta A_{x/IMU} + \text{Noise}\}$$
$$A_{y/acc} = B413\{A_{y/IMU} + \Delta A_{y/IMU} + \text{Noise}\}$$
$$A_{z/acc} = B414\{A_{z/IMU} + \Delta A_{z/IMU} + \text{Noise}\}$$

NON-GRAVITY ACCELEROMETER VELOCITY OUTPUTS

NOTE: $\Delta V_{x/acc}$ IS [ ] TERM

21

$$(V_{x/acc})_i = B406\left[\int_{i-1}^{i} A_{x/acc}\,dt + (\Delta V_{xe})B409\right]_{i-1}^{i} + (V_{x/acc})_0 + (V_{x/acc})_{i-1}$$
$$(V_{y/acc})_i = B407\left[\int_{i-1}^{i} A_{y/acc}\,dt + (\Delta V_{ye})B410\right]_{i-1}^{i} + (V_{y/acc})_0 + (V_{y/acc})_{i-1}$$
$$(V_{z/acc})_i = B408\left[\int_{i-1}^{i} A_{z/acc}\,dt + (\Delta V_{ze})B411\right]_{i-1}^{i} + (V_{z/acc})_0 + (V_{z/acc})_{i-1}$$

$\frac{(V_{i/acc})_0}{(L-01)}$

ACCELEROMETER MEASUREMENT ERRORS

22

$$\Delta A_{x/acc} = C_x + C_{1x}A_{x/IMU} + C_{2x}A^2_{x/IMU} + C_{3x}A_{y/IMU} + C_{4x}A_{y/IMU}A_{x/IMU} + C_{5x}A_{z/IMU} + C_{xT}\Delta T_a$$
$$\Delta A_{y/acc} = C_y + C_{1y}A_{y/IMU} + C_{2y}A^2_{y/IMU} + C_{3y}A_{z/IMU} + C_{4y}A_{z/IMU}A_{y/IMU} + C_{5y}A_{x/IMU} + C_{yT}\Delta T_a$$
$$\Delta A_{z/acc} = C_z + C_{1z}A_{z/IMU} + C_{2z}A^2_{z/IMU} + C_{3z}A_{x/IMU} + C_{4z}A_{x/IMU}A_{z/IMU} + C_{5z}A_{y/IMU} + C_{zT}\Delta T_a$$

MALFUNCTIONS MAY BE SIMULATED BY ALTERING CONSTANTS

$\frac{C_{ij}}{(L-01)}$

$\frac{\Delta T_a}{L-21b}$

$\frac{\Delta T_a}{L01}$

TEMPERATURE MODEL

L-21b

$$\Delta T_a = \frac{0.01^\circ}{sec}(t - t_g)B627 + \frac{0.005^\circ}{sec}(t_f - t)\overline{B323}\ \overline{B324}$$
$$T_A = 129.95^\circ F + \Delta T_a$$
$$T_G = 134.95^\circ F + \Delta T_a$$

ΔT_a

GG2300 T_A

GG2301 T_G

L-51

L-22a

IF $-5^\circ \geqq \Delta T_a \leqq 5^\circ$
ISSUE B5 = 1
IMU TEMP. OUT of LIMITS

B5

LGC (C&W)
L-50

NON-GRAVITY ACCELERATIONS MEASURED ALONG PLATFORM AXIS

23

$$\begin{bmatrix} A_{x/IMU} \\ A_{y/IMU} \\ A_{z/IMU} \end{bmatrix} = d'^{\,T}_{ij} \begin{bmatrix} A_{x/B} \\ A_{y/B} \\ A_{z/B} \end{bmatrix}$$

d'_{ij}
(L-17) or
(L-16) or
(L-15)

NON-GRAVITY ACCELERATIONS MEASURED ALONG BODY AXES AT IMU-CG

24

$\frac{(F_x, F_y, F_z)_B}{(A-81)}$

$$A_{x/B} = \frac{F_{x/B}}{m_L} - \bar{\alpha}_{IMU}(q_B^2 + r_B^2) + \bar{\beta}_{IMU}(p_B q_B - \dot{r}_B) + \bar{\gamma}_{IMU}(r_B p_B - \dot{q}_B)$$
$$A_{y/B} = \frac{F_{y/B}}{m_L} - \bar{\beta}_{IMU}(r_B^2 + p_B^2) + \bar{\gamma}_{IMU}(q_B r_B - \dot{p}_B) + \bar{\alpha}_{IMU}(p_B q_B - \dot{r}_B)$$
$$A_{z/B} = \frac{F_{z/B}}{m_L} - \bar{\gamma}_{IMU}(p_B^2 + q_B^2) + \bar{\alpha}_{IMU}(r_B p_B - \dot{q}_B) + \bar{\beta}_{IMU}(q_B r_B - \dot{p}_B)$$

$\frac{(\dot{p}, \dot{q}, \dot{r})_B}{(C-10)}$

$\frac{(p, q, r)_B}{(C-11)}$

$\frac{m_L}{(I-10)}$

ACCELEROMETER ERROR

L21

L21a

If $\Delta V_{x/acc} \geq K_{x1}$ $B_{12} = 1$

If $\Delta V_{x/acc} \leq K_{x2}$ $B_{12} = 1$

If $\Delta V_{y/acc} \geq K_{y1}$ $B13 = 1$

If $\Delta V_{y/acc} \leq K_{y2}$ $B13 = 1$

If $\Delta V_{z/acc} \geq K_{z1}$ $B14 = 1$

If $\Delta V_{z/acc} \leq K_{z2}$ $B14 = 1$

THEN $B18 = B12 + B13 + B14$

PIPA FAIL B18

LGC (C&W)
L-50

GYRO DRIFT RATES MEASURED ALONG PLATFORM AXES

26

$\frac{R_i, U_{si}, U_i}{(L-01)}$

$\frac{(S_{ss} - S_{ii})}{(L-01)}$

$\frac{S_{si}, S_{is}}{(L-01)}$

$$\omega_{x_d} = R_x + U_{sx}A_{x/IMU} + U_x A_{y/IMU} - (S_{ss} - S_{xx})A_{y/IMU}A_{y/IMU} + U_{Tx}\Delta T_a$$
$$\omega_{y_d} = R_y + U_{sy}A_{y/IMU} + U_y A_{z/IMU} - (S_{ss} - S_{yy})A_{y/IMU}A_{z/IMU} + U_{Ty}\Delta T_a$$
$$\omega_{z_d} = R_z + U_{sz}A_{z/IMU} - U_z A_{y/IMU} + (S_{ss} - S_{zz})A_{y/IMU}A_{z/IMU} + U_{Tz}\Delta T_a$$

GYRO MALFUNCTIONS MAY BE SIMULATED BY ALTERING CONSTANTS

$\frac{U_{Tx}, U_{Ty}, U_{Tz}}{(L-01)}$

$\frac{\Delta T_a}{L-21b}$

DISPLACEMENT BETWEEN IMU-CG AND LEM-CG

25

$$\bar{\alpha}_{IMU} = \alpha_{IMU} - \alpha_{CG}$$
$$\bar{\beta}_{IMU} = \beta_{IMU} - \beta_{CG}$$
$$\bar{\gamma}_{IMU} = \gamma_{IMU} - \gamma_{CG}$$

$\frac{(\alpha, \beta, \gamma)_{IMU}}{(L-01)}$

$\frac{(\alpha, \beta, \gamma)_{CG}}{(I-20)}$

AOT - COARSE AND FINE ALIGN MODES

30

	COARSE ALIGN ON COMMAND		
	IF:	THEN SLEW GIMBALS SEQUENTIALLY AT CONSTANT VELOCITY	UNTIL COARSE ALIGN ERRORS ARE REDUCED TO SOME PREDETERMINED VALUE:
$\frac{(\theta, \psi, \phi)_{ec}}{\text{DSKY OR Q35}}$	$\theta_{ec} \neq 0$	$\dot{\theta}_{ec}$	$\int \dot{\theta}_{ec}\,dt - \theta_{ec} \leqq \Delta\theta_{ec}$
$\frac{(\theta, \psi, \phi)_{ec}}{(L-01)}$	$\psi_{ec} \neq 0$	$\dot{\psi}_{ec}$	$\int \dot{\psi}_{ec}\,dt - \psi_{ec} \leqq \Delta\psi_{ec}$
$\frac{(\Delta\theta, \Delta\psi, \Delta\phi)_{ec}}{(L-01)}$	$\phi_{ec} \neq 0$	$\dot{\phi}_{ec}$	$\int \dot{\phi}_{ec} - \phi_{ec} \leqq \Delta\phi_{ec}$

31

	FINE ALIGN ON COMMAND		
	IF:	THEN DRIVE PLATFORM SEQUENTIALLY:	UNTIL FINE ALIGN ERROR ARE REDUCED TO SOME PREDETERMINED VALUE:
$\frac{(\theta, \psi, \phi)_{ef}}{(Q-35)}$	$\theta_{ef} \neq 0$	$\dot{\theta}_{ef}$	$\int \dot{\theta}_{ef}\,dt - \theta_{ef} \leqq \Delta\theta_{ef}$
$\frac{(\Delta\theta, \Delta\psi, \Delta\phi)_{ef}}{(L-01)}$	$\psi_{ef} \neq 0$	$\dot{\psi}_{ef}$	$\int \dot{\psi}_{ef}\,dt - \psi_{ef} \leqq \Delta\psi_{ef}$
	$\phi_{ef} \neq 0$	$\dot{\phi}_{ef}$	$\int \dot{\phi}_{ef}\,dt - \phi_{ef} \leqq \Delta\phi_{ef}$

L-12

11/65

IMU - LED-440-3 PART II SECTION 2-2.TRUE MOTION EQUATIONS (CONT)

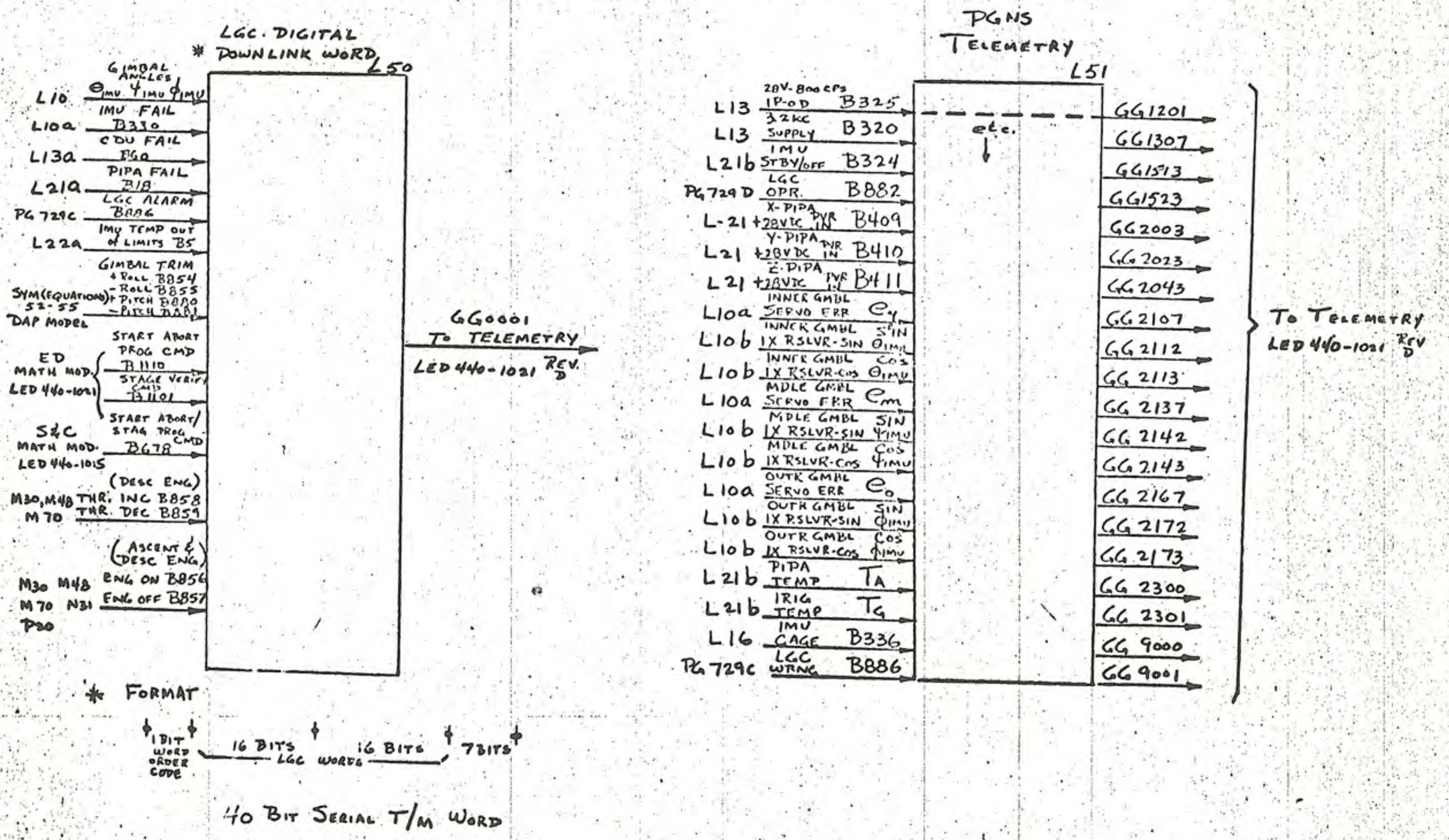

M - LGC SEPARATION TO TOUCHDOWN-PRIMARY

M-1

SHEET 1 OF 3

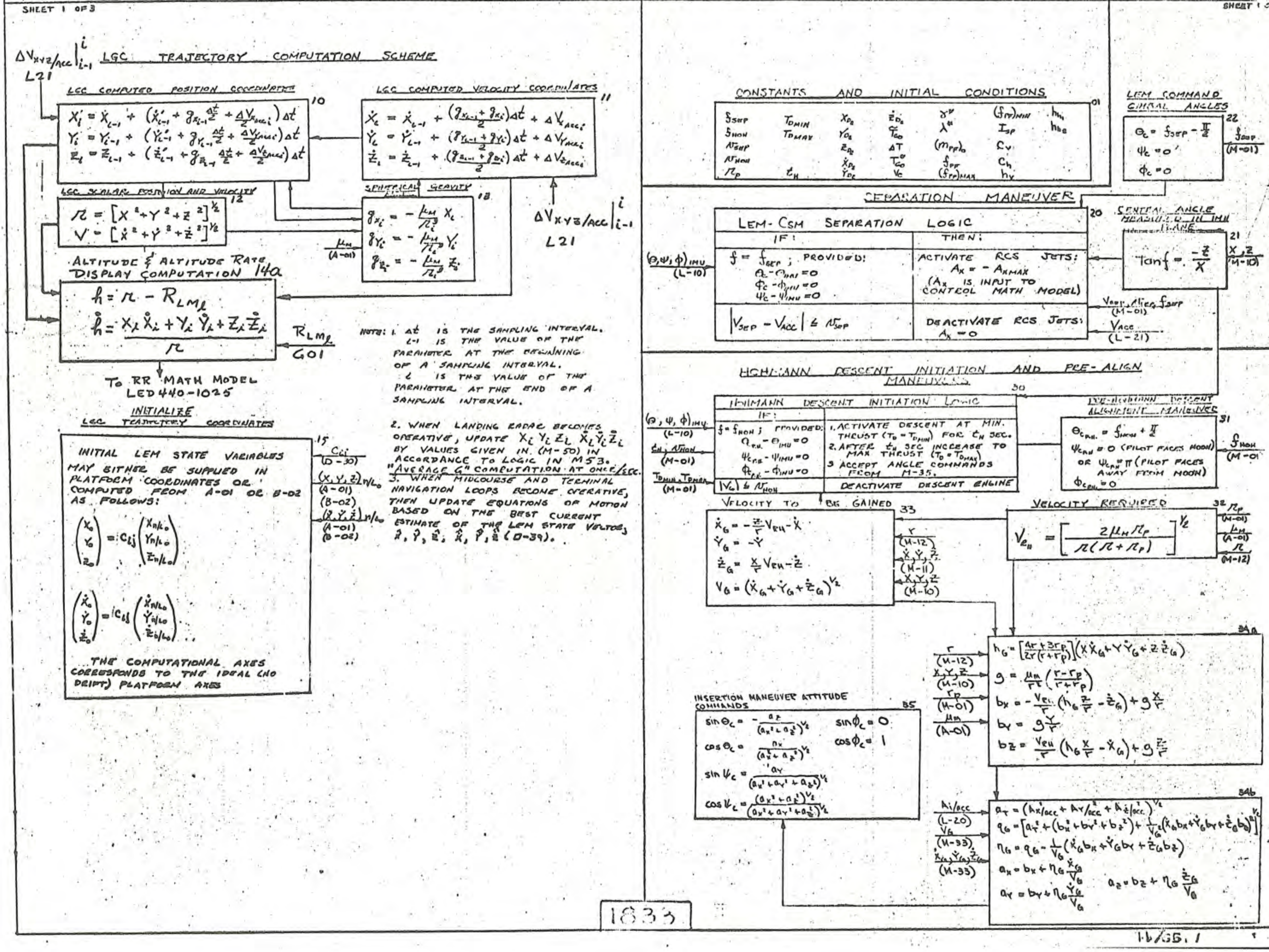

NOTE: 1. Δt IS THE SAMPLING INTERVAL.
$i-1$ IS THE VALUE OF THE PARAMETER AT THE BEGINNING OF A SAMPLING INTERVAL.
i IS THE VALUE OF THE PARAMETER AT THE END OF A SAMPLING INTERVAL.

2. WHEN LANDING RADAR BECOMES OPERATIVE, UPDATE $X_i\ Y_i\ Z_i\ \dot{X}_i\ \dot{Y}_i\ \dot{Z}_i$ BY VALUES GIVEN IN (M-50) IN ACCORDANCE TO LOGIC IN M53.
"AVERAGE G" COMPUTATION AT ONCE/SEC.

3. WHEN MIDCOURSE AND TERMINAL NAVIGATION LOOPS BECOME OPERATIVE, THEN UPDATE EQUATIONS OF MOTION BASED ON THE BEST CURRENT ESTIMATE OF THE LEM STATE VECTOR, $\hat{X}, \hat{Y}, \hat{Z}; \hat{\dot{X}}, \hat{\dot{Y}}, \hat{\dot{Z}}$ (D-39).

1833

M - LGC SEPARATION TO TOUCHDOWN-PRIMARY M

SHEET 2 OF 3

SHEET 2 OF 3

PRIMARY GUIDANCE LAWS FOR PHASE 1 AND 2 POWERED DESCENT

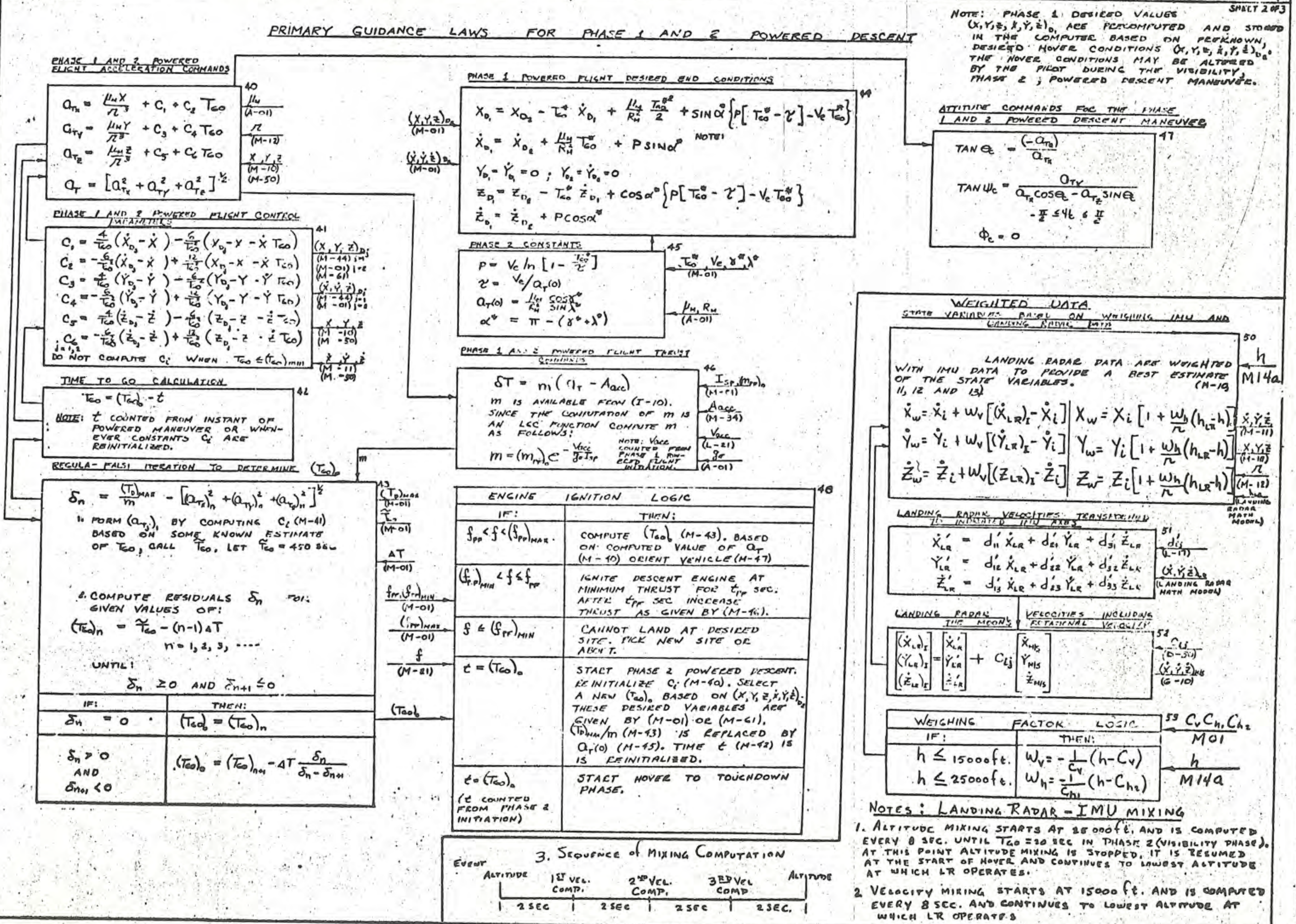

NOTE: PHASE 1 DESIRED VALUES $(X,Y,Z,\dot{X},\dot{Y},\dot{Z})_{D_1}$ ARE PRECOMPUTED AND STORED IN THE COMPUTER BASED ON PREKNOWN, DESIRED HOVER CONDITIONS $(X,Y,Z,\dot{X},\dot{Y},\dot{Z})_{D_2}$. THE HOVER CONDITIONS MAY BE ALTERED BY THE PILOT DURING THE VISIBILITY, PHASE 2 ; POWERED DESCENT MANEUVER.

PHASE 1 AND 2 POWERED FLIGHT ACCELERATION COMMANDS

40

$$a_{T_X} = \frac{\mu_M X}{r^3} + C_1 + C_2 T_{GO}$$
$$a_{T_Y} = \frac{\mu_M Y}{r^3} + C_3 + C_4 T_{GO}$$
$$a_{T_Z} = \frac{\mu_M Z}{r^3} + C_5 + C_6 T_{GO}$$
$$a_T = \left[a_{T_X}^2 + a_{T_Y}^2 + a_{T_Z}^2\right]^{1/2}$$

$\frac{\mu_M}{(A-01)}$ $\frac{r}{(M-12)}$ $\frac{X,Y,Z}{(M-10)\,(M-50)}$

PHASE 1 AND 2 POWERED FLIGHT CONTROL PARAMETERS

41

$$C_1 = \frac{4}{T_{GO}}(\dot{X}_{D_j} - \dot{X}) - \frac{6}{T_{GO}^2}(X_{D_j} - X - \dot{X}T_{GO})$$
$$C_2 = -\frac{6}{T_{GO}^2}(\dot{X}_{D_j} - \dot{X}) + \frac{12}{T_{GO}^3}(X_{D_j} - X - \dot{X}T_{GO})$$
$$C_3 = \frac{4}{T_{GO}}(\dot{Y}_{D_j} - \dot{Y}) - \frac{6}{T_{GO}^2}(Y_{D_j} - Y - \dot{Y}T_{GO})$$
$$C_4 = -\frac{6}{T_{GO}^2}(\dot{Y}_{D_j} - \dot{Y}) + \frac{12}{T_{GO}^3}(Y_{D_j} - Y - \dot{Y}T_{GO})$$
$$C_5 = \frac{4}{T_{GO}}(\dot{Z}_{D_j} - \dot{Z}) - \frac{6}{T_{GO}^2}(Z_{D_j} - Z - \dot{Z}T_{GO})$$
$$C_6 = -\frac{6}{T_{GO}^2}(\dot{Z}_{D_j} - \dot{Z}) + \frac{12}{T_{GO}^3}(Z_{D_j} - Z - \dot{Z}T_{GO})$$

$j = 1, 2$

DO NOT COMPUTE C_i WHEN $T_{GO} \le (T_{GO})_{MIN}$

$\frac{(X,Y,Z)_{D_j}}{(M-44)\,j=1 \quad (M-01)\,j=2 \quad (M-61)}$ $\frac{(\dot{X},\dot{Y},\dot{Z})_{D_j}}{(M-44)\,j=1 \quad (M-01)\,j=2}$ $\frac{X,Y,Z}{(M-10)\,(M-50)}$ $\frac{\dot{X},\dot{Y},\dot{Z}}{(M-11)\,(M-50)}$

TIME TO GO CALCULATION

42

$$T_{GO} = (T_{GO})_0 - t$$

NOTE: t COUNTED FROM INSTANT OF POWERED MANEUVER OR WHENEVER CONSTANTS C_i ARE REINITIALIZED.

REGULA-FALSI ITERATION TO DETERMINE $(T_{GO})_0$

43

$$\delta_n = \frac{(T_D)_{MAX}}{m} - \left[(a_{T_X})_n^2 + (a_{T_Y})_n^2 + (a_{T_Z})_n^2\right]^{1/2}$$

1. FORM $(a_{T_j})_1$ BY COMPUTING C_i (M-41) BASED ON SOME KNOWN ESTIMATE OF T_{GO}, CALL $\tilde{T}_{GO}$, LET $\tilde{T}_{GO} = 450$ SEC

2. COMPUTE RESIDUALS δ_n FOR GIVEN VALUES OF:

$$(T_{GO})_n = \tilde{T}_{GO} - (n-1)\Delta T$$
$$n = 1, 2, 3, \cdots$$

UNTIL:

$$\delta_n \ge 0 \text{ AND } \delta_{n+1} \le 0$$

IF:	THEN:
$\delta_n = 0$	$(T_{GO})_0 = (T_{GO})_n$
$\delta_n > 0$ AND $\delta_{n+1} < 0$	$(T_{GO})_0 = (T_{GO})_{n+1} - \Delta T \frac{\delta_n}{\delta_n - \delta_{n+1}}$

$\frac{(T_D)_{MAX}}{(M-01)}$ $\frac{\tilde{T}_{GO}}{(M-01)}$ $\frac{\Delta T}{(M-01)}$ m $(T_{GO})_0$

PHASE 1 POWERED FLIGHT DESIRED END CONDITIONS

44

$$X_{D_1} = X_{D_2} - T_{GO}^{*}\dot{X}_{D_1} + \frac{\mu_M}{R_M^2}\frac{T_{GO}^{*2}}{2} + \sin\alpha^{*}\left\{P\left[T_{GO}^{*} - \tau\right] - V_e T_{GO}^{*}\right\}$$
$$\dot{X}_{D_1} = \dot{X}_{D_2} + \frac{\mu_M}{R_M^2}T_{GO}^{*} + P\sin\alpha^{*}$$
$$Y_{D_1} = \dot{Y}_{D_1} = 0 \;;\; Y_{D_2} = \dot{Y}_{D_2} = 0$$
$$Z_{D_1} = Z_{D_2} - T_{GO}^{*}\dot{Z}_{D_1} + \cos\alpha^{*}\left\{P\left[T_{GO}^{*} - \tau\right] - V_e T_{GO}^{*}\right\}$$
$$\dot{Z}_{D_1} = \dot{Z}_{D_2} + P\cos\alpha^{*}$$

NOTE1

$\frac{(X,Y,Z)_{D_2}}{(M-01)}$ $\frac{(\dot{X},\dot{Y},\dot{Z})_{D_2}}{(M-01)}$

PHASE 2 CONSTANTS

45

$$P = V_e \ln\left[1 - \frac{T_{GO}^{*}}{\tau}\right]$$
$$\tau = V_e / a_T(0)$$
$$a_T(0) = \frac{\mu_M}{R_M^2}\frac{\cos\gamma^{*}}{\sin\lambda^{*}}$$
$$\alpha^{*} = \pi - (\gamma^{*} + \lambda^{*})$$

$\frac{T_{GO}^{*},\, V_e,\, \gamma^{*},\, \lambda^{*}}{(M-01)}$ $\frac{\mu_M, R_M}{(A-01)}$

PHASE 1 AND 2 POWERED FLIGHT THRUST COMMANDS

46

$$\delta T = m(a_T - A_{acc})$$

m IS AVAILABLE FROM (I-10). SINCE THE COMPUTATION OF m IS AN LGC FUNCTION COMPUTE m AS FOLLOWS:

$$m = (m_{PP})_0 e^{-\frac{V_{acc}}{g_0 I_{SP}}}$$

NOTE: V_{acc} COUNTED FROM PHASE 1 POWERED FLIGHT INITIATION.

$\frac{I_{SP}, (m_{PP})_0}{(M-01)}$ $\frac{A_{acc}}{(M-34)}$ $\frac{V_{acc}}{(L-21)}$ $\frac{g_0}{(A-01)}$

ATTITUDE COMMANDS FOR THE PHASE 1 AND 2 POWERED DESCENT MANEUVER

47

$$\tan\theta_c = \frac{(-a_{T_Z})}{a_{T_X}}$$
$$\tan\psi_c = \frac{a_{T_Y}}{a_{T_X}\cos\theta_c - a_{T_Z}\sin\theta_c}$$
$$-\frac{\pi}{2} \le \psi_c \le \frac{\pi}{2}$$
$$\phi_c = 0$$

48

ENGINE IGNITION LOGIC

IF:	THEN:
$f_{PP} < f < (f_{PP})_{MAX}$	COMPUTE $(T_{GO})_0$ (M-43). BASED ON COMPUTED VALUE OF a_T (M-40) ORIENT VEHICLE (M-47)
$(f_{PP})_{MIN} < f \le f_{PP}$	IGNITE DESCENT ENGINE AT MINIMUM THRUST FOR t_{PP} SEC. AFTER t_{PP} SEC INCREASE THRUST AS GIVEN BY (M-46).
$f \le (f_{PP})_{MIN}$	CANNOT LAND AT DESIRED SITE. PICK NEW SITE OR ABORT.
$t = (T_{GO})_0$	START PHASE 2 POWERED DESCENT. REINITIALIZE C_i (M-40). SELECT A NEW $(T_{GO})_0$ BASED ON $(X,Y,Z,\dot{X},\dot{Y},\dot{Z})_{D_2}$. THESE DESIRED VARIABLES ARE GIVEN BY (M-01) OR (M-61). $(T_D)_{MAX}/m$ (M-43) IS REPLACED BY $a_T(0)$ (M-45). TIME t (M-42) IS IS REINITIALIZED.
$t = (T_{GO})_0$ (t COUNTED FROM PHASE 2 INITIATION)	START HOVER TO TOUCHDOWN PHASE.

$\frac{f_{PP}, (f_{PP})_{MIN}}{(M-01)}$ $\frac{(f_{PP})_{MAX}}{(M-01)}$ $\frac{f}{(M-21)}$ $(T_{GO})_0$

WEIGHTED DATA

STATE VARIABLES BASED ON WEIGHING IMU AND LANDING RADAR DATA

50

LANDING RADAR DATA ARE WEIGHTED WITH IMU DATA TO PROVIDE A BEST ESTIMATE OF THE STATE VARIABLES. (M-10, 11, 12 AND 13)

$$\dot{X}_w = \dot{X}_i + W_v\left[(\dot{X}_{LR})_I - \dot{X}_i\right] \quad X_w = X_i\left[1 + \frac{W_h}{r}(h_{LR} - h)\right]$$
$$\dot{Y}_w = \dot{Y}_i + W_v\left[(\dot{Y}_{LR})_I - \dot{Y}_i\right] \quad Y_w = Y_i\left[1 + \frac{W_h}{r}(h_{LR} - h)\right]$$
$$\dot{Z}_w = \dot{Z}_i + W_v\left[(Z_{LR})_I - \dot{Z}_i\right] \quad Z_w = Z_i\left[1 + \frac{W_h}{r}(h_{LR} - h)\right]$$

$\frac{h}{M14a}$ $\frac{\dot{X},\dot{Y},\dot{Z}}{(M-11)}$ $\frac{X,Y,Z}{(M-10)}$ $\frac{r}{(M-12)}$ h_{LR} (LANDING RADAR MATH MODEL)

LANDING RADAR VELOCITIES TRANSFORMED TO INDICATED IMU AXES

51

$$\dot{X}_{LR}' = d_{11}'\dot{X}_{LR} + d_{21}'\dot{Y}_{LR} + d_{31}'\dot{Z}_{LR}$$
$$\dot{Y}_{LR}' = d_{12}'\dot{X}_{LR} + d_{22}'\dot{Y}_{LR} + d_{32}'\dot{Z}_{LR}$$
$$\dot{Z}_{LR}' = d_{13}'\dot{X}_{LR} + d_{23}'\dot{Y}_{LR} + d_{33}'\dot{Z}_{LR}$$

$\frac{d_{ij}'}{(L-17)}$ $(\dot{X},\dot{Y},\dot{Z})_{LR}$ (LANDING RADAR MATH MODEL)

LANDING RADAR VELOCITIES INCLUDING THE MOON'S ROTATIONAL VELOCITY

52

$$\begin{bmatrix}(\dot{X}_{LR})_I\\(\dot{Y}_{LR})_I\\(\dot{Z}_{LR})_I\end{bmatrix} = \begin{bmatrix}\dot{X}_{LR}'\\\dot{Y}_{LR}'\\\dot{Z}_{LR}'\end{bmatrix} + C_{ij}\begin{bmatrix}\dot{X}_{MIS}\\\dot{Y}_{MIS}\\\dot{Z}_{MIS}\end{bmatrix}$$

$\frac{C_{ij}}{(D-50)}$ $\frac{(\dot{X},\dot{Y},\dot{Z})_{MS}}{(G-10)}$

53

WEIGHING FACTOR LOGIC

IF:	THEN:
$h \le 15000$ ft.	$W_v = -\frac{1}{C_v}(h - C_v)$
$h \le 25000$ ft.	$W_h = \frac{-1}{C_{h_1}}(h - C_{h_2})$

$\frac{C_v C_{h_1} C_{h_2}}{M01}$ $\frac{h}{M14a}$

NOTES: LANDING RADAR - IMU MIXING

1. ALTITUDE MIXING STARTS AT 25 000 ft. AND IS COMPUTED EVERY 8 SEC. UNTIL T_{GO} = 30 SEC IN PHASE 2 (VISIBILITY PHASE). AT THIS POINT ALTITUDE MIXING IS STOPPED. IT IS RESUMED AT THE START OF HOVER AND CONTINUES TO LOWEST ALTITUDE AT WHICH LR OPERATES.
2. VELOCITY MIXING STARTS AT 15000 ft. AND IS COMPUTED EVERY 8 SEC. AND CONTINUES TO LOWEST ALTITUDE AT WHICH LR OPERATES

3. SEQUENCE of MIXING COMPUTATION

M - LGC SEPARATION TO TOUCHDOWN-PRIMARY

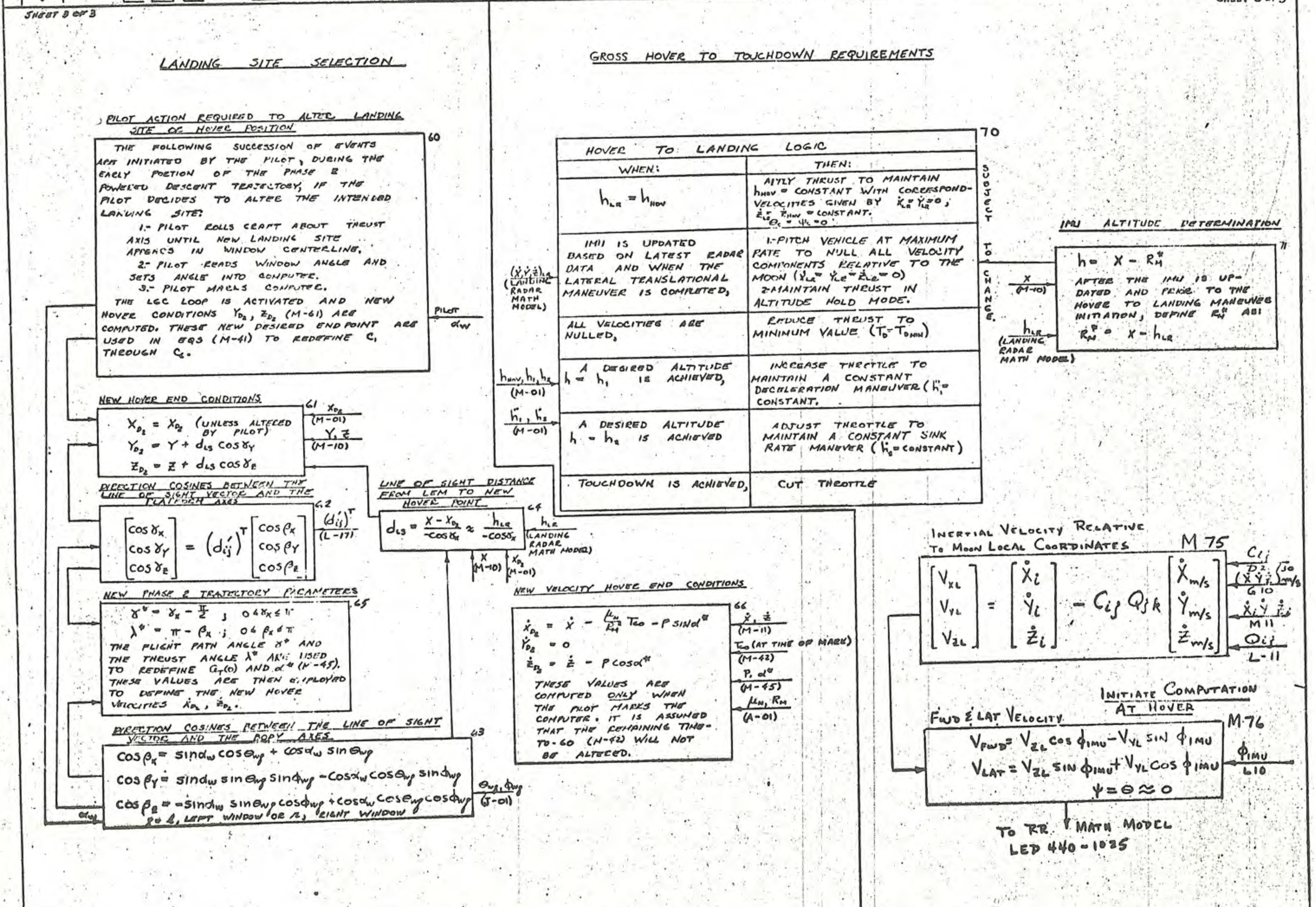

LANDING SITE SELECTION

PILOT ACTION REQUIRED TO ALTER LANDING SITE OF HOVER POSITION

THE FOLLOWING SUCCESSION OF EVENTS ARE INITIATED BY THE PILOT, DURING THE EARLY PORTION OF THE PHASE 2 POWERED DESCENT TRAJECTORY, IF THE PILOT DECIDES TO ALTER THE INTENDED LANDING SITE:

1.- PILOT ROLLS CRAFT ABOUT THRUST AXIS UNTIL NEW LANDING SITE APPEARS IN WINDOW CENTERLINE.

2.- PILOT READS WINDOW ANGLE AND SETS ANGLE INTO COMPUTER.

3.- PILOT MARKS COMPUTER.

THE LGC LOOP IS ACTIVATED AND NEW HOVER CONDITIONS Y_{D_2}, Z_{D_2} (M-61) ARE COMPUTED. THESE NEW DESIRED END POINT ARE USED IN EQS (M-41) TO REDEFINE C_1 THROUGH C_6.

NEW HOVER END CONDITIONS

$$X_{D_2} = X_{D_2} \quad \text{(UNLESS ALTERED BY PILOT)}$$
$$Y_{D_2} = Y + d_{LS}\cos\gamma_Y$$
$$Z_{D_2} = Z + d_{LS}\cos\gamma_Z$$

DIRECTION COSINES BETWEEN THE LINE OF SIGHT VECTOR AND THE PLATFORM AXES

$$\begin{bmatrix}\cos\gamma_X\\ \cos\gamma_Y\\ \cos\gamma_Z\end{bmatrix} = \left(d_{ij}'\right)^T \begin{bmatrix}\cos\beta_X\\ \cos\beta_Y\\ \cos\beta_Z\end{bmatrix}$$

NEW PHASE 2 TRAJECTORY PARAMETERS

$$\gamma^* = \gamma_X - \frac{\pi}{2} \;;\quad 0 \le \gamma_X \le \pi$$
$$\lambda^* = \pi - \beta_X \;;\quad 0 \le \beta_X \le \pi$$

THE FLIGHT PATH ANGLE γ^* AND THE THRUST ANGLE λ^* ARE USED TO REDEFINE $G_T(0)$ AND α^* (M-45). THESE VALUES ARE THEN EMPLOYED TO DEFINE THE NEW HOVER VELOCITIES $\dot{X}_{D_2}$, $\dot{Z}_{D_2}$.

DIRECTION COSINES BETWEEN THE LINE OF SIGHT VECTOR AND THE BODY AXES

$$\cos\beta_X = \sin\alpha_w\cos\theta_{wp} + \cos\alpha_w\sin\theta_{wp}$$
$$\cos\beta_Y = \sin\alpha_w\sin\theta_{wp}\sin\phi_{wp} - \cos\alpha_w\cos\theta_{wp}\sin\phi_{wp}$$
$$\cos\beta_Z = -\sin\alpha_w\sin\theta_{wp}\cos\phi_{wp} + \cos\alpha_w\cos\theta_{wp}\cos\phi_{wp}$$

$p = L$, LEFT WINDOW OR R, RIGHT WINDOW

LINE OF SIGHT DISTANCE FROM LEM TO NEW HOVER POINT

$$d_{LS} = \frac{X - X_{D_2}}{-\cos\gamma_X} \approx \frac{h_{LR}}{-\cos\gamma_X}$$

NEW VELOCITY HOVER END CONDITIONS

$$\dot{X}_{D_2} = \dot{X} - \frac{\mu_M}{R_M^2}T_{GO} - P\sin\alpha^*$$
$$\dot{Y}_{D_2} = 0$$
$$\dot{Z}_{D_2} = \dot{Z} - P\cos\alpha^*$$

THESE VALUES ARE COMPUTED ONLY WHEN THE PILOT MARKS THE COMPUTER. IT IS ASSUMED THAT THE REMAINING TIME-TO-GO (M-42) WILL NOT BE ALTERED.

GROSS HOVER TO TOUCHDOWN REQUIREMENTS

HOVER TO LANDING LOGIC

WHEN:	THEN:
$h_{LR} = h_{HOV}$	APPLY THRUST TO MAINTAIN h_{HOV} = CONSTANT WITH CORRESPONDING VELOCITIES GIVEN BY $\dot{X}_{LR} = \dot{Y}_{LR} = 0$; $\dot{Z}_{LR} = \dot{Z}_{HOV}$ = CONSTANT. $\theta_c = \psi_c = 0$
IMU IS UPDATED BASED ON LATEST RADAR DATA AND WHEN THE LATERAL TRANSLATIONAL MANEUVER IS COMPLETED,	1.-PITCH VEHICLE AT MAXIMUM RATE TO NULL ALL VELOCITY COMPONENTS RELATIVE TO THE MOON ($\dot{X}_{LR} = \dot{Y}_{LR} = \dot{Z}_{LR} = 0$) 2-MAINTAIN THRUST IN ALTITUDE HOLD MODE.
ALL VELOCITIES ARE NULLED,	REDUCE THRUST TO MINIMUM VALUE ($T_D = T_{DMIN}$)
A DESIRED ALTITUDE $h = h_1$ IS ACHIEVED,	INCREASE THROTTLE TO MAINTAIN A CONSTANT DECELERATION MANEUVER ($\ddot{h}_1$ = CONSTANT.
A DESIRED ALTITUDE $h = h_2$ IS ACHIEVED	ADJUST THROTTLE TO MAINTAIN A CONSTANT SINK RATE MANEUVER ($\dot{h}_2$ = CONSTANT)
TOUCHDOWN IS ACHIEVED,	CUT THROTTLE

IMU ALTITUDE DETERMINATION

$$h = X - R_M^*$$

AFTER THE IMU IS UPDATED AND PRIOR TO THE HOVER TO LANDING MANEUVER INITIATION, DEFINE R_M^* AS

$$R_M^* = X - h_{LR}$$

INERTIAL VELOCITY RELATIVE TO MOON LOCAL COORDINATES

$$\begin{bmatrix}V_{XL}\\ V_{YL}\\ V_{ZL}\end{bmatrix} = \begin{bmatrix}\dot{X}_i\\ \dot{Y}_i\\ \dot{Z}_i\end{bmatrix} - C_{ij}\,Q_{jk}\begin{bmatrix}\dot{X}_{m/s}\\ \dot{Y}_{m/s}\\ \dot{Z}_{m/s}\end{bmatrix}$$

FWD & LAT VELOCITY

INITIATE COMPUTATION AT HOVER

$$V_{FWD} = V_{ZL}\cos\phi_{IMU} - V_{YL}\sin\phi_{IMU}$$
$$V_{LAT} = V_{ZL}\sin\phi_{IMU} + V_{YL}\cos\phi_{IMU}$$
$$\psi = \theta \approx 0$$

TO RR. MATH MODEL LED 440-1035

N-LGC ASCENT TO RENDEZVOUS - PRIMARY N

SHEET 1 OF 6

SHEET 1 OF 5

PRE-LAUNCH COMPUTATIONS

PROBLEM INITIALIZATION

10

$\frac{R_M^*}{(M-71)}$

$\frac{\phi_{s/L}, \lambda_{s/L}}{(N-01)}$

$\frac{a_{ij}^T}{(D-10)}$

$\frac{C_{ij}}{(D-30)}$

1. THE CSM ORBIT HAS BEEN DETERMINED. STATE VECTORS $\bar{r}_{MK_0}, \dot{\bar{r}}_{MK_0}$ ARE KNOWN AT SOME EPOCH CALL d_0 (E-01).

2. THE TAKE-OFF SIGHT IS ACCURATELY KNOWN IN SELENOGRAPHIC COORDINATES:

$$\bar{r}_{S/LO} = R_M^* \left[\cos\phi_{s/L} \cos\lambda_{s/L} \hat{i}_s + \cos\phi_{s/L} \sin\lambda_{s/L} \hat{j}_s + \sin\phi_{s/L} \hat{k}_s \right]$$

THUS THE LIFT-OFF VECTOR, AT ANY TIME, IN M-FRAME COORDINATES IS:

$$\bar{r}_{L/LO} = a_{ij}^T \bar{r}_{S/LO}$$

3. IF IT IS DESIRED TO COMPUTE ALL PRE-LAUNCH OPERATIONS IN THE LANDING IMU FRAME, THEN THE FOLLOWING TRANSFORMATION IS APPROPRIATE:

$$\bar{r}_{IMU} = C_{ij_{OLD}} \bar{r}_{M_0}$$

TIME AND CENTRAL ANGLE MEASURED FROM CSM AT EPOCH TO CSM AT LEM LIFT OFF

12

$\frac{U_0', \Delta U}{(N-01)}$

$\frac{j_{MAX}}{(N-01)}$

$\frac{\Delta t_{BO}}{(N-01)}$

1. SELECT A LEAD ANGLE MEASURED IN THE CSM PLANE FROM THE PROJECTION OF THE LAUNCH SITE, AT EPOCH, TO THE CSM AT LIFT-OFF:

$$U_j' = U_0' \mp j\Delta U \quad ; \quad j = 0, 1, 2, \cdots j_{MAX}$$

2. COMPUTE THE CSM ECCENTRIC ANOMALY FROM REFERENCE TO CSM AT LEM LIFT-OFF:

$$\tan\frac{E_{LO_j}}{2} = \sqrt{\frac{1-e_c}{1+e_c}} \tan\frac{f_{co} + (f_{LO})_0 + U_j'}{2}$$

3. COMPUTE TIME MEASURED FROM CSM AT EPOCH TO CSM AT LEM LIFT-OFF.

a) ENTER B-25, LET:

$E = E_{LO_j} + n2\pi$

$E_0 = E_{CO}$

b) SOLVE FOR $t_{c_{LO}}$. NOTE THAT

n IS THE INTEGER VALUE OF THE QUOTIENT:

$$\frac{f_{co} + (f_{LO})_0 + U_j'}{2\pi}$$

4. COMPUTE THE ACTUAL LEM LIFT-OFF VECTOR AND LEAD ANGLE U_j: (DURING TIME $t_{c_{LO_j}}$ THE LAUNCH SITE MOVES FROM THE EPOCH POSITION TO THE TAKE OFF POSITION. THIS MOTION IS REFLECTED IN a_{ij}^T AND HENCE $\bar{r}_{L/LO}$ (SEE N-10)).

$$\tan f_{LO_j} = \frac{\bar{r}_{L/LO_j} \times \hat{h}_c \cdot \bar{r}_{MK_0}}{\hat{h}_c \times (\bar{r}_{L/LO_j} \times \hat{h}_c) \cdot \bar{r}_{MK_0}}$$

$$U_j = U_j' - [f_{LO_j} - (f_{LO})_0]$$

4. COMPUTE THE CSM POSITION AT LEM BURNOUT:

a) $t_{c_{BO_j}} = t_{c_{LO_j}} + \Delta t_{BO}$

b) ENTER LOOP B-25. ITERATE FOR $E - E_0$

c) $E_{c_{BO_j}} = (E - E_0) + E_{c_0}$

d) $\tan\frac{f_{BO_j}}{2} = \sqrt{\frac{1+e_c}{1-e_c}} \tan\frac{E_{c_{BO_j}}}{2}$

INITIALIZATION OF PERTINENT CSM PARAMETERS

$\bar{r}_{MK_0}$, $\dot{\bar{r}}_{MK_0}$ $(\bar{r}_{L/L})$

11

$\frac{(H_x, H_y, H_z)_{MC}}{(B-22)}$

$\frac{H_{MC}}{(B-24)}$

$\frac{\mu_M}{(A-01)}$

$\frac{a_c}{(B-25)}$

1. BASED ON (B-22) AND (B-24) DEFINE:

$$\hat{h}_c = h_{x_c} \hat{i}_M + h_{y_c} \hat{j}_M + h_{z_c} \hat{k}_M$$

$$h_{x_c} = \frac{H_{x_{MC}}}{H_{MC}} \; ; \; h_{y_c} = \frac{H_{y_{MC}}}{H_{MC}} \; ; \; h_{z_c} = \frac{H_{z_{MC}}}{H_{MC}}$$

2. DEFINE CSM INCLINATION:

$$\cos i_c = h_{z_c} \qquad 0 \le i_c \le \pi$$

3. DEFINE DIRECTION OF ASCENDING NODE AND RIGHT ASCENSION OF ASCENDING NODE:

$$\hat{N}_c = \frac{\hat{k}_M \times \hat{h}_c}{\sin i_c}$$

IF: $i_c = 0$ THEN: $\hat{N}_c = \hat{i}_M$

IF: $i_c = \pi$ THEN: $\hat{N}_c = -\hat{i}_M$

$$\tan\Omega_c = \frac{(\hat{N}_c \times \hat{k}_M) \cdot \hat{i}_M}{\hat{N}_c \cdot \hat{i}_M}$$

4. COMPUTE CSM ECCENTRICITY:

$$e_c = \left[1 - \frac{H_{MC}^2}{\mu_M a_c}\right]^{1/2}$$

5. COMPUTE CSM ECCENTRIC ANOMALY AND TRUE ANOMALY AT EPOCH:

a) ENTER (B-25) WITH $t = E = 0$

b) SOLVE FOR E_{c_0}

c) THEN

$$\tan\frac{f_{c_0}}{2} = \sqrt{\frac{1+e_c}{1-e_c}} \tan\frac{E_{c_0}}{2}$$

6. COMPUTE THE CENTRAL ANGLE FROM $\bar{r}_{MK_0}$ AT EPOCH TO THE PROJECTION OF THE TAKE-OFF SITE, AT EPOCH, INTO THE CSM PLANE:

$$\tan(f_{LO})_0 = \frac{(\bar{r}_{L/LO})_0 \times \hat{h}_c \cdot \bar{r}_{MK_0}}{\hat{h}_c \times ((\bar{r}_{L/LO})_0 \times \hat{h}_c) \cdot \bar{r}_{MK_0}}$$

TIME OF FLIGHT FROM LEM BURNOUT TO LEM-CSM INTERCEPT AND CSM STATE VECTORS AT INTERCEPT

13

$\frac{\Phi_{ff_0}, \Delta\Phi_{ff}}{(N-01)}$

$\frac{\ell_{MAX}}{(N-01)}$

1. SELECT A CENTRAL ANGLE MEASURED FROM THE CSM AT LEM BURNOUT TO THE CSM AT INTERCEPT:

$$\Phi_{ff_\ell} = \Phi_{ff_0} \mp \ell\Delta\Phi_{ff} \quad ; \; \ell = 0, 1, 2, - \ell_{MAX}$$

2. COMPUTE THE CSM ECCENTRIC ANOMALY FROM REFERENCE TO INTERCEPT:

$$\tan\frac{E_I}{2} = \sqrt{\frac{1-e_c}{1+e_c}} \tan\frac{f_{BO_j} + f_{co} + \Phi_{ff_\ell}}{2}$$

3. COMPUTE FREE FLIGHT TIME FOR LAMBERT EQ:

a) ENTER B-25, LET

$E = E_I + n2\pi$

$E_0 = E_{c_0}$

n = INTEGER VALUE OF $\frac{f_{BO_j} + f_{co} + \Phi_{ff_\ell}}{2\pi}$

b) SOLVE FOR $t_{c/I}$

$$t_{ff} = t_{c/I} - t_{c_{BO}}$$

4 COMPUTE CSM STATE VECTOR AT INTERCEPT

a) ENTER LOOP B-20 WITH $t = t_{c/I}$ AND $\bar{r}_{MK_0}$, $\dot{\bar{r}}_{MK_0}$

b) SOLVE FOR $\dot{\bar{r}}_{c/I}$, $\bar{r}_{c/I}$.

N-LGC ASCENT TO RENDEZVOUS - PRIMARY N

SHEET 2 OF 5

PRE-LAUNCH COMPUTATIONS - CONTINUED

LEM BURNOUT VECTOR

14

A DECISION HAS NOT BEEN REACHED WHETHER TO PROGRAM:

1) A THREE DIMENSIONAL ASCENT STEERING LOOP TO FORCE LEM BURNOUT IN THE CSM PLANE.

2) AN ASCENT STEERING THAT FORCES BURNOUT IN A GREAT CIRCLE PLANE DEFINED BY $\bar{r}_{L/LO}$ AND $\bar{r}_{C/I}$

LEM BURNOUT VECTOR COMPUTATIONS FOR EACH CASE ARE GIVEN:

I THREE DIMENSIONAL STEERING

1. DETERMINE THE CENTRAL ANGLE FROM THE NODE TO THE PROJECTION OF THE TAKE-OFF SITE AT LIFT-OFF:

$$\text{TAN } u_{L/LO} = \frac{\hat{N}_c \cdot (\bar{r}_{L/LO} \times \hat{h}_c)}{\hat{N}_c \cdot [\hat{h}_c \times (\bar{r}_{L/LO} \times \hat{h}_c)]}$$

2. COMPUTE THE CENTRAL ANGLE FROM THE NODE TO LEM BURNOUT:

$$u_{L/BO} = u_{L/LO} + \theta_{L/BO}$$

3. COMPUTE LEM BURNOUT VECTOR:

$$\bar{r}_{L/BO} = (R_M^* + h_{BO}) \Big[(\cos\Omega_c \cos u_{L/BO} - \sin\Omega_c \cos i_c \sin u_{L/BO}) \hat{i}_M + (\sin\Omega_c \cos u_{L/BO} + \cos\Omega_c \cos i_c \sin u_{L/BO}) \hat{j}_M + \sin i_c \sin u_{L/BO} \hat{k}_M \Big]$$

4. COMPUTE LEM FREE FLIGHT ANGLE:

$$\phi_{ff} = \Phi_{ff_k} + (f_{BO} - f_{LO}) - \theta_{L/BO}$$

II GREAT CIRCLE STEERING

1a. DEFINE THE LEM ANGULAR MOMENTUM DIRECTION; $\hat{h}_L$:

$$\hat{h}_L^* = \frac{\bar{r}_{L/LO} \times \bar{r}_{C/I}}{|\bar{r}_{L/LO} \times \bar{r}_{C/I}|} ; \quad \chi = \hat{h}_L^* \cdot \hat{h}_c$$

IF	THEN:
$\bar{r}_{L/LO} \times \bar{r}_{C/I} = 0$	$\hat{h}_L = \hat{h}_c$
$\chi = 0$	$\hat{h}_L = \hat{h}_c$
$\chi > 0$	$\hat{h}_L = \hat{h}_L^*$
$\chi < 0$	$\hat{h}_L = -\hat{h}_L^*$

2a. COMPUTE GREAT CIRCLE NODE AND INCLINATION:

$$\hat{N}_L = \frac{\hat{k}_M \times \hat{h}_L}{\sin i_L}$$

IF	THEN
$i_L = 0$	$\hat{N}_L = \hat{i}_M$
$i_L = \pi$	$\hat{N}_L = -\hat{i}_M$

$$\text{TAN } \Omega_L = \frac{\hat{N}_L \times \hat{k}_M \cdot \hat{i}_M}{\hat{N}_L \cdot \hat{i}_M}$$

$$\cos i_L = h_{z_L} ; \quad 0 \le i_L \le \pi$$

3a. COMPUTE CENTRAL ANGLE FROM LEM NODE TO TAKE-OFF SITE AT LIFT-OFF:

$$\text{TAN } u_{L/LO} = \frac{\hat{N}_L \cdot (\bar{r}_{L/LO} \times \hat{h}_L)}{\hat{N}_L \cdot [\hat{h}_L \times (\bar{r}_{L/LO} \times \hat{h}_L)]}$$

4a. COMPUTE CENTRAL ANGLE FROM LEM NODE TO LEM BURNOUT:

$$u_{L/BO} = u_{L/LO} + \theta_{L/BO}$$

5a. COMPUTE LEM BURNOUT VECTOR SAME AS I-3 EXCEPT:

$$\Omega_c = \Omega_L$$
$$i_c = i_L$$

6a. COMPUTE LEM FREE FLIGHT ANGLE:

$$\text{TAN } \phi_{ff} = \frac{(\hat{h}_L \times \bar{r}_{L/BO}) \cdot \bar{r}_{C/I}}{\bar{r}_{L/BO} \cdot \bar{r}_{C/I}}$$

$\hat{N}_c, \hat{h}_c$ (N-11)

R_M^* (M-71)

$\bar{r}_{L/LO}$ (N-10)

$\theta_{L/BO}, h_{BO}$ (N-01)

Ω_c, i_c (N-11)

Φ_{ff_k} (N-13)

U_j (N-12)

$\bar{r}_{C/I}$ (N-13)

INSTRUCTIONS

15

GENERAL PROCEDURE FOR DEFINING DIRECT LAUNCH WINDOW

1. GIVEN:
   - a) $\bar{r}_{MC_0}$ AND $\dot{\bar{r}}_{MC_0}$ AT SOME EPOCH d_0 (E-01)
   - b) TAKE-OFF SIGHT LATITUDE ϕ_{SL} AND LONGITUDE λ_{SL}

   INITIALIZE PROBLEM, FIND:
   - a) $(\bar{r}_{L/LO})_0$
   - b) ALL CONSTANTS SPECIFIED IN (N-11).

2. SELECT AN INITIAL VALUE FOR:
   - a) THE CSM LEAD ANGLE U_0'
   - b) THE CSM FREE FLIGHT ANGLE Φ_{ff_0} $(\Phi_{ff_0} = \pi)$

3. FOR THE VALUE OF U_0' AND Φ_{ff_0} GIVEN ABOVE FIND:
   - a) THE FREE FLIGHT TIME t_{ff} (N-13)
   - b) THE CSM INTERCEPT VECTORS $\bar{r}_{C/I}$, $\dot{\bar{r}}_{C/I}$ (N-13)
   - c) THE LEM FREE FLIGHT ANGLE ϕ_{ff} (N-14)
   - d) THE LEM BURNOUT VECTOR $\bar{r}_{L/BO}$ (N-14)

4. ENTER LAMBERT'S ROUTINE (N-20) AND COMPUTE ΔV AND R_p

5. DECREMENT AND INCREMENT U_j' $(U_j' = U_0' \pm j\Delta U)$, AT A FIXED VALUE OF Φ_{ff}, UNTIL EITHER $\Delta V \ge \Delta V_{MAX}$ OR $R_p \le R_{PMIN}$. AT BOUNDARY RECORD:

DECREMENT	INCREMENT
a) $t_{C_{LOj-}}$ (N-12)	a) $t_{C_{LOj+}}$
b) U_{j-} (N-12)	b) U_{j+}
c) $\phi_{ff_{j-}}$ (N-14)	c) ϕ_{ffj+}

6. DECREMENT Φ_{ff_k} $(\Phi_{ff_k} = \Phi_{ff_0} - k\Delta\Phi_{ff})$. FOR EACH VALUE OF Φ_{ff} REPEAT STEP 5.

7. COMPARE EACH VALUE OF $t_{C_{LOj-}}$ FOR ALL VALUES OF Φ_{ff_k}. SELECT THE SMALLEST VALUE $(t_{C_{LO}})_{MIN}$.
   COMPARE EACH VALUE OF $t_{C_{LOj+}}$ FOR ALL VALUES OF Φ_{ff_k}. SELECT THE LARGEST VALUE $(t_{C_{LO}})_{1 MAX}$.
   THE LAUNCH WINDOW, WHEN $\Phi_{ff} < \pi$ IS:
   $$\Delta t_{LW_1} = (t_{LO})_{1 MAX} - (t_{LO})_{1 MIN}$$
   RECORD CORRESPONDING VALUES OF U_j

8. INCREMENT Φ_{ff_k}. FOR EACH VALUE OF Φ_{ff} REPEAT STEPS 5 AND 7. RECORD $(t_{LO})_{2 MAX}$, $(t_{LO})_{2 MIN}$. THE LAUNCH WINDOW, WHEN $\Phi_{ff} > \pi$ IS:
   $$\Delta t_{LW_2} = (t_{LO})_{2 MAX} - (t_{LO})_{2 MIN}$$

9. THE DIRECT LAUNCH WINDOW IS DETERMINED BY SELECTING THE LARGEST VALUE OF $(t_{C_{LO}})_{MAX}$, FROM STEPS 7 AND 8, AND THE SMALLEST VALUE OF $(t_{C_{LO}})_{MIN}$, FROM STEPS 7 AND 8, THUS:
   $$\Delta t_{LW} = (t_{LO})_{MAX} - (t_{C_{LO}})_{MIN}$$

SHEET 2 OF 5

N-LGC ASCENT TO RENDEZVOUS - PRIMARY N

SHEET 3 OF 5

PRE-LAUNCH COMPUTATIONS - CONTINUED

APPROXIMATE PARKING ORBIT LAUNCH WINDOW

16

1. CORRESPONDING TO $(t_{c_{LO}})_{MAX}$ AND $(t_{c_{LO}})_{MIN}$, STEP 9 (N-15), IS THE MINIMUM AND MAXIMUM CSM LEAD ANGLE AT LIFT-OFF. LET:

$$\Delta U_{LW} = U_{MAX} - U_{MIN}$$

REPRESENT THE REGION OF ACCESSIBILITY.

2. COMPUTE THE BEAT FREQUENCY:

$$\Delta\omega = \omega_L - \omega_c$$

$$\omega_L = \sqrt{\frac{\mu_M}{(R_M^* + h_{BO})^3}}$$

$$\omega_c = \sqrt{\frac{\mu_M}{a_c^3}}$$

3. COMPUTE THE MAXIMUM CENTRAL ANGLE MEASURED FROM U_{MAX} TERMINUS TO POSITION OF CSM BEYOND WHICH A PARKING ORBIT IS NO LONGER CONSIDERED:

$$\Delta U_{MAX} = \frac{\frac{\Delta\omega}{\omega_c}(2\pi - \Delta U_{LW})}{1 + \frac{\Delta\omega}{\omega_c}}$$

4. COMPUTE THE INCREMENTAL PARKING ORBIT LAUNCH WINDOW:

$$\Delta t_{PW} \cong \frac{1}{\omega_c}(\Delta U_{LW} + \Delta U_{MAX})$$

h_{BO} (N-01)

R_M^* (M-71)

μ_M (A-01)

$U_{MAX} - U_{MIN}$ (N-15)

$(t_{c_{LO}})_{MAX}, (t_{c_{LO}})_{MIN}$ (N-15)

a_c (B-25)

IDEAL PLATFORM REFERENCE FRAME

17

$(t_{c_{LO}})_{MAX}$ (N-15)

$(t_{c_{LO}})_{MIN}$ (N-15)

d_0 (E-01)

1. THE IDEAL PLATFORM DIRECTION IS A FUNCTION OF T^* (E-01) AND $\hat{h}_0$ (N-11 OR B-22). IF $\hat{h}_0$ AND LIFT-OFF TIME t^*, MEASURED FROM SOME EPOCH d_0 (E-01), TOGETHER WITH t_{ff} AND U ARE SUPPLIED AS INITIAL CONDITIONS; THEN THERE IS NO NEED TO COMPUTE THE LAUNCH WINDOW. SHOULD THIS BE THE CASE THEN DO NOT PROGRAM N-11 THROUGH N-16.

2. IF LAUNCH WINDOW COMPUTATIONS ARE EMPLOYED, THEN DETERMINE t^* BASED ON THE CENTER OF THE LAUNCH WINDOW. THUS:

$$t^* = \frac{(t_{c_{LO}})_{MAX} + (t_{c_{LO}})_{MIN}}{2}$$

WHEREUPON FROM (E-01):

$$T^* = \frac{d_0 + \frac{t^*}{24(3,600)}}{36,525}$$

3. ACTIVATE COARSE ALIGN MODE (Q-30) PRIOR TO $t = t^*$.

CONSTANTS AND INITIAL CONDITIONS

01

1) THE FOLLOWING DATA MUST BE SUPPLIED FOR PRE-LAUNCH COMPUTATIONS:

$(X, Y, Z)_{M/C_0}$ U_0', ΔU, i_{MAX}

$(\dot{X}, \dot{Y}, \dot{Z})_{M/C_0}$ Φ_{ff_0}, $\Delta\Phi$, ℓ_{MAX}

2) THE FOLLOWING DATA MUST BE SUPPLIED AT ASCENT INITIATION:

t_{ff}, ϕ_{ff}, U

3) THE FOLLOWING DATA ARE ALWAYS REQUIRED

Δt_{BO} $T_{CO_{MIN}}$ $\phi_{S/L}$ $\lambda_{S/L}$

$\theta_{L/BO}$

h_{BO} t_{VR}

$R_{P_{MIN}}$

ΔV_{MAX}

$f(V_{L/BO})$ STORED FUNCTION

T_E

IF LAUNCH WINDOW COMPUTATIONS NOT REQUIRED THEN SUPPLY:

t_{ff} $(X, Y, Z)_{M/C_0}$ OR $(X, Y, Z)_c$

ϕ_{ff} $(\dot{X}, \dot{Y}, \dot{Z})_{M/C_0}$ OR $(\dot{X}, \dot{Y}, \dot{Z})_c$

U Δt_{LW}

t^* ΔU_{LW}

LAMBERT ROUTINE - DEFINE LEM TRANSFER ORBIT FROM BURNOUT TO INTERCEPT

SHEET 3 OF 5

GEOMETRIC CONSTANTS

21

$R_{L/BO}$ (N-46)

$R_{C/I}$ (B-27) @ $t = T_I$

ϕ_{ff} (N-45)

$$C = \left[R_{L/BO}^2 + R_{C/I}^2 - 2 R_{L/BO} R_{C/I} \cos\phi_{ff}\right]^{1/2}$$

$$S = \frac{R_{L/BO} + R_{C/I} + C}{2}$$

ϕ_{ff} (N-14) PRE-LAUNCH

$R_{C/I}$ (N-13) PRE-LAUNCH

LAMBERT'S EQUATION

20

$$F(\lambda) = \sqrt{\mu_M}\, t_{ff} - \left(\frac{S}{1-\cos\lambda}\right)^{3/2}\left[\lambda - \sin\lambda - \frac{\sin\phi_{ff}}{|\sin\phi_{ff}|}(\beta - \sin\beta)\right]$$

$$\cos\beta = 1 - \frac{S-C}{S}(1-\cos\lambda)$$

USE NEWTON RAPHSON ITERATION TO DEFINE λ. LET:

$$\lambda_0 = \pi$$

$$\lambda_{i+1} = \lambda_i - \frac{F(\lambda_i)}{F'(\lambda_i)}$$

$$F'(\lambda_i) = -\left(\frac{S}{1-\cos\lambda}\right)^{3/2}\left\{1-\cos\lambda - \frac{3}{2}\frac{\sin\lambda}{1-\cos\lambda}\left[\lambda - \sin\lambda - \frac{\sin\phi_{ff}}{|\sin\phi_{ff}|}(\beta - \sin\beta)\right] - \left(\frac{S-C}{S}\right)\frac{\sin\lambda}{\sin\beta}\frac{\sin\phi_{ff}}{|\sin\phi_{ff}|}(1-\cos\beta)\right\}$$

μ_M (A-01)

t_{ff} (N-45) (N-01)

ϕ_{ff} (N-45) (N-01)

t_{ff} (N-13) PRE-LAUNCH

ϕ_{ff} (N-14) PRE-LAUNCH

TRANSFER ORBIT SEMI-MAJOR AXIS AND MINIMUM ENERGY TRANSFER TIME

22

$$a_L = \frac{S}{1-\cos\lambda}$$

$$t_m = \sqrt{\frac{S^3}{8\mu_M}}\left[\pi - \frac{\sin\phi_{ff}}{|\sin\phi_{ff}|}(\beta_m - \sin\beta_m)\right]$$

$$\sin\frac{\beta_m}{2} = \sqrt{\frac{S-C}{S}} \qquad 0 \le \frac{\beta_m}{2} \le \frac{\pi}{2}$$

μ_M (A-01)

TRANSFER ORBIT PARAMETER

23

$$P_L = \frac{2S(S-R_{L/BO})(S-R_{C/I})(S-C)}{C^2}\left[\sqrt{\frac{1}{S-C} - \frac{1}{2a_L}} + \frac{\sin\phi_{ff}}{|\sin\phi_{ff}|}\left\{SNG(t_m - t_{ff})\right\}\sqrt{\frac{1}{S} - \frac{1}{2a_L}}\right]^2$$

ϕ_{ff} (N-45)

$R_{L/BO}$ (N-46)

$R_{C/I}$ (B-27) @ $t = T_I$

TRANSFER ORBIT PERICYNTHION CRITERION

24

$$R_p = a_L\left(1 - \sqrt{1 - \frac{P_L}{a_L}}\right)$$

IF:	THEN:
$R_p > R_{P_{MIN}}$	FIND ΔV (N-25)
$R_p \le R_{P_{MIN}}$	FOR PRE-LAUNCH, RECORD DATA (N-15, STEP 5); OTHERWISE REJECT ORBIT AND CONTINUE ITERATION.

$R_{P_{MIN}}$ (N-01)

a_L (N-22)

TOTAL CHARACTERISTIC VELOCITY REQ TO ACHIEVE TRANSFER ORBIT

25

$$\Delta V = V_{L/BO} + f(V_{L/BO}) + \Delta V_E$$

IF:	THEN:
$\Delta V < \Delta V_{MAX}$	TRAJECTORY SATISFACTORY
$\Delta V \ge \Delta V_{MAX}$	FOR PRE-LAUNCH, RECORD DATA (N-15, STEP 5); OTHERWISE REJECT ORBIT AND CONTINUE ITERATION.

$f(V_{L/BO})$ (N-01)

ΔV_{MAX} (N-01)

$V_{L/BO}$ (N-20)

ΔV_E (N-20)

N-LGC ASCENT TO RENDEZVOUS - PRIMARY N

SHEET 4 OF 5

LAMBERT ROUTINE - CONTINUED

LEM BURNOUT VELOCITY

26

$$\dot{\bar{r}}_{L/BO} = u_1\left[\bar{r}_{C/I} + \nu_1 \bar{r}_{L/BO}\right],$$

$$\dot{X}_{L/BO} = u_1(X_{C/I} + \nu_1 X_{L/BO})$$
$$\dot{Y}_{L/BO} = u_1(Y_{C/I} + \nu_1 Y_{L/BO})$$
$$\dot{Z}_{L/BO} = u_1(Z_{C/I} + \nu_1 Z_{L/BO})$$

$$u_1 = \frac{\sqrt{\mu_M P_L}}{r_{L/BO}\, r_{C/I} \sin\phi_{ff}}$$

$$\nu_1 = -\left[1 - \frac{r_{C/I}}{P_L}(1-\cos\phi_{ff})\right]$$

$$V_{L/BO} = \left[\dot{X}^2_{L/BO} + \dot{Y}^2_{L/BO} + \dot{Z}^2_{L/BO}\right]^{1/2}$$

$r_{L/BO}$ (N-46)
$r_{C/I}$ (B-27) EVALUATED AT $t = T_I$
P_L (N-23)
ϕ_{ff} (N-45)
μ_M (A-01)

FLIGHT PATH ANGLE AND RADIAL VELOCITY AT BURNOUT

27

$$\sin\gamma_{L/BO} = \frac{\bar{r}_{L/BO}\cdot\dot{\bar{r}}_{L/BO}}{r_{L/BO} V_{L/BO}}, \quad -\frac{\pi}{2} \le \gamma_{L/B} \le \frac{\pi}{2}$$

$$\sin\gamma_{L/BO} = \frac{X_{L/BO}\dot{X}_{L/BO} + Y_{L/BO}\dot{Y}_{L/BO} + Z_{L/BO}\dot{Z}_{L/BO}}{r_{L/BO} V_{L/BO}}$$

$$\dot{r}_{L/BO} = V_{L/BO} \sin\gamma_{L/BO}$$

$r_{L/BO}$ (N-46)
$(X,Y,Z)_{L/BO}$ (N-43)
NOTE: FOR PRE-LAUNCH $\bar{r}_{L/BO}$ (N-14).

LEM VELOCITY AT INTERCEPT

28

$$\dot{\bar{r}}_{L/I} = u_2 \bar{r}_{L/BO} + \nu_2 \dot{\bar{r}}_{L/BO},$$

$$\dot{X}_{L/I} = u_2 X_{L/BO} + \nu_2 \dot{X}_{L/BO}$$
$$\dot{Y}_{L/I} = u_2 Y_{L/BO} + \nu_2 \dot{Y}_{L/BO}$$
$$\dot{Z}_{L/I} = u_2 Z_{L/BO} + \nu_2 \dot{Z}_{L/BO}$$

$$u_2 = \frac{\dot{r}_{L/BO}}{P_L}(1-\cos\phi_{ff}) - \frac{1}{r_{L/BO}}\sqrt{\frac{\mu_M}{P_L}}\sin\phi_{ff}$$

$$\nu_2 = 1 - \frac{r_{L/BO}}{P_L}(1-\cos\phi_{ff})$$

$$V_{L/I} = \left[\dot{X}^2_{L/I} + \dot{Y}^2_{L/I} + \dot{Z}^2_{L/I}\right]^{1/2}$$

$r_{L/BO}$ (N-46)
$(X,Y,Z)_{L/BO}$ (N-43)
ϕ_{ff} (N-45)
P_L (N-23)
μ_M (A-01)

CHARACTERISTIC VELOCITY REQ TO ACHIEVE CSM ORBIT

29

$$\Delta\dot{X}_2 = \dot{X}_{C/I} - \dot{X}_{L/I}$$
$$\Delta\dot{Y}_2 = \dot{Y}_{C/I} - \dot{Y}_{L/I}$$
$$\Delta\dot{Z}_2 = \dot{Z}_{C/I} - \dot{Z}_{L/I}$$

$$\Delta V_2 = \left[\Delta\dot{X}_2^2 + \Delta\dot{Y}_2^2 + \Delta\dot{Z}_2^2\right]^{1/2}$$

LIFT-OFF AND VERTICAL RISE MANEUVER

POWERED ASCENT INITIALIZATION INSTRUCTIONS

30

1. ALIGN PLATFORM BASED ON t^* (EITHER GIVEN AS AN IC OR COMPUTED AS PER N-17).

2. DEFINE THE TAKE-OFF SITE VECTOR IN TERMS OF PLATFORM COORDINATES:

a) AT TIME OF PLATFORM ALIGNMENT:

$$\bar{r}_{L/LO} = R_M^* \hat{i}$$

b) AT ANY SUBSEQUENT TIME

$$\bar{r}_{L/LO} = C_{ij}\, a^T_{ij}\, \bar{R}_{S/L} \quad \text{(NOTE; IN G-13 } R'_M \text{ IS REPLACED BY } R^*_M \text{ M-71).}$$

$$\dot{\bar{r}}_{L/LO} = C_{ij}\, \dot{\bar{R}}_{M/S}$$

3. DEFINE CSM COORDINATES IN PLATFORM COORDINATES. EITHER:

a) RE-INITIALIZE THE M-FRAME CSM STATE VECTOR IN PLATFORM COORDINATES ($\bar{r}_{C_0} = C_{ij}\bar{r}_{M/C_0}$; $\dot{\bar{r}}_{C_0} = C_{ij}\dot{\bar{r}}_{M/C_0}$) AND THEN ENTER KEPLER ROUTINE (B-20) TO DEFINE INSTANTANEOUS VALUES $\bar{r}_C$ AND $\dot{\bar{r}}_C$ OR:

b) USE INITIAL M-FRAME CSM COORDINATES IN LOOP (B-20). AFTER EACH COMPUTATION TRANSFORM TO PLATFORM COORDINATES ($\bar{r}_C = C_{ij}\bar{r}_{M/C}$; $\dot{\bar{r}}_C = C_{ij}\dot{\bar{r}}_{M/C}$).

THE FOREGOING APPLIES TO INDEPENDENT LMS OPERATION ONLY.

4. PILOT ACTIVATES ASCENT ENGINE FOR DIRECT LAUNCH TO INTERCEPT WHENEVER THE CSM IS WITHIN THE DESIRED, DIRECT LAUNCH WINDOW. THE LEAD ANGLE, U, AT LIFT-OFF IS KNOWN. COUNT TIME, DURING ASCENT, FROM THIS INSTANT.

5. THE INITIAL FREE FLIGHT PARAMETERS, t_{ff} AND ϕ_{ff}, ARE KNOWN. THESE VALUES CORRESPOND TO A PARTICULAR ASCENT PATH DEFINED BY ΔV_{min} FOR ALL ACCEPTABLE VALUES OF U (SEE PRE-LAUNCH OPERATION N-15). HENCE:

a) THE CSM INTERCEPT VECTORS $\bar{r}_{C/I}$, $\dot{\bar{r}}_{C/I}$ ARE KNOWN BASED ON FIXED T_I. (SEE B-20).

b) THE TOTAL TIME MEASURED FROM LIFT-OFF TO INTERCEPT IS KNOWN:

$$T_I = \text{CONSTANT} = \Delta t_{BO} + t_{ff}$$

6. DEFINE A DIRECTION NORMAL TO THE DESIRED ASCENT PLANE. IF:

$\hat{h}_L = \hat{h}_C$ WHEN $\bar{r}_{L/LO} \times \bar{r}_{C/I} = 0$

a) GREAT CIRCLE STEERING:

$$\hat{h}_L = \frac{\bar{r}_{L/LO} \times \bar{r}_{C/I}}{|\bar{r}_{L/LO} \times \bar{r}_{C/I}|}\,\frac{\sin(\theta_{L/BO} + \phi_{ff})}{|\sin(\theta_{L/BO} + \phi_{ff})|}$$

b) 3-D STEERING (ALSO USE FOR PARKING ORBIT):

$$\hat{h}_C = \frac{\bar{r}_{C_0} \times \dot{\bar{r}}_{C_0}}{|\bar{r}_{C_0} \times \dot{\bar{r}}_{C_0}|}$$

R^*_M
C_{ij} (D-30)
a^T_{ij} (D-10)
$\bar{R}_{S/L}$ (G-14)
$\dot{\bar{R}}_{M/S}$ (G-10)
$\bar{r}_{M/C_0}$ (N-01)
$\dot{\bar{r}}_{M/C_0}$ (N-01)
U_{LO} (N-01)
t_{ff} (N-01)
ϕ_{ff} (N-01)
Δt_{BO} (N-01)
$\bar{r}_{L/LO}$ (N-30) STEP-2
$\bar{r}_{C/I}$ (N-30) STEP 5
θ_{BO} (N-01)
$\bar{r}_{C_0}, \dot{\bar{r}}_{C_0}$ (N-30) STEP-3

31

VERTICAL RISE MANEUVER	
IF:	THEN:
GREAT CIRCLE STEERING.	$\tan\phi_C = \frac{-h_{X/L}}{-h_{Y/L}}$ $\theta_C = \psi_C = 0$
3-D STEERING	THE COMMAND ROLL ANGLE ϕ_C MUST BE PROGRAMMED AS SOME FUNCTION OF THE INITIAL OUT OF PLANE ANGLE δ: $\sin\delta = \frac{\bar{r}_{L/LO}\cdot\hat{h}_C}{r_{L/LO}}$ $\theta_C = \psi_C = 0$
$t = t_{VR}$	STOP VERTICAL RISE MANEUVER. INITIALIZE C_1, C_2, C_3, C_4 USING $\bar{r}_D = \bar{r}_{L/BO}$ AND $\dot{\bar{r}}_D = \dot{\bar{r}}_{L/BO}$ GIVEN BY t_{ff} AND ϕ_{ff} IN LOOP N-30, STEP 5

$h_{X/L}$
$h_{Y/L}$
$\hat{h}_C$
$\bar{r}_{L/LO}$

POWERED ASCENT MANEUVER

POWERED ASCENT STEERING CONSTANTS

40

$$C_1 = \frac{4}{T_{CO}}(\dot{r}_D - \dot{r}) - \frac{6}{T_{CO}^2}(r_D - r - \dot{r}T_{CO})$$

$$C_2 = -\frac{6}{T_{CO}^2}(\dot{r}_D - \dot{r}) + \frac{12}{T_{CO}^3}(r_D - r - \dot{r}T_{CO})$$

$$C_3 = \frac{4}{T_{CO}}(\dot{Y}^*_D - \dot{Y}^*) - \frac{6}{T_{CO}^2}(Y^*_D - Y^* - \dot{Y}^*T_{CO})$$

$$C_4 = -\frac{6}{T_{CO}^2}(\dot{Y}^*_D - \dot{Y}^*) + \frac{12}{T_{CO}^3}(Y^*_D - Y^* - \dot{Y}^*T_{CO})$$

DO NOT EVALUATE C_1, C_2, C_3, C_4 WHEN $T_{CO} \le T_{COMIN}$.

$r_D, \dot{r}_D$ (N-46)
$Y^*_D, \dot{Y}^*_D$ (N-46)
$Y^*, \dot{Y}^*$ (N-46)
$\dot{r}, r$ (M-12)
T_{CO} (N-41)
T_{COMIN} (N-01)

N-LGC ASCENT TO RENDEZVOUS - PRIMARY N

SHEET 5 OF 5

SHEET 5 OF 5

POWERED ASCENT MANEUVER - CONTINUED

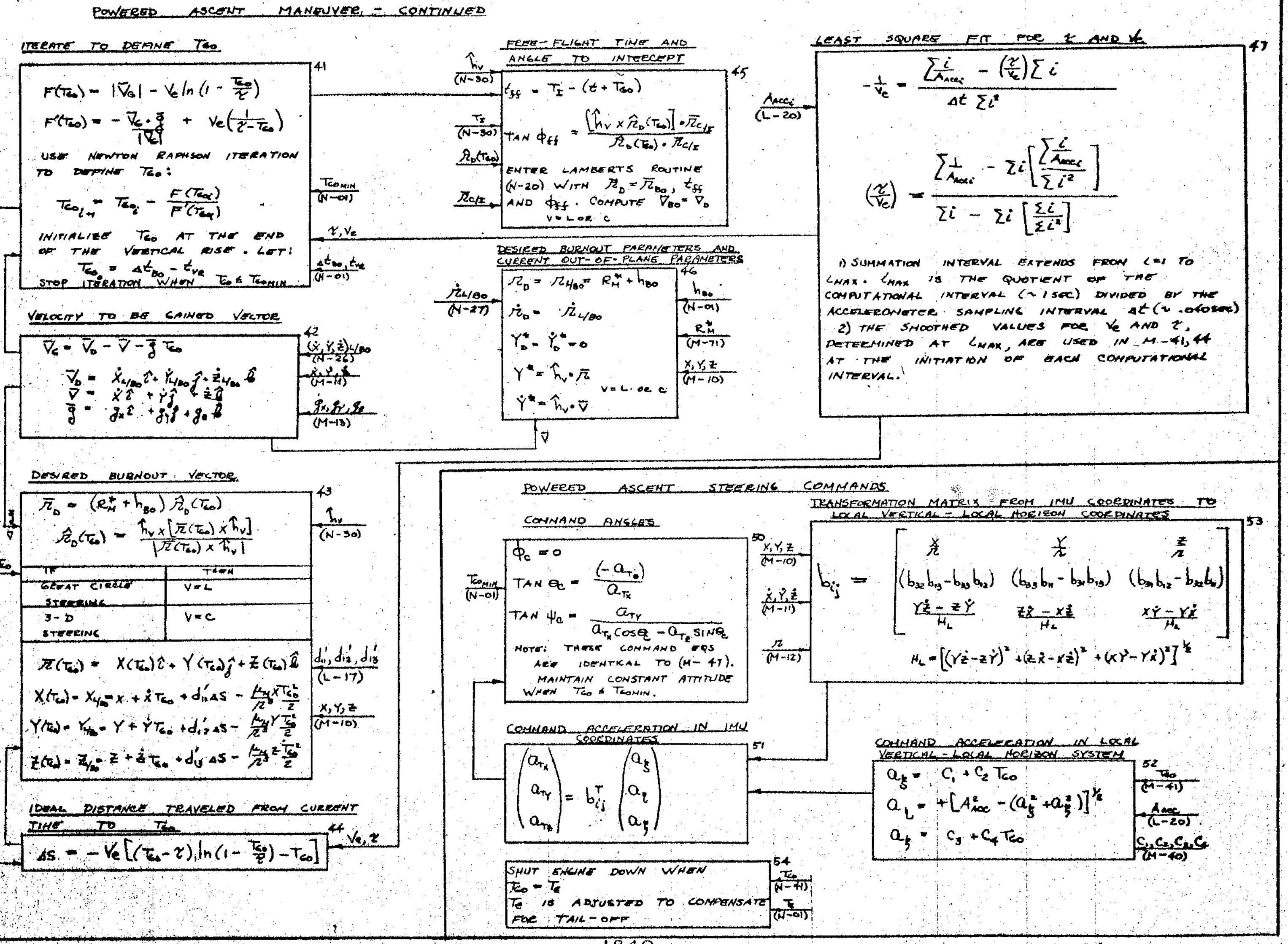

ITERATE TO DEFINE T_{GO}

41

$$F(T_{GO}) = |\bar{V}_G| - V_e \ln\left(1 - \frac{T_{GO}}{\tau}\right)$$

$$F'(T_{GO}) = -\frac{\bar{V}_G \cdot \bar{g}}{|\bar{V}_G|} + V_e\left(\frac{1}{\tau - T_{GO}}\right)$$

USE NEWTON RAPHSON ITERATION TO DEFINE T_{GO}:

$$T_{GO_{i+1}} = T_{GO_i} - \frac{F(T_{GO_i})}{F'(T_{GO_i})}$$

INITIALIZE T_{GO} AT THE END OF THE VERTICAL RISE. LET:

$$T_{GO_0} = \Delta t_{BO} - t_{VR}$$

STOP ITERATION WHEN $T_{GO} \leq T_{GO_{MIN}}$

VELOCITY TO BE GAINED VECTOR

42

$$\bar{V}_G = \bar{V}_D - \bar{V} - \bar{g}\,T_{GO}$$

$$\bar{V}_D = \dot{X}_{L/BO}\hat{i} + \dot{Y}_{L/BO}\hat{j} + \dot{Z}_{L/BO}\hat{k}$$

$$\bar{V} = \dot{X}\hat{i} + \dot{Y}\hat{j} + \dot{Z}\hat{k}$$

$$\bar{g} = g_x\hat{i} + g_y\hat{j} + g_z\hat{k}$$

DESIRED BURNOUT VECTOR

43

$$\bar{r}_D = (R_M^* + h_{BO})\,\hat{r}_D(T_{GO})$$

$$\hat{r}_D(T_{GO}) = \frac{\hat{h}_V \times [\bar{r}(T_{GO}) \times \hat{h}_V]}{|\bar{r}(T_{GO}) \times \hat{h}_V|}$$

IF	THEN
GREAT CIRCLE STEERING	V = L
3-D STEERING	V = C

$$\bar{r}(T_{GO}) = X(T_{GO})\hat{i} + Y(T_{GO})\hat{j} + Z(T_{GO})\hat{k}$$

$$X(T_{GO}) = X_{L/BO} = X + \dot{X}T_{GO} + d'_{11}\Delta S - \frac{\mu_M}{r^3}X\frac{T_{GO}^2}{2}$$

$$Y(T_{GO}) = Y_{L/BO} = Y + \dot{Y}T_{GO} + d'_{12}\Delta S - \frac{\mu_M}{r^3}Y\frac{T_{GO}^2}{2}$$

$$Z(T_{GO}) = Z_{L/BO} = Z + \dot{Z}T_{GO} + d'_{13}\Delta S - \frac{\mu_M}{r^3}Z\frac{T_{GO}^2}{2}$$

IDEAL DISTANCE TRAVELED FROM CURRENT TIME TO T_{GO}

44

$$\Delta S = -V_e\left[(T_{GO} - \tau)\ln\left(1 - \frac{T_{GO}}{\tau}\right) - T_{GO}\right]$$

FREE-FLIGHT TIME AND ANGLE TO INTERCEPT

45

$$t_{ff} = T_I - (t + T_{GO})$$

$$\tan\phi_{ff} = \frac{[\hat{h}_V \times \hat{r}_D(T_{GO})] \cdot \bar{r}_{C/I}}{\hat{r}_D(T_{GO}) \cdot \bar{r}_{C/I}}$$

ENTER LAMBERTS ROUTINE (N-20) WITH $\bar{r}_D = \bar{r}_{BO}$, t_{ff} AND ϕ_{ff}. COMPUTE $\bar{V}_{BO} = \bar{V}_D$

V = L OR C

DESIRED BURNOUT PARAMETERS AND CURRENT OUT-OF-PLANE PARAMETERS

46

$$r_D = r_{H/BO} = R_M^* + h_{BO}$$

$$\dot{r}_D = \dot{r}_{L/BO}$$

$$Y_D^* = \dot{Y}_D^* = 0$$

$$Y^* = \hat{h}_V \cdot \bar{r}$$

V = L OR C

$$\dot{Y}^* = \hat{h}_V \cdot \bar{V}$$

LEAST SQUARE FIT FOR τ AND V_e

47

$$-\frac{1}{V_e} = \frac{\sum\frac{i}{A_{ACC_i}} - \left(\frac{\tau}{V_e}\right)\sum i}{\Delta t \sum i^2}$$

$$\left(\frac{\tau}{V_e}\right) = \frac{\sum\frac{1}{A_{ACC_i}} - \sum i\left[\frac{\sum\frac{i}{A_{ACC_i}}}{\sum i^2}\right]}{\sum i - \sum i\left[\frac{\sum i}{\sum i^2}\right]}$$

1) SUMMATION INTERVAL EXTENDS FROM $i = 1$ TO i_{MAX}. i_{MAX} IS THE QUOTIENT OF THE COMPUTATIONAL INTERVAL (~ 1 SEC) DIVIDED BY THE ACCELEROMETER SAMPLING INTERVAL Δt (~ .0405 SEC)

2) THE SMOOTHED VALUES FOR V_e AND τ, DETERMINED AT i_{MAX}, ARE USED IN M-41, 44 AT THE INITIATION OF EACH COMPUTATIONAL INTERVAL.

POWERED ASCENT STEERING COMMANDS

COMMAND ANGLES

50

$$\phi_c = 0$$

$$\tan\theta_c = \frac{(-a_{T_Z})}{a_{T_X}}$$

$$\tan\psi_c = \frac{a_{T_Y}}{a_{T_X}\cos\theta_c - a_{T_Z}\sin\theta_c}$$

NOTE: THESE COMMAND EQS ARE IDENTICAL TO (M-47). MAINTAIN CONSTANT ATTITUDE WHEN $T_{GO} \leq T_{GO_{MIN}}$.

COMMAND ACCELERATION IN IMU COORDINATES

51

$$\begin{pmatrix} a_{T_X} \\ a_{T_Y} \\ a_{T_Z} \end{pmatrix} = b_{ij}^T \begin{pmatrix} a_\xi \\ a_\eta \\ a_\zeta \end{pmatrix}$$

TRANSFORMATION MATRIX FROM IMU COORDINATES TO LOCAL VERTICAL - LOCAL HORIZON COORDINATES

53

$$b_{ij} = \begin{bmatrix} \frac{X}{r} & \frac{Y}{r} & \frac{Z}{r} \\ (b_{32}b_{13} - b_{33}b_{12}) & (b_{33}b_{11} - b_{31}b_{13}) & (b_{31}b_{12} - b_{32}b_{11}) \\ \frac{Y\dot{Z} - Z\dot{Y}}{H_L} & \frac{Z\dot{X} - X\dot{Z}}{H_L} & \frac{X\dot{Y} - Y\dot{X}}{H_L} \end{bmatrix}$$

$$H_L = \left[(Y\dot{Z} - Z\dot{Y})^2 + (Z\dot{X} - X\dot{Z})^2 + (X\dot{Y} - Y\dot{X})^2\right]^{1/2}$$

COMMAND ACCELERATION IN LOCAL VERTICAL - LOCAL HORIZON SYSTEM

52

$$a_\xi = C_1 + C_2 T_{GO}$$

$$a_\eta = +\left[A_{ACC}^2 - (a_\xi^2 + a_\zeta^2)\right]^{1/2}$$

$$a_\zeta = C_3 + C_4 T_{GO}$$

54

SHUT ENGINE DOWN WHEN $T_{GO} = T_E$

T_E IS ADJUSTED TO COMPENSATE FOR TAIL-OFF

MIDCOURSE GUIDANCE

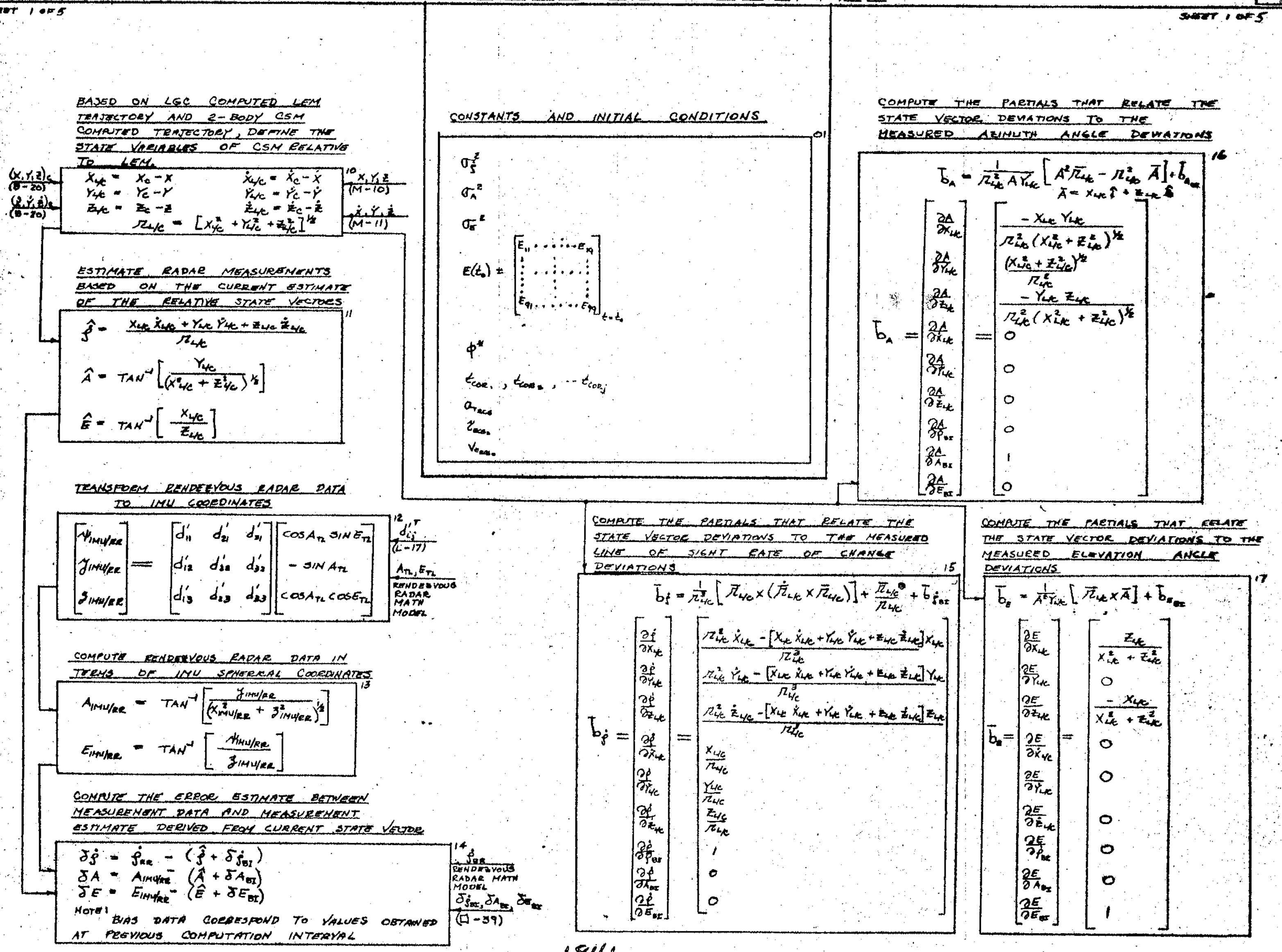

1841

MIDCOURSE GUIDANCE

SHEET 2 OF 5

SHEET 2 OF 5

TRANSITION AND COVARIANCE MATRIX COMPUTATIONS

TRANSITION MATRIX

20

$$P(t,t_0) = \left[\begin{array}{c|c} \Phi(t,t_0) & 0 \\ \hline 0 & \Phi_{BIAS} \end{array}\right] ; \quad \Phi_{BIAS} = \begin{bmatrix} 1 & 0 & 0 \\ 0 & 1 & 0 \\ 0 & 0 & 1 \end{bmatrix} ; \quad \Phi(t,t_0) = \left[\begin{array}{c|c} \frac{\partial x_i}{\partial x_{0j}} & \frac{\partial x_i}{\partial \dot{x}_{0j}} \\ \hline \frac{\partial \dot{x}_i}{\partial x_{0j}} & \frac{\partial \dot{x}_i}{\partial \dot{x}_{0j}} \end{array}\right]$$

NOTES:

$i = 1,2,3$; $j = 1,2,3$

SUBSCRIPT 0 DENOTES VALUE OF PARAMETER AT PREVIOUS TIME STEP

$X_1 = X$; $X_2 = Y$; $X_3 = Z$

$\dot{X}_1 = \dot{X}$; $\dot{X}_2 = \dot{Y}$; $\dot{X}_3 = \dot{Z}$

COVARIANCE MATRIX

22

$P(t_{n+1},t_n)$

$P^T(t_{n+1},t_n)$

$E(t_0)$ (□-01)

$$E'(t) = P(t,t_0)\, E(t_0)\, P^T(t,t_0)$$

NOTES:

1. THE ELEMENTS OF THE COVARIANCE MATRIX ARE GIVEN AT LEM BURNOUT $E(t_0)$.

2. AT AN OBSERVATION TIME, CALL t_n, THE MEASURED PARAMETERS ARE WEIGHTED AND A BEST ESTIMATE FOR THE COVARIANCE MATRIX $\hat{E}(t_n)$ AT THAT TIME IS COMPUTED (□-35). THE COVARIANCE MATRIX $\hat{E}(t_n)$ IS THEN EXTRAPOLATED TO THE NEXT OBSERVATION TIME t_{n+1} AS FOLLOWS:

$$E'(t_{n+1}) = P(t_{n+1},t_n)\, \hat{E}(t_n)\, P^T(t_{n+1},t_n)$$

TWO TECHNIQUES CAN BE EMPLOYED TO GENERATE THE STATE TRANSITION MATRIX. TECHNIQUE 1 REQUIRES THE SOLUTION OF 36 FIRST ORDER DIFFERENTIAL EQUATIONS DURING EACH UPDATE OR OBSERVATIONAL INTERVAL. TECHNIQUE 2 REQUIRES THE SOLUTION OF SIMPLE ALGEBRAIC EQUATIONS AND KEPLER'S EQUATION (B-25). PROGRAM THE SIMPLEST TECHNIQUE.

TECHNIQUE 1

21a

X,Y,Z (M-10)

r (M-12)

μ_M (A-01)

$$\dot{\Phi}(t,t_0) = A\, \Phi(t,t_0)$$

WHERE:

$$A = \left[\begin{array}{c|c} 0 & I \\ \hline G & 0 \end{array}\right]$$

AND

$$G = \frac{3\mu_M}{r^5}\begin{bmatrix} X^2 - \frac{r^2}{3} & XY & XZ \\ XY & Y^2 - \frac{r^2}{3} & YZ \\ XZ & YZ & Z^2 - \frac{r^2}{3} \end{bmatrix}$$

NOTES:

1. MATRIX $\Phi(t,0)$ IS INITIALIZED AT LEM BURNOUT BY COMPUTING [A] BASED ON THE LEM STATE VECTOR AT BURNOUT (M-10). THE FIRST INCREMENT GIVES:

$$\dot{\Phi}(t,0) = [A]\big|_{t_0}$$

2. $\dot{\Phi}$ IS INTEGRATED AT APPROXIMATELY 1 SEC INTERVALS UNTIL THE FIRST OBSERVATION PERIOD (EVERY 60 SEC) IS REACHED, WHEREUPON, [G] IS RE-INITIALIZED, BASED ON OBSERVATIONAL DATA, AND THE PROCESS REPEATED.

TECHNIQUE 2

21b

$$\frac{\partial x_i}{\partial x_{0j}} = f\delta_{ij} + \frac{a_L x_{0j}}{r_0^3}\Big\{\big[\dot{x}_i - \dot{x}_{0i}\big]\Big[g - \frac{r_0^2 r}{\mu_M}\dot{f}\Big(1 - \frac{r_0}{a_L}\Big)\Big] + 3\big[x_i - x_{0i} - (t-t_0)\dot{x}_i\big] - (f-1)\Big(1 + \frac{r_0}{a_L}\Big)x_{0i}\Big\} + \frac{r_0}{\mu_M}(f-1)\,\dot{x}_{0j}(\dot{x}_i - \dot{x}_{0i})$$

$$\frac{\partial x_i}{\partial \dot{x}_{0j}} = g\delta_{ij} + \frac{a_L \dot{x}_{0j}}{\mu_M}\Big\{3\big[x_i - x_{0i} - (t-t_0)\dot{x}_i\big] - (f-1)x_{0i}\Big\} + \frac{a_L}{\mu_M}(\dot{x}_i - \dot{x}_{0i})\Big[\Big(g - \frac{r_0^2 r}{\mu_M}\dot{f}\Big)\dot{x}_{0j} + \frac{r_0}{a_L}(f-1)x_{0j}\Big]$$

$$\frac{\partial \dot{x}_i}{\partial x_{0j}} = \dot{f}\delta_{ij} - \frac{\mu_M a_L x_{0j} x_i}{r_0 r^3}\Big\{g - 3(t-t_0) - \frac{r_0^2 r}{\mu_M}\dot{f}\Big(1 - \frac{r_0}{a_L}\Big)\Big\} - \frac{r_0}{r^3}(f-1)\dot{x}_{0j}x_i - \frac{a_L}{r_0^3}\dot{f}\Big(1 + \frac{r_0}{a_L}\Big)x_{0i}x_{0j} + \frac{r_0}{\mu_M}\dot{f}(\dot{x}_i - \dot{x}_{0i})\dot{x}_{0j} + \frac{a_L}{r_0^3}(\dot{x}_i - \dot{x}_{0i})\Big\{\dot{g} + \Big(1 - \frac{r_0}{a_L}\Big)\Big[\frac{r_0}{a_L}(\dot{g}-1) + \frac{r_0}{r}\Big]\Big\}x_{0j}$$

$$\frac{\partial \dot{x}_i}{\partial \dot{x}_{0j}} = \dot{g}\delta_{ij} - \frac{a_L}{r^3}x_i\Big\{\Big[g - 3(t-t_0) - \frac{r_0^2 r}{\mu_M}\dot{f}\Big]\dot{x}_{0j} + \frac{r}{a_L}(\dot{g}-1)x_{0j}\Big\} - \frac{a_L}{\mu_M}\dot{f}\,x_{0i}\dot{x}_{0j} + \frac{r_0}{\mu_M}(\dot{x}_i - \dot{x}_{0i})\Big\{\Big[\Big(\frac{a_L}{r_0}+1\Big)\dot{g} + \frac{a_L}{r} - 1\Big]\dot{x}_{0j} + \dot{f}x_{0j}\Big\}$$

NOTES:

1. δ_{ij} = KRONECKER DELTA

2. AT LEM BURNOUT THE BURNOUT STATE VECTOR $\bar{r}_0, \dot{\bar{r}}_0$ (M-10,11) IS SUBSTITUTED IN B-21, 23, 25, 26. FUNCTIONS $f, \dot{f}, g, \dot{g}$ ARE COMPUTED (B-26) BASED ON THE NEXT OBSERVATION TIME INTERVAL ($t - t_0 = 60$ SEC). NOTE THAT A NEWTON-RAPHSON ITERATION IS REQUIRED TO DETERMINE $E - E_0$ (B-27).

3. HAVING FOUND $f, \dot{f}, g, \dot{g}$ THEN THE LEM STATE VECTOR $\bar{r}, \dot{\bar{r}}$ CAN BE COMPUTED AT TIME t (NEXT OBSERVATION PERIOD) FROM EQUATIONS (B-20). THESE VALUE $\bar{r}, \dot{\bar{r}}$ ARE SUBSTITUTED IN M-21b TO DEFINE THE MATRIX ELEMENTS.

4. AT AN OBSERVATION TIME, CALL t_n, THE MEASURED PARAMETERS ARE WEIGHTED AND A NEW VALUE OF THE STATE VECTOR IS ASCERTAINED (□-39), $\bar{r} + \delta\bar{r}$, $\dot{\bar{r}} + \delta\dot{\bar{r}}$). THIS NEW ESTIMATE OF THE STATE VECTOR IS THEN USED AT TIME t_n TO ESTIMATE $\bar{r}(t_{n+1})$, $\dot{\bar{r}}(t_{n+1})$. HENCE, A NEW TRANSITION MATRIX $\Phi(t_{n+1}, t_n)$ IS COMPUTED FOR THE NEXT OBSERVATION TIME t_{n+1}.

$t_{n+1} - t_n$ UPDATE INTERVAL

$(X,Y,Z)_0\ t_n$ (M-10)

$(\dot{X},\dot{Y},\dot{Z})_0\ t_n$

$(X,Y,Z)\ t_{n+1}$ (B-20)

$(\dot{X},\dot{Y},\dot{Z})\ t_{n+1}$ (B-20)

$r_0\ t_n$ (M-12)

$r\ t_{n+1}$ (B-21)

$f, \dot{f}, g, \dot{g}$ (B-26)

a_L (B-23)

μ_M (A-01)

5/65

MIDCOURSE GUIDANCE

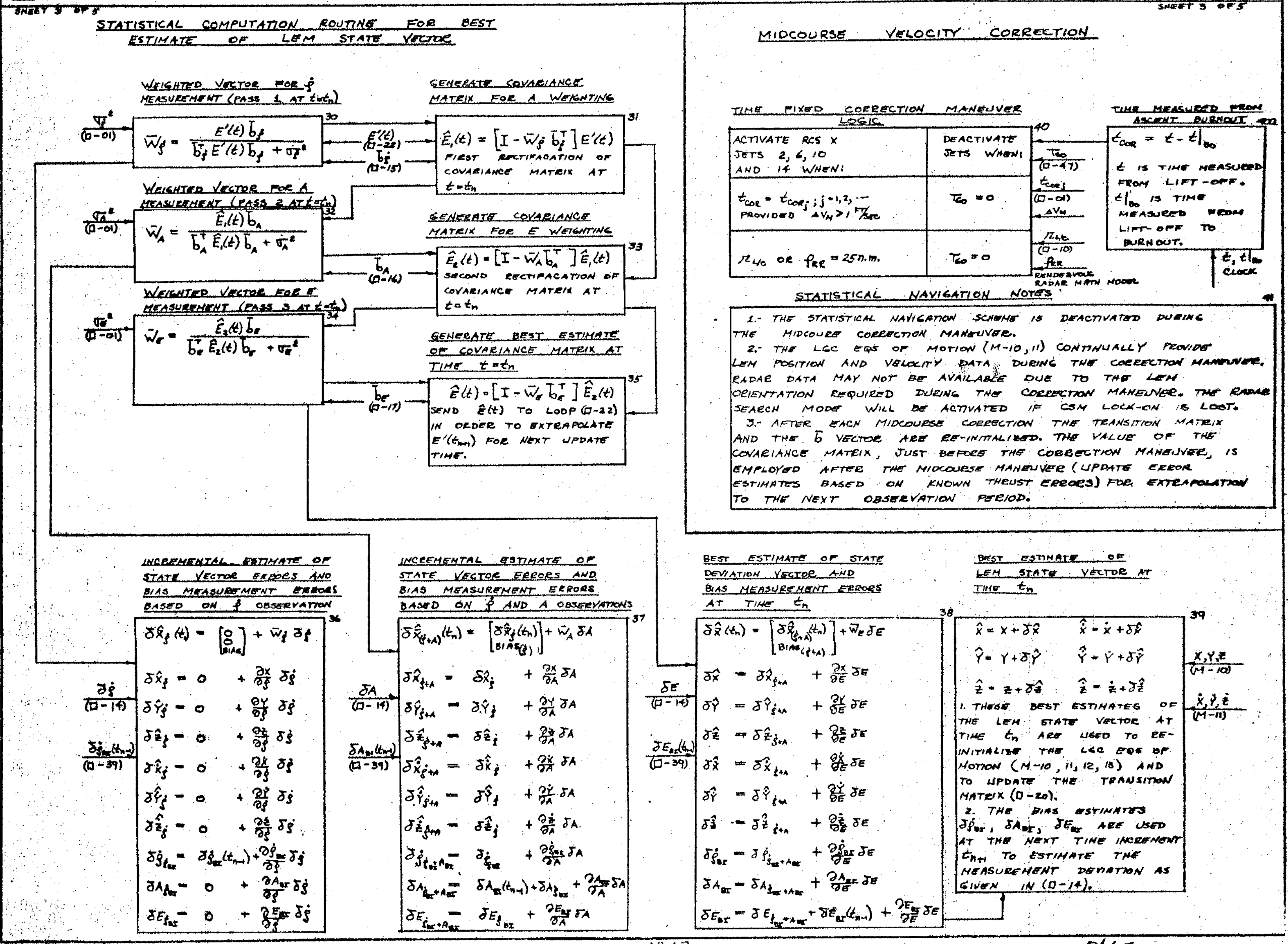

STATISTICAL COMPUTATION ROUTINE FOR BEST ESTIMATE OF LEM STATE VECTOR

WEIGHTED VECTOR FOR $\dot\rho$ MEASUREMENT (PASS 1 AT $t = t_n$)

$$\bar W_{\dot\rho} = \frac{E'(t)\,\bar b_{\dot\rho}}{\bar b_{\dot\rho}^T E'(t)\,\bar b_{\dot\rho} + \sigma_{\dot\rho}^2}$$

WEIGHTED VECTOR FOR A MEASUREMENT (PASS 2 AT $t = t_n$)

$$\bar W_A = \frac{\hat E_1(t)\,\bar b_A}{\bar b_A^T \hat E_1(t)\,\bar b_A + \sigma_A^2}$$

WEIGHTED VECTOR FOR E MEASUREMENT (PASS 3 AT $t = t_n$)

$$\bar W_E = \frac{\hat E_2(t)\,\bar b_E}{\bar b_E^T \hat E_2(t)\,\bar b_E + \sigma_E^2}$$

GENERATE COVARIANCE MATRIX FOR A WEIGHTING

$$\hat E_1(t) = \left[I - \bar W_{\dot\rho}\,\bar b_{\dot\rho}^T\right] E'(t)$$

FIRST RECTIFACATION OF COVARIANCE MATRIX AT $t = t_n$

GENERATE COVARIANCE MATRIX FOR E WEIGHTING

$$\hat E_2(t) = \left[I - \bar W_A\,\bar b_A^T\right] \hat E_1(t)$$

SECOND RECTIFACATION OF COVARIANCE MATRIX AT $t = t_n$

GENERATE BEST ESTIMATE OF COVARIANCE MATRIX AT TIME $t = t_n$

$$\hat E(t) = \left[I - \bar W_E\,\bar b_E^T\right] \hat E_2(t)$$

SEND $\hat E(t)$ TO LOOP (□-22) IN ORDER TO EXTRAPOLATE $E'(t_{n+1})$ FOR NEXT UPDATE TIME.

INCREMENTAL ESTIMATE OF STATE VECTOR ERRORS AND BIAS MEASUREMENT ERRORS BASED ON $\dot\rho$ OBSERVATION

$$\delta\hat X_{\dot\rho}(t_n) = \begin{bmatrix} 0 \\ 0 \\ \text{BIAS} \end{bmatrix} + \bar W_{\dot\rho}\,\delta\dot\rho$$

$$\delta\hat x_{\dot\rho} = 0 + \frac{\partial x}{\partial\dot\rho}\,\delta\dot\rho$$

$$\delta\hat y_{\dot\rho} = 0 + \frac{\partial y}{\partial\dot\rho}\,\delta\dot\rho$$

$$\delta\hat z_{\dot\rho} = 0 + \frac{\partial z}{\partial\dot\rho}\,\delta\dot\rho$$

$$\delta\hat{\dot x}_{\dot\rho} = 0 + \frac{\partial\dot x}{\partial\dot\rho}\,\delta\dot\rho$$

$$\delta\hat{\dot y}_{\dot\rho} = 0 + \frac{\partial\dot y}{\partial\dot\rho}\,\delta\dot\rho$$

$$\delta\hat{\dot z}_{\dot\rho} = 0 + \frac{\partial\dot z}{\partial\dot\rho}\,\delta\dot\rho$$

$$\delta\dot\rho_{\dot\rho_{BI}} = \delta\dot\rho_{BI}(t_{n-1}) + \frac{\partial\dot\rho_{BI}}{\partial\dot\rho}\,\delta\dot\rho$$

$$\delta A_{\dot\rho_{BI}} = 0 + \frac{\partial A_{BI}}{\partial\dot\rho}\,\delta\dot\rho$$

$$\delta E_{\dot\rho_{BI}} = 0 + \frac{\partial E_{BI}}{\partial\dot\rho}\,\delta\dot\rho$$

INCREMENTAL ESTIMATE OF STATE VECTOR ERRORS AND BIAS MEASUREMENT ERRORS BASED ON $\dot\rho$ AND A OBSERVATIONS

$$\delta\hat X_{(\dot\rho+A)}(t_n) = \begin{bmatrix} \delta\hat X_{\dot\rho}(t_n) \\ \text{BIAS}_{(\dot\rho)} \end{bmatrix} + \bar W_A\,\delta A$$

$$\delta\hat x_{\dot\rho+A} = \delta\hat x_{\dot\rho} + \frac{\partial x}{\partial A}\,\delta A$$

$$\delta\hat y_{\dot\rho+A} = \delta\hat y_{\dot\rho} + \frac{\partial y}{\partial A}\,\delta A$$

$$\delta\hat z_{\dot\rho+A} = \delta\hat z_{\dot\rho} + \frac{\partial z}{\partial A}\,\delta A$$

$$\delta\hat{\dot x}_{\dot\rho+A} = \delta\hat{\dot x}_{\dot\rho} + \frac{\partial\dot x}{\partial A}\,\delta A$$

$$\delta\hat{\dot y}_{\dot\rho+A} = \delta\hat{\dot y}_{\dot\rho} + \frac{\partial\dot y}{\partial A}\,\delta A$$

$$\delta\hat{\dot z}_{\dot\rho+A} = \delta\hat{\dot z}_{\dot\rho} + \frac{\partial\dot z}{\partial A}\,\delta A$$

$$\delta\dot\rho_{\dot\rho_{BI}+A_{BI}} = \delta\dot\rho_{\dot\rho_{BI}} + \frac{\partial\dot\rho_{BI}}{\partial A}\,\delta A$$

$$\delta A_{\dot\rho_{BI}+A_{BI}} = \delta A_{BI}(t_{n-1}) + \delta A_{\dot\rho_{BI}} + \frac{\partial A_{BI}}{\partial A}\,\delta A$$

$$\delta E_{\dot\rho_{BI}+A_{BI}} = \delta E_{\dot\rho_{BI}} + \frac{\partial E_{BI}}{\partial A}\,\delta A$$

BEST ESTIMATE OF STATE DEVIATION VECTOR AND BIAS MEASUREMENT ERRORS AT TIME t_n

$$\delta\hat X(t_n) = \begin{bmatrix} \delta\hat X_{(\dot\rho+A)}(t_n) \\ \text{BIAS}_{(\dot\rho+A)} \end{bmatrix} + \bar W_E\,\delta E$$

$$\delta\hat x = \delta\hat x_{\dot\rho+A} + \frac{\partial x}{\partial E}\,\delta E$$

$$\delta\hat y = \delta\hat y_{\dot\rho+A} + \frac{\partial y}{\partial E}\,\delta E$$

$$\delta\hat z = \delta\hat z_{\dot\rho+A} + \frac{\partial z}{\partial E}\,\delta E$$

$$\delta\hat{\dot x} = \delta\hat{\dot x}_{\dot\rho+A} + \frac{\partial\dot x}{\partial E}\,\delta E$$

$$\delta\hat{\dot y} = \delta\hat{\dot y}_{\dot\rho+A} + \frac{\partial\dot y}{\partial E}\,\delta E$$

$$\delta\hat{\dot z} = \delta\hat{\dot z}_{\dot\rho+A} + \frac{\partial\dot z}{\partial E}\,\delta E$$

$$\delta\dot\rho_{BI} = \delta\dot\rho_{\dot\rho_{BI}+A_{BI}} + \frac{\partial\dot\rho_{BI}}{\partial E}\,\delta E$$

$$\delta A_{BI} = \delta A_{\dot\rho_{BI}+A_{BI}} + \frac{\partial A_{BI}}{\partial E}\,\delta E$$

$$\delta E_{BI} = \delta E_{\dot\rho_{BI}+A_{BI}} + \delta E_{BI}(t_{n-1}) + \frac{\partial E_{BI}}{\partial E}\,\delta E$$

BEST ESTIMATE OF LEM STATE VECTOR AT TIME t_n

$$\hat x = x + \delta\hat x \qquad \hat{\dot x} = \dot x + \delta\hat{\dot x}$$

$$\hat y = y + \delta\hat y \qquad \hat{\dot y} = \dot y + \delta\hat{\dot y}$$

$$\hat z = z + \delta\hat z \qquad \hat{\dot z} = \dot z + \delta\hat{\dot z}$$

1. THESE BEST ESTIMATES OF THE LEM STATE VECTOR AT TIME t_n ARE USED TO RE-INITIALIZE THE LGC EQS OF MOTION (M-10, 11, 12, 13) AND TO UPDATE THE TRANSITION MATRIX (□-20).

2. THE BIAS ESTIMATES $\delta\dot\rho_{BI}$, δA_{BI}, δE_{BI} ARE USED AT THE NEXT TIME INCREMENT t_{n+1} TO ESTIMATE THE MEASUREMENT DEVIATION AS GIVEN IN (□-14).

MIDCOURSE VELOCITY CORRECTION

TIME FIXED CORRECTION MANEUVER LOGIC

ACTIVATE RCS X JETS 2, 6, 10 AND 14 WHEN:	DEACTIVATE JETS WHEN:
$t_{COR} = t_{COR_j};\ j = 1, 2, \text{--}$ PROVIDED $\Delta V_H > 1$ FT/SEC	$T_{GO} = 0$
r_{LC} OR $\rho_{RR} = 25$ n.m.	$T_{GO} = 0$

TIME MEASURED FROM ASCENT BURNOUT

$$t_{COR} = t - t|_{BO}$$

t IS TIME MEASURED FROM LIFT-OFF. $t|_{BO}$ IS TIME MEASURED FROM LIFT-OFF TO BURNOUT.

STATISTICAL NAVIGATION NOTES

1.- THE STATISTICAL NAVIGATION SCHEME IS DEACTIVATED DURING THE MIDCOURSE CORRECTION MANEUVER.

2.- THE LGC EQS OF MOTION (M-10, 11) CONTINUALLY PROVIDE LEM POSITION AND VELOCITY DATA DURING THE CORRECTION MANEUVER. RADAR DATA MAY NOT BE AVAILABLE DUE TO THE LEM ORIENTATION REQUIRED DURING THE CORRECTION MANEUVER. THE RADAR SEARCH MODE WILL BE ACTIVATED IF CSM LOCK-ON IS LOST.

3.- AFTER EACH MIDCOURSE CORRECTION THE TRANSITION MATRIX AND THE $\bar b$ VECTOR ARE RE-INITIALIZED. THE VALUE OF THE COVARIANCE MATRIX, JUST BEFORE THE CORRECTION MANEUVER, IS EMPLOYED AFTER THE MIDCOURSE MANEUVER (UPDATE ERROR ESTIMATES BASED ON KNOWN THRUST ERRORS) FOR EXTRAPOLATION TO THE NEXT OBSERVATION PERIOD.

MIDCOURSE GUIDANCE

MIDCOURSE VELOCITY CORRECTION - CONTINUED

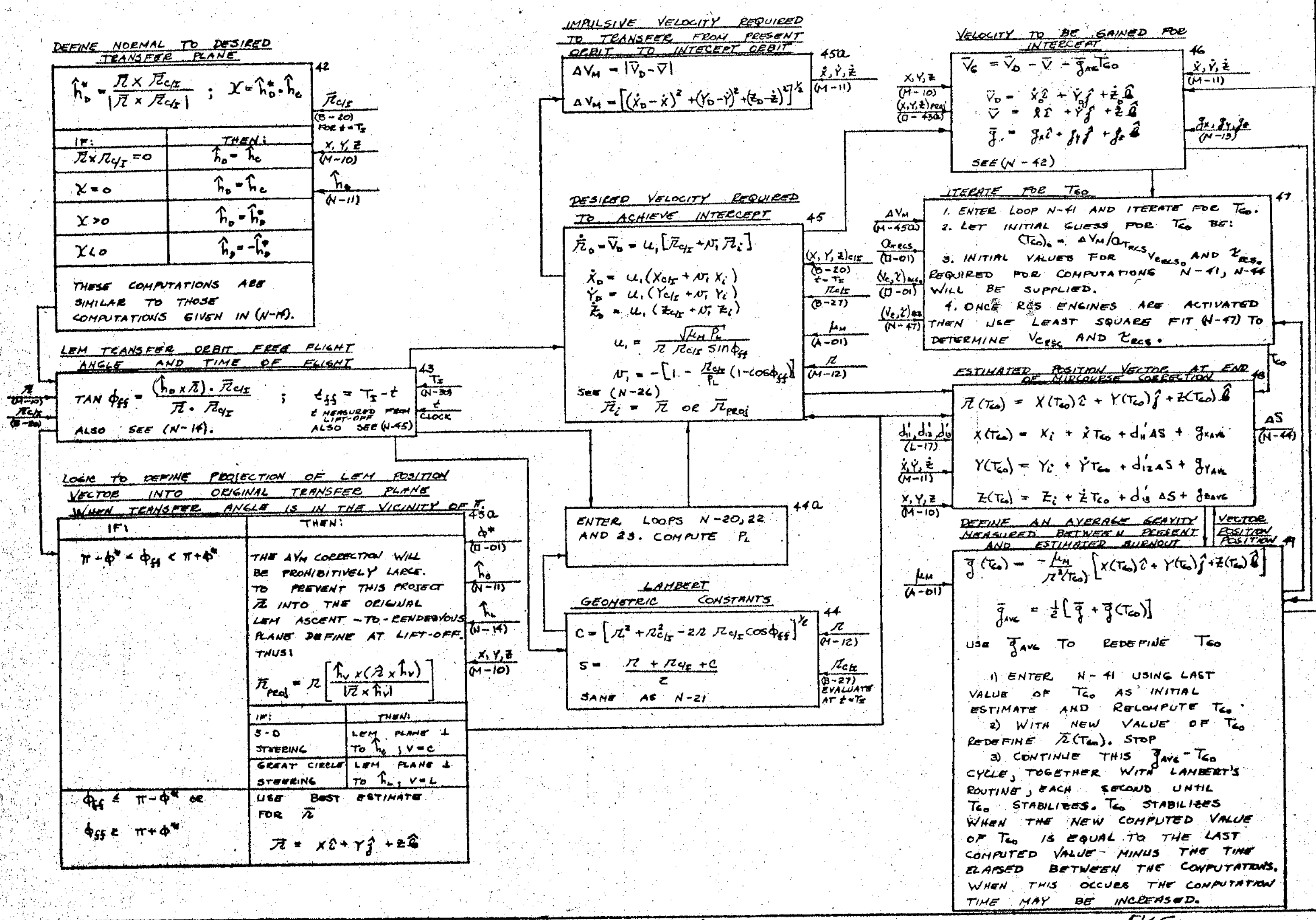

DEFINE NORMAL TO DESIRED TRANSFER PLANE 42

$$\hat{h}_D^* = \frac{\bar{R} \times \bar{R}_{c/I}}{|\bar{R} \times \bar{R}_{c/I}|} \; ; \; \chi = \hat{h}_D^* \cdot \hat{h}_c$$

IF:	THEN:
$\bar{R} \times R_{c/I} = 0$	$\hat{h}_D = \hat{h}_c$
$\chi = 0$	$\hat{h}_D = \hat{h}_c$
$\chi > 0$	$\hat{h}_D = \hat{h}_D^*$
$\chi < 0$	$\hat{h}_D = -\hat{h}_D^*$

THESE COMPUTATIONS ARE SIMILAR TO THOSE COMPUTATIONS GIVEN IN (N-14).

LEM TRANSFER ORBIT FREE FLIGHT ANGLE AND TIME OF FLIGHT 43

$$\tan \phi_{ff} = \frac{(\hat{h}_D \times \bar{R}) \cdot \bar{R}_{c/I}}{\bar{R} \cdot \bar{R}_{c/I}} \; ; \; t_{ff} = T_I - t$$

ALSO SEE (N-14).

t MEASURED FROM LIFT-OFF ALSO SEE (N-45)

LOGIC TO DEFINE PROJECTION OF LEM POSITION VECTOR INTO ORIGINAL TRANSFER PLANE WHEN TRANSFER ANGLE IS IN THE VICINITY OF π. 43a

IF:	THEN:
$\pi - \phi^* < \phi_{ff} < \pi + \phi^*$	THE ΔV_M CORRECTION WILL BE PROHIBITIVELY LARGE. TO PREVENT THIS PROJECT $\bar{R}$ INTO THE ORIGINAL LEM ASCENT-TO-RENDEZVOUS PLANE DEFINE AT LIFT-OFF. THUS: $\bar{R}_{PROJ} = R \left[\frac{\hat{h}_v \times (\bar{R} \times \hat{h}_v)}{\lvert \bar{R} \times \hat{h}_v \rvert} \right]$ IF: 3-D STEERING — THEN: LEM PLANE ⊥ TO $\hat{h}_c$; $v = c$ IF: GREAT CIRCLE STEERING — THEN: LEM PLANE ⊥ TO $\hat{h}_L$; $v = L$
$\phi_{ff} \leq \pi - \phi^*$ OR $\phi_{ff} \geq \pi + \phi^*$	USE BEST ESTIMATE FOR $\bar{R}$ $\bar{R} = X\hat{i} + Y\hat{j} + Z\hat{k}$

IMPULSIVE VELOCITY REQUIRED TO TRANSFER FROM PRESENT ORBIT TO INTERCEPT ORBIT 45a

$$\Delta V_M = |\bar{V}_D - \bar{V}|$$

$$\Delta V_M = \left[(\dot{X}_D - \dot{X})^2 + (\dot{Y}_D - \dot{Y})^2 + (\dot{Z}_D - \dot{Z})^2 \right]^{1/2}$$

DESIRED VELOCITY REQUIRED TO ACHIEVE INTERCEPT 45

$$\dot{\bar{R}}_D = \bar{V}_D = u_1 \left[\bar{R}_{c/I} + N_1 \bar{R}_i \right]$$

$$\dot{X}_D = u_1 (X_{c/I} + N_1 X_i)$$
$$\dot{Y}_D = u_1 (Y_{c/I} + N_1 Y_i)$$
$$\dot{Z}_D = u_1 (Z_{c/I} + N_1 Z_i)$$

$$u_1 = \frac{\sqrt{\mu_M P_L}}{R \, R_{c/I} \sin\phi_{ff}}$$

$$N_1 = -\left[1 - \frac{R_{c/I}}{P_L} (1 - \cos\phi_{ff}) \right]$$

SEE (N-26)

$$\bar{R}_i = \bar{R} \text{ OR } \bar{R}_{PROJ}$$

ENTER LOOPS N-20, 22 AND 23. COMPUTE P_L 44a

LAMBERT GEOMETRIC CONSTANTS 44

$$C = \left[R^2 + R_{c/I}^2 - 2R \, R_{c/I} \cos\phi_{ff} \right]^{1/2}$$

$$S = \frac{R + R_{c/I} + C}{2}$$

SAME AS N-21

VELOCITY TO BE GAINED FOR INTERCEPT 46

$$\bar{V}_G = \bar{V}_D - \bar{V} - \bar{g}_{AVE} T_{GO}$$

$$\bar{V}_D = \dot{X}_D \hat{i} + \dot{Y}_D \hat{j} + \dot{Z}_D \hat{k}$$
$$\bar{V} = \dot{X} \hat{i} + \dot{Y} \hat{j} + \dot{Z} \hat{k}$$
$$\bar{g} = g_X \hat{i} + g_Y \hat{j} + g_Z \hat{k}$$

SEE (N-42)

ITERATE FOR T_{GO} 47

1. ENTER LOOP N-41 AND ITERATE FOR T_{GO}.
2. LET INITIAL GUESS FOR T_{GO} BE: $(T_{GO})_0 = \Delta V_M / a_{T_{RCS}}$
3. INITIAL VALUES FOR $V_{e_{RCS_0}}$ AND τ_{RCS_0} REQUIRED FOR COMPUTATIONS N-41, N-44 WILL BE SUPPLIED.
4. ONCE RCS ENGINES ARE ACTIVATED THEN USE LEAST SQUARE FIT (N-47) TO DETERMINE $V_{e_{RCS}}$ AND τ_{RCS}.

ESTIMATED POSITION VECTOR AT END OF MIDCOURSE CORRECTION 48

$$\bar{R}(T_{GO}) = X(T_{GO})\hat{i} + Y(T_{GO})\hat{j} + Z(T_{GO})\hat{k}$$

$$X(T_{GO}) = X_i + \dot{X} T_{GO} + d_{11}' \Delta S + g_{X_{AVE}}$$

$$Y(T_{GO}) = Y_i + \dot{Y} T_{GO} + d_{12}' \Delta S + g_{Y_{AVE}}$$

$$Z(T_{GO}) = Z_i + \dot{Z} T_{GO} + d_{13}' \Delta S + g_{Z_{AVE}}$$

DEFINE AN AVERAGE GRAVITY MEASURED BETWEEN PRESENT AND ESTIMATED BURNOUT 49

$$\bar{g}(T_{GO}) = -\frac{\mu_M}{R^3(T_{GO})} \left[X(T_{GO})\hat{i} + Y(T_{GO})\hat{j} + Z(T_{GO})\hat{k} \right]$$

$$\bar{g}_{AVE} = \frac{1}{2} \left[\bar{g} + \bar{g}(T_{GO}) \right]$$

USE $\bar{g}_{AVE}$ TO REDEFINE T_{GO}

1) ENTER N-41 USING LAST VALUE OF T_{GO} AS INITIAL ESTIMATE AND RECOMPUTE T_{GO}.

2) WITH NEW VALUE OF T_{GO} REDEFINE $\bar{R}(T_{GO})$. STOP

3) CONTINUE THIS $\bar{g}_{AVE} - T_{GO}$ CYCLE, TOGETHER WITH LAMBERT'S ROUTINE, EACH SECOND UNTIL T_{GO} STABILIZES. T_{GO} STABILIZES WHEN THE NEW COMPUTED VALUE OF T_{GO} IS EQUAL TO THE LAST COMPUTED VALUE MINUS THE TIME ELAPSED BETWEEN THE COMPUTATIONS. WHEN THIS OCCURS THE COMPUTATION TIME MAY BE INCREASED.

5165

MIDCOURSE GUIDANCE

MIDCOURSE STEERING COMMANDS

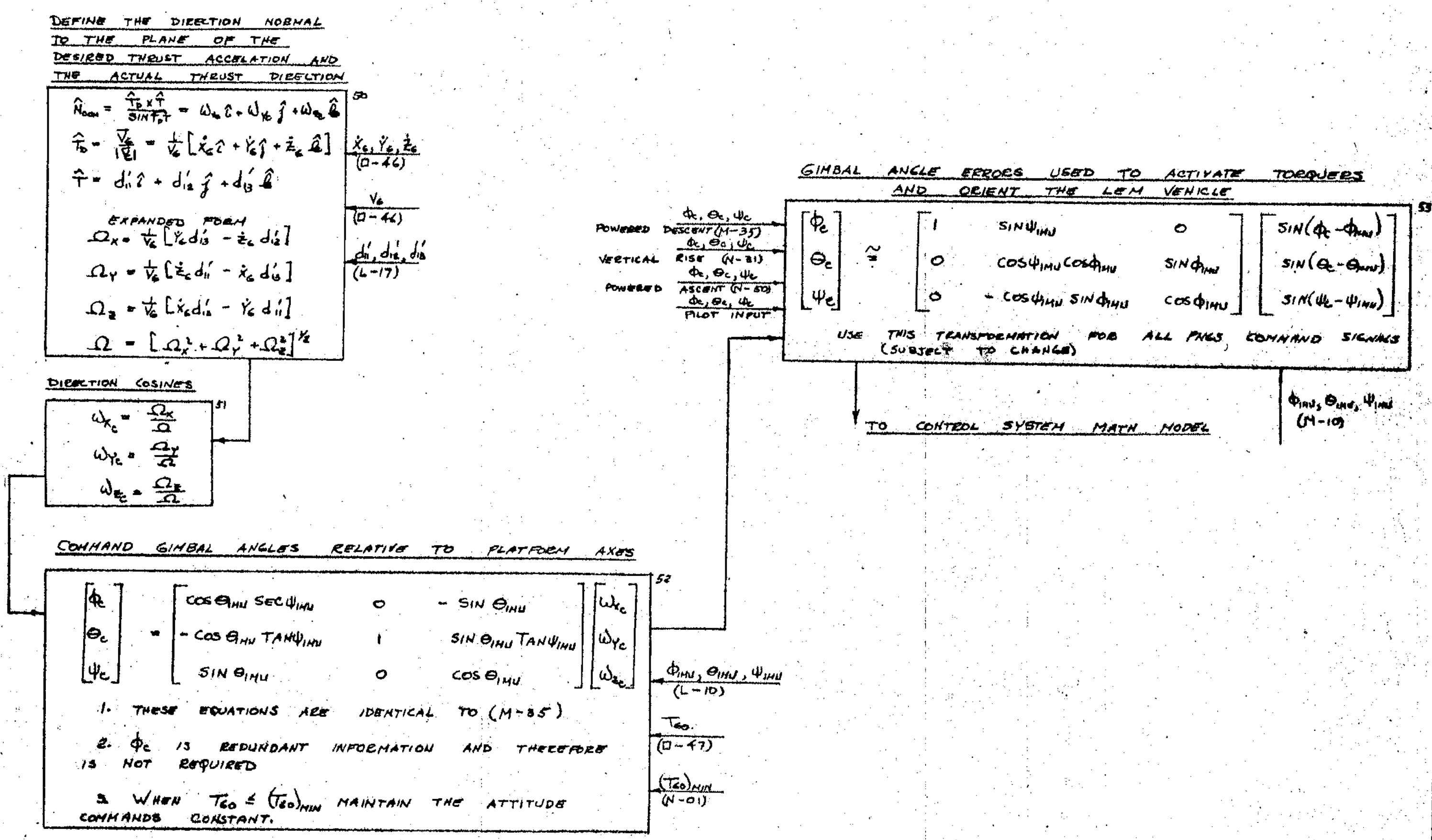

DEFINE THE DIRECTION NORMAL TO THE PLANE OF THE DESIRED THRUST ACCELATION AND THE ACTUAL THRUST DIRECTION

$$\hat{N}_{com} = \frac{\hat{T}_D \times \hat{T}}{SIN\,\hat{T}_D\hat{T}} = \omega_{x_c}\hat{i} + \omega_{y_c}\hat{j} + \omega_{z_c}\hat{k}$$

$$\hat{T}_D = \frac{\bar{V}_c}{|\bar{V}_c|} = \frac{1}{V_c}\left[\dot{x}_c\hat{i} + \dot{y}_c\hat{j} + \dot{z}_c\hat{k}\right]$$

$$\hat{T} = d_{11}'\hat{i} + d_{12}'\hat{j} + d_{13}'\hat{k}$$

EXPANDED FORM

$$\Omega_X = \frac{1}{V_c}\left[\dot{y}_c d_{13}' - \dot{z}_c d_{12}'\right]$$

$$\Omega_Y = \frac{1}{V_c}\left[\dot{z}_c d_{11}' - \dot{x}_c d_{13}'\right]$$

$$\Omega_Z = \frac{1}{V_c}\left[\dot{x}_c d_{12}' - \dot{y}_c d_{11}'\right]$$

$$\Omega = \left[\Omega_X^2 + \Omega_Y^2 + \Omega_Z^2\right]^{1/2}$$

DIRECTION COSINES

$$\omega_{x_c} = \frac{\Omega_X}{\Omega}$$

$$\omega_{y_c} = \frac{\Omega_Y}{\Omega}$$

$$\omega_{z_c} = \frac{\Omega_Z}{\Omega}$$

COMMAND GIMBAL ANGLES RELATIVE TO PLATFORM AXES

$$\begin{bmatrix}\phi_c\\ \theta_c\\ \psi_c\end{bmatrix} = \begin{bmatrix} COS\,\theta_{IMU}\,SEC\,\psi_{IMU} & 0 & -SIN\,\theta_{IMU}\\ -COS\,\theta_{IMU}\,TAN\,\psi_{IMU} & 1 & SIN\,\theta_{IMU}\,TAN\,\psi_{IMU}\\ SIN\,\theta_{IMU} & 0 & COS\,\theta_{IMU}\end{bmatrix}\begin{bmatrix}\omega_{x_c}\\ \omega_{y_c}\\ \omega_{z_c}\end{bmatrix}$$

1. THESE EQUATIONS ARE IDENTICAL TO (M-35)

2. ϕ_c IS REDUNDANT INFORMATION AND THEREFORE IS NOT REQUIRED

3. WHEN $T_{GO} \leq (T_{GO})_{MIN}$ MAINTAIN THE ATTITUDE COMMANDS CONSTANT.

GIMBAL ANGLE ERRORS USED TO ACTIVATE TORQUERS AND ORIENT THE LEM VEHICLE

$$\begin{bmatrix}\phi_e\\ \theta_e\\ \psi_e\end{bmatrix} \cong \begin{bmatrix} 1 & SIN\,\psi_{IMU} & 0\\ 0 & COS\,\psi_{IMU}\,COS\,\phi_{IMU} & SIN\,\phi_{IMU}\\ 0 & -COS\,\psi_{IMU}\,SIN\,\phi_{IMU} & COS\,\phi_{IMU}\end{bmatrix}\begin{bmatrix}SIN(\phi_c - \phi_{IMU})\\ SIN(\theta_c - \theta_{IMU})\\ SIN(\psi_c - \psi_{IMU})\end{bmatrix}$$

USE THIS TRANSFORMATION FOR ALL PNGS COMMAND SIGNALS (SUBJECT TO CHANGE)

TO CONTROL SYSTEM MATH MODEL

TERMINAL GUIDANCE

P- SHEET 1 OF 2

P SHEET 1 OF 2

TERMINAL NAVIGATION COMPUTATIONS

10

AFTER THE LAST MIDCOURSE CORRECTION, $\rho_{RR} = 25$ n.m., REDUCE THE 9X9 TRANSITION AND COVARIANCE MATRICES TO 6X6 MATRICES AS FOLLOWS:

ALTER	TO READ
$P(t, t_0)$ (□-20)	$P(t, t_{TR_0}) = \Phi(t, t_{TR_0})$
$E(t_{TR_0})$ (□-22)	$E(t_{TR_0}) = 100 \ \hat{E}(t)\big\vert_{t=t_{TR_0}}$

THE MATRIX ELEMENTS GIVEN ABOVE CORRESPOND TO THOSE VALUES GIVEN AT THE TIME OF TERMINAL RENDEZVOUS INITIATION (CALL t_{TR_0}, OCCURS WHEN $\rho_{RR} \leq 25$ n.m.)

12

1. BIAS ESTIMATES REMAIN CONSTANT DURING THE TERMINAL RENDEZVOUS MANEUVER, THUS δA_{BI}, δE_{BI} (□-14) AND $\delta\rho_{BI}$ (P-11) ESTIMATES REMAIN CONSTANT AT THE VALUES GIVEN AT TIME $t = t_{TR_0}$

2. ALL BIAS PARTIALS GIVEN IN (□-36, 37 AND 38 ARE ZEROED

3. STATISTICAL NAVIGATION NOTES GIVEN IN □-41 ALSO APPLY TO THE TERMINAL PHASE.

11

WITH REGARD TO THE NAVIGATION PHASE THE RANGE RATE MEASUREMENT IS REPLACED BY THE RANGE MEASUREMENT, THUS:

ALTER:		
$\hat{\rho}$ (□-11)	$\hat{\rho} = \left[X_{L/C}^2 + Y_{L/C}^2 + Z_{L/C}^2 \right]^{1/2}$	$\frac{(X, Y, Z)_{L/C}}{(□-10)}$
$\delta\hat{\rho}$ (□-14)	$\delta\hat{\rho} = \rho_{RR} - (\hat{\rho} + \delta\rho_{BI})$	$\frac{\delta\rho_{BI}}{(P-01)}$
$\bar{b}_\rho$ (□-16)	$\bar{b}_\rho = \frac{\bar{r}_{L/C}}{r_{L/C}}$	ρ_{RR} (RENDEZVOUS RADAR MATH MODEL)
	$\bar{b}_\rho = \begin{array}{lcl} \frac{\partial\rho}{\partial X_{L/C}} & = & \frac{X_{L/C}}{r_{L/C}} \\ \frac{\partial\rho}{\partial Y_{L/C}} & & \frac{Y_{L/C}}{r_{L/C}} \\ \frac{\partial\rho}{\partial Z_{L/C}} & & \frac{Z_{L/C}}{r_{L/C}} \\ \frac{\partial\rho}{\partial \dot{X}_{L/C}} & & 0 \\ \frac{\partial\rho}{\partial \dot{Y}_{L/C}} & & 0 \\ \frac{\partial\rho}{\partial \dot{Z}_{L/C}} & & 0 \end{array}$	$\frac{r_{L/C}}{(□-10)}$
$\bar{b}_A$ (□-16)	$\frac{\partial A}{\partial \rho_{BI}} = \frac{\partial A}{\partial A_{BI}} = \frac{\partial A}{\partial E_{BI}} = 0$	
$\bar{b}_E$ (□-17)	$\frac{\partial E}{\partial \rho_{BI}} = \frac{\partial E}{\partial A_{BI}} = \frac{\partial E}{\partial E_{BI}}$	
$\bar{W}_\rho$ (□-30)	$\bar{W}_\rho = \frac{E'(t)\,\bar{b}_\rho}{\bar{b}_\rho^T E'(t)\,\bar{b}_\rho + \sigma_\rho^2}$	$\frac{\sigma_\rho^2}{(P-01)}$
$\hat{E}_1(t)$ (□-31)	$\hat{E}_1(t) = \left[I - \bar{W}_\rho \bar{b}_\rho^T \right] E'(t)$	

DETERMINE BEST ESTIMATE OF STATE VECTOR (□-39). USE THIS ESTIMATE TO RE-INITIALIZE THE LGC EQ OF MOTION (M-10, 11, 12, 13).

CONSTANTS AND INITIAL CONDITIONS

01

ρ_1
ρ_2
ρ_3
$\dot{\rho}_{D_1}$
$\dot{\rho}_{D_2}$
$\dot{\rho}_{D_3}$
σ_ρ^2
$\delta\rho_{BI}$
ΔV_{MAX}

ENGINE IGNITE LOGIC

20

Inputs: $\frac{\rho_1, \rho_2, \rho_3}{(P-01)}$; $\frac{\dot{\rho}_{D_1}, \dot{\rho}_{D_2}, \dot{\rho}_{D_3}}{(P-01)}$; $\frac{\Delta V_{MAX}}{(P-01)}$; $\frac{\Delta V_{TR}}{(P-22)}$; ρ_{RR} (RENDEZVOUS RADAR MATH MODEL)

ACTIVATE ENGINE WHEN:	COMPUTE TIME TO-GO-TO-INTERCEPT (USED TO REDEFINE AIM POINT):	THRUST SUPPLIED BY:	DEACTIVATE ENGINE WHEN:
$\rho_{RR} = \rho_1$	$T_{I_1} = \frac{\rho_{RR}}{\dot{\rho}_{D_1}}$	ASCENT ENGINE IF: $\Delta V_{TR} \geq \Delta V_{MAX}$ RCS JETS 2, 6, 10, 14 (X) IF: $\Delta V_{TR} < \Delta V_{MAX}$	$T_{EO} = 0$
$\rho_{RR} = \rho_2$	$T_{I_2} = \frac{\rho_{RR}}{\dot{\rho}_{D_2}}$	RCS (+Z) JETS 3, 15	$T_{EO} = 0$
$\rho_{RR} = \rho_3$	$T_{I_3} = \frac{\rho_{RR}}{\dot{\rho}_{D_3}}$	RCS (+Z) JET 3, 15	$T_{EO} = 0$

TERMINAL GUIDANCE VELOCITY COMMANDS

COMPUTE THE FREE FLIGHT TIME AND THE AIM POINT REQUIRED TO ACHIEVE INTERCEPT

21

Inputs: T_{I_j}; $\frac{\bar{r}_c, \dot{\bar{r}}_c}{(B-20)}$; $\frac{T_{EO}}{(P-22)}$; $\frac{t_j}{\text{CLOCK}}$

1. DISCARD t_{ff} AS GIVEN IN (□-43). REDEFINE t_{ff} AS:
$$t_{ff} = T_{I_j} - t_j \qquad j = 1, 2, 3$$
WHERE t_j DENOTES THE TIME COUNTED FROM THE INSTANT T_{I_j} IS DETERMINED.
2. REINITIALIZE $\bar{r}_c$ AND $\dot{\bar{r}}_c$ AT TIME $t_j = 0$
3. ENTER ROUTINE (B-20) WITH $\bar{r}_{c_0}$ AND $\dot{\bar{r}}_{c_0}$. PROJECT CSM STATE VECTOR AHEAD BY T_{I_j} SECONDS. COMPUTE NEW AIM POINT $\bar{r}_{c/I}$ AND $\dot{\bar{r}}_{c/I}$.

TERMINAL GUIDANCE

SHEET 2 OF 2

SHEET 2 OF 2

TERMINAL GUIDANCE VELOCITY COMMANDS - CONTINUED

22

LAMBERT ROUTINE AND T_{GO} CALCULATIONS

ENTER LOOP:	COMPUTE:	NOTES:
□-42	$\hat{h}_D$	$\hat{h}_D \neq -\hat{h}_D^*$; $\bar{R}_{C/I}$ GIVEN BY (P-21)
□-43	ϕ_{ff}	t_{ff} GIVEN BY (□-13) IS INAPPROPRIATE. USE (P-21) DISCARD LOOP (□-43a)
□-44, 44a, 45	C, S P_L $\bar{V}_D$	AS MENTIONED PREVIOUSLY $\bar{R}_{C/I}$ IS EVALUATED BASED ON NEW AIM POINT CONSIDERATIONS GIVEN BY T_{I_j}.
□-45a	ΔV_M	FOR TERMINAL RENDEZVOUS CALL $\Delta V_{TR} = \Delta V_M$
□-47	T_{GO}	NOTES ALSO APPLY TO ASCENT ENGINE. IF ASCENT ENGINE IS ACTIVATED (P-20) THEN FOR INITIAL GUESS REPLACE $(a_T, V_e, \tau)_{BSC}$ BY LAST VALUE OF a_T, V_e AND DEFINED BY (N-47, 51).
□-48	$\bar{R}(T_{GO})$	FIRST ESTIMATE
□-49	$\bar{g}_{AVG}$	SEND BACK TO (□-47) AND REDEFINE T_{GO}
□-46	$\bar{V}_G$	REQUIRED FOR STEERING COMMANDS.

TERMINAL GUIDANCE STEERING COMMANDS

50

LOOP (□-50) APPLIES TO (-X) RCS JETS AS WELL AS THE ASCENT ENGINE. WHEN THE +Z RCS JETS ARE ACTIVATED (P-20) THEN REDEFINE LOOP (□-50) AS FOLLOWS:

$$\hat{T} = -\left[d_{31}' \hat{i} + d_{32}' \hat{j} + d_{33}' \hat{k} \right]$$

$$\Omega_X = -\frac{1}{V_G}\left[\dot{Y}_G d_{33}' - \dot{Z}_G d_{32}' \right]$$

$$\Omega_Y = -\frac{1}{V_G}\left[\dot{Z}_G d_{31}' - \dot{X}_G d_{33}' \right]$$

$$\Omega_Z = -\frac{1}{V_G}\left[\dot{X}_G d_{32}' - \dot{Y}_G d_{31}' \right]$$

LOOPS □-51, 52 AND 53 ARE UNCHANGED.

$d_{31}', d_{32}', d_{33}'$
(L-17)

CONSTANTS AND INITIAL CONDITIONS

01

AGC Catalogue Number	Star Name	Mag.	Right Ascension Hr. Min. Sec. RA_s	Declination Dg. Min Sec. δ_s
01	α Andromedae	2.1		
02	β Ceti	2.2		
03	α Eridani (Achernar)	0.6		
04	α Ursae Minoris (Polaris)	2.1		
05	α Arietis	2.2		
06	α Fornacis	3.9		
07	α Persei	1.9		
08	α Tauri (Aldebaran)	1.1		
09	α Canis Majoris (Sirius)	-1.6		
10	β Geminorum (Pollux)	1.2		
11	γ Velorum	1.9		
12	β Carinae	1.8		
13	α Hydrae	2.2		
14	α Leonis (Regulus)	1.3		
15	α Ursae Majoris	1.9		
16	γ Centauri	2.4		
17	α Virginis (Spica)	1.2		
18	η Ursae Majoris	1.9		
19	α Bootis (Arcturus)	0.2		
20	α Centauri	0.1		
21	α Scorpii (Antares)	1.2		
22	α Ophiuchi	2.1		
23	α Lyrae (Vega)	0.1		
24	β Capricorni	3.2		
25	α Pavonis	2.1		
26	α Cygni (Deneb)	1.3		
27	ε Pegasi	2.5		
28	α Piscis Austrini (Fomalhaut)	1.3		
29	α Cassiopeiae	2.3		
30	α Ceti	2.8		
31	β Leonis	2.2		
32	α Carinae	-0.9		
33	α Columbae	2.7		
34	α Aurigae	.2		
35	α Lancis	3.3		
36	α Canis Minoris	.5		
37	γ Eridani	3.2		
38	γ Corvi	2.8		
39	α Aquilae	.9		
40	α Coronae Borealis	2.3		
41	σ Sagittarii	2.1		
42	θ Centauri	2.3		
43	β Pegasi	2.6		
44	ψ Velorum	3.6		
45	η Ophiuchi	2.6		
46	β Arae	2.0		
47	α Indi	3.2		
48	α Cephei	2.6		
49	γ Piscis Austrini	3.8		
50	β Hydri	2.9		
51	β Librae	2.7		
52	α Orionis	0-1		
53	ε Virginis	2.9		
54	ζ Hydrae	3.7		

K_s

NOTE: STAR DATA MAY BE GIVEN WITH RESPECT TO A MEAN EQUINOX MEAN EQUATOR AT SOME EPOCH. SHOULD THIS BE THE CASE THEN, PROPER MOTION CORRECTIONS. (SEE E-30, E-31) MUST BE INCLUDED TO DEFINE STAR DATA RELATIVE TO THE MEAN EQUINOX OF DATE.

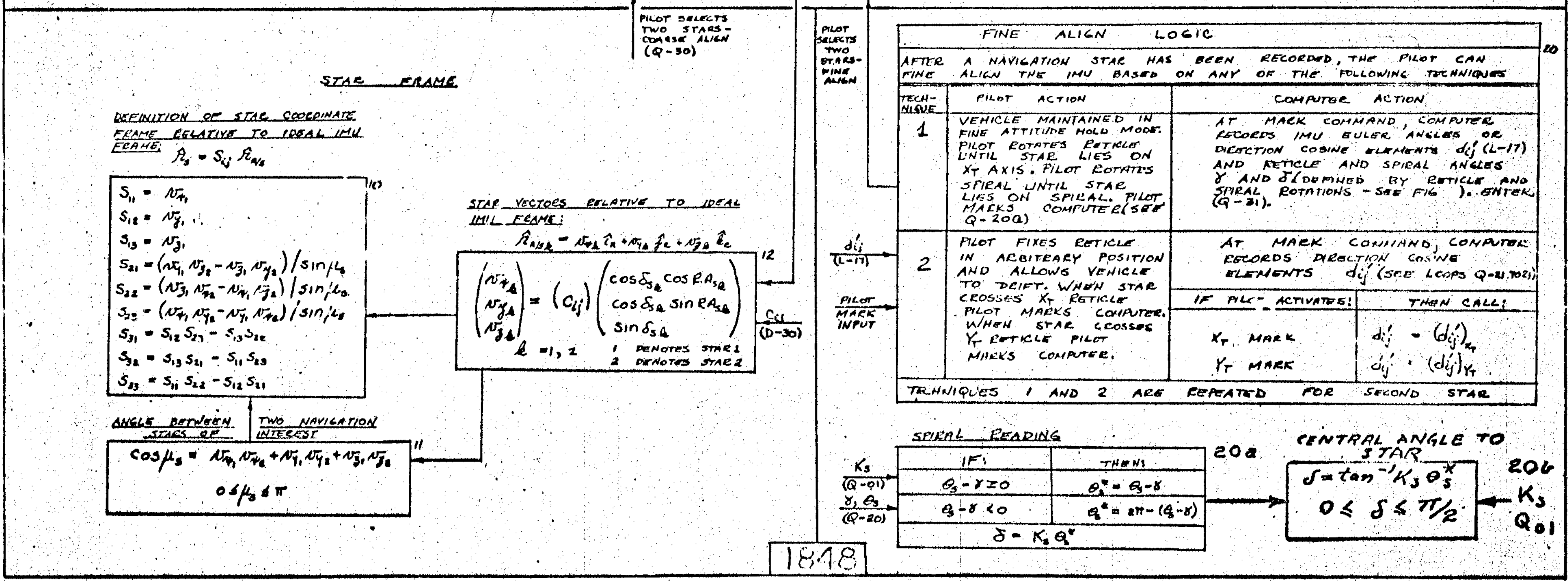

STAR FRAME

DEFINITION OF STAR COORDINATE FRAME RELATIVE TO IDEAL IMU FRAME: $R_s = S_{ij} R_{N/s}$

10

$$S_{11} = u_{x_1}$$
$$S_{12} = u_{y_1}$$
$$S_{13} = u_{z_1}$$
$$S_{21} = (u_{y_1} u_{z_2} - u_{z_1} u_{y_2}) / \sin \mu_s$$
$$S_{22} = (u_{z_1} u_{x_2} - u_{x_1} u_{z_2}) / \sin \mu_s$$
$$S_{23} = (u_{x_1} u_{y_2} - u_{y_1} u_{x_2}) / \sin \mu_s$$
$$S_{31} = S_{12} S_{23} - S_{13} S_{22}$$
$$S_{32} = S_{13} S_{21} - S_{11} S_{23}$$
$$S_{33} = S_{11} S_{22} - S_{12} S_{21}$$

ANGLE BETWEEN TWO NAVIGATION STARS OF INTEREST

11

$$\cos \mu_s = u_{x_1} u_{x_2} + u_{y_1} u_{y_2} + u_{z_1} u_{z_2}$$
$$0 \le \mu_s \le \pi$$

STAR VECTORS RELATIVE TO IDEAL IMU FRAME:

12

$$\hat{R}_{A/S_k} = u_{x_k} \hat{i}_c + u_{y_k} \hat{j}_c + u_{z_k} \hat{k}_c$$

$$\begin{pmatrix} u_{x_k} \\ u_{y_k} \\ u_{z_k} \end{pmatrix} = (C_{ij}) \begin{pmatrix} \cos \delta_{s_k} \cos RA_{s_k} \\ \cos \delta_{s_k} \sin RA_{s_k} \\ \sin \delta_{s_k} \end{pmatrix}$$

$k = 1, 2$ 1 DENOTES STAR 1 2 DENOTES STAR 2

FINE ALIGN LOGIC

20

AFTER A NAVIGATION STAR HAS BEEN RECORDED, THE PILOT CAN FINE ALIGN THE IMU BASED ON ANY OF THE FOLLOWING TECHNIQUES

TECHNIQUE	PILOT ACTION	COMPUTER ACTION
1	VEHICLE MAINTAINED IN FINE ATTITUDE HOLD MODE. PILOT ROTATES RETICLE UNTIL STAR LIES ON X_T AXIS. PILOT ROTATES SPIRAL UNTIL STAR LIES ON SPIRAL. PILOT MARKS COMPUTER (SEE Q-20a)	AT MARK COMMAND, COMPUTER RECORDS IMU EULER ANGLES OR DIRECTION COSINE ELEMENTS d'_{ij} (L-17) AND RETICLE AND SPIRAL ANGLES γ AND δ (DEFINED BY RETICLE AND SPIRAL ROTATIONS - SEE FIG). ENTER (Q-31).
2	PILOT FIXES RETICLE IN ARBITRARY POSITION AND ALLOWS VEHICLE TO DRIFT. WHEN STAR CROSSES X_T RETICLE PILOT MARKS COMPUTER. WHEN STAR CROSSES Y_T RETICLE PILOT MARKS COMPUTER.	AT MARK COMMAND, COMPUTER RECORDS DIRECTION COSINE ELEMENTS d'_{ij} (SEE LOOPS Q-21 TO 21) IF PILOT ACTIVATES: X_T MARK — THEN CALL: $d'_{ij} = (d'_{ij})_{X_T}$ IF PILOT ACTIVATES: Y_T MARK — THEN CALL: $d'_{ij} = (d'_{ij})_{Y_T}$

TECHNIQUES 1 AND 2 ARE REPEATED FOR SECOND STAR

SPIRAL READING

20a

IF:	THEN:
$\theta_s - \gamma \geq 0$	$\theta_s^* = \theta_s - \gamma$
$\theta_s - \gamma < 0$	$\theta_s^* = 2\pi - (\theta_s - \gamma)$

$$\delta = K_s \theta_s^*$$

CENTRAL ANGLE TO STAR

20b

$$\delta = \tan^{-1} K_s \theta_s^*$$
$$0 \leq \delta \leq \pi/2$$

ADT

SHEET 2 OF 2

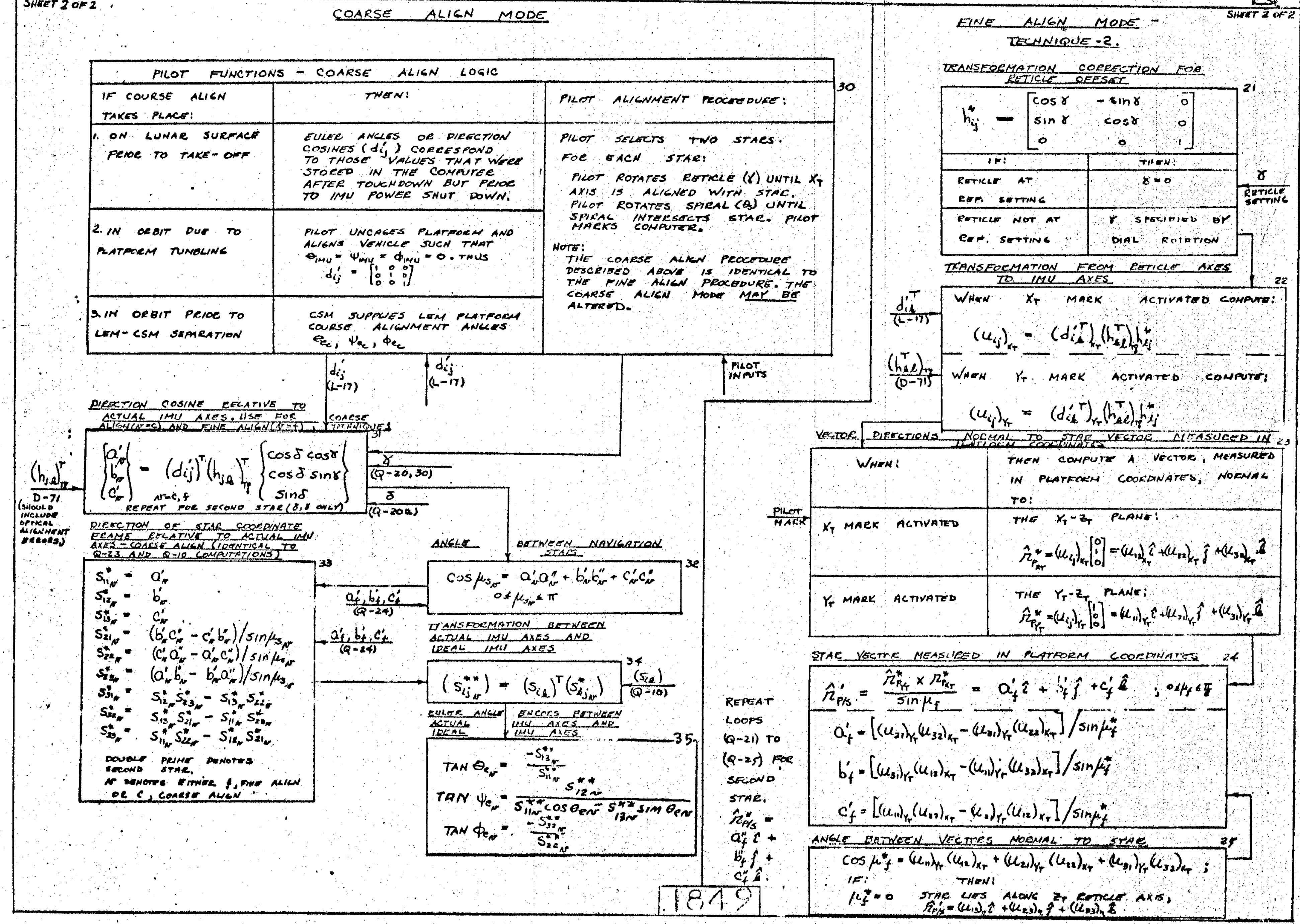

COARSE ALIGN MODE

PILOT FUNCTIONS - COARSE ALIGN LOGIC 30

IF COURSE ALIGN TAKES PLACE:	THEN:	PILOT ALIGNMENT PROCEDURE:
1. ON LUNAR SURFACE PRIOR TO TAKE-OFF	EULER ANGLES OR DIRECTION COSINES (d'_{ij}) CORRESPOND TO THOSE VALUES THAT WERE STORED IN THE COMPUTER AFTER TOUCHDOWN BUT PRIOR TO IMU POWER SHUT DOWN.	PILOT SELECTS TWO STARS. FOR EACH STAR: PILOT ROTATES RETICLE (γ) UNTIL X_T AXIS IS ALIGNED WITH STAR. PILOT ROTATES SPIRAL (θ_s) UNTIL SPIRAL INTERSECTS STAR. PILOT MARKS COMPUTER. NOTE: THE COARSE ALIGN PROCEDURE DESCRIBED ABOVE IS IDENTICAL TO THE FINE ALIGN PROCEDURE. THE COARSE ALIGN MODE MAY BE ALTERED.
2. IN ORBIT DUE TO PLATFORM TUMBLING	PILOT UNCAGES PLATFORM AND ALIGNS VEHICLE SUCH THAT $\theta_{IMU} = \psi_{IMU} = \phi_{IMU} = 0$. THUS $d'_{ij} = \begin{bmatrix}1&0&0\\0&1&0\\0&0&1\end{bmatrix}$	
3. IN ORBIT PRIOR TO LEM-CSM SEPARATION	CSM SUPPLIES LEM PLATFORM COURSE ALIGNMENT ANGLES $\theta_{ec}, \psi_{ec}, \phi_{ec}$	

DIRECTION COSINE RELATIVE TO ACTUAL IMU AXES. USE FOR ALIGN(ν=C) AND FINE ALIGN(ν=f) 31

$$\begin{Bmatrix}a'_\nu\\b'_\nu\\c'_\nu\end{Bmatrix} = (d'_{ij})^T (h_{j\ell})^T_{\pi} \begin{Bmatrix}\cos\delta\cos\gamma\\\cos\delta\sin\gamma\\\sin\delta\end{Bmatrix} \quad \nu = c, f$$

REPEAT FOR SECOND STAR (δ, γ ONLY)

DIRECTION OF STAR COORDINATE FRAME RELATIVE TO ACTUAL IMU AXES - COARSE ALIGN (IDENTICAL TO Q-23 AND Q-10 COMPUTATIONS) 33

$$S^*_{11_\nu} = a'_\nu$$
$$S^*_{12_\nu} = b'_\nu$$
$$S^*_{13_\nu} = c'_\nu$$
$$S^*_{21_\nu} = (b'_\nu c''_\nu - c'_\nu b''_\nu)/\sin\mu_{s_\nu}$$
$$S^*_{22_\nu} = (c'_\nu a''_\nu - a'_\nu c''_\nu)/\sin\mu_{s_\nu}$$
$$S^*_{23_\nu} = (a'_\nu b''_\nu - b'_\nu a''_\nu)/\sin\mu_{s_\nu}$$
$$S^*_{31_\nu} = S^*_{12_\nu} S^*_{23_\nu} - S^*_{13_\nu} S^*_{22_\nu}$$
$$S^*_{32_\nu} = S^*_{13_\nu} S^*_{21_\nu} - S^*_{11_\nu} S^*_{23_\nu}$$
$$S^*_{33_\nu} = S^*_{11_\nu} S^*_{22_\nu} - S^*_{12_\nu} S^*_{21_\nu}$$

DOUBLE PRIME DENOTES SECOND STAR.
ν DENOTES EITHER f, FINE ALIGN OR C, COARSE ALIGN

ANGLE BETWEEN NAVIGATION STARS 32

$$\cos\mu_{s_\nu} = a'_\nu a''_\nu + b'_\nu b''_\nu + c'_\nu c''_\nu \qquad 0 \le \mu_{s_\nu} \le \pi$$

TRANSFORMATION BETWEEN ACTUAL IMU AXES AND IDEAL IMU AXES 34

$$(S^{**}_{ij_\nu}) = (S_{i\ell})^T (S^*_{\ell j_\nu})$$

EULER ANGLE ERRORS BETWEEN ACTUAL IMU AXES AND IDEAL IMU AXES 35

$$\tan\theta_{e_\nu} = \frac{-S^{**}_{13_\nu}}{S^{**}_{11_\nu}}$$
$$\tan\psi_{e_\nu} = \frac{S^{**}_{12_\nu}}{S^{**}_{11_\nu}\cos\theta_{e_\nu} - S^{**}_{13_\nu}\sin\theta_{e_\nu}}$$
$$\tan\phi_{e_\nu} = \frac{-S^{**}_{32_\nu}}{S^{**}_{22_\nu}}$$

REPEAT LOOPS (Q-21) TO (Q-25) FOR SECOND STAR.
$\hat{r}''_{P/S} = a''_f \hat{i} + b''_f \hat{j} + c''_f \hat{k}$.

FINE ALIGN MODE - TECHNIQUE - 2.

TRANSFORMATION CORRECTION FOR RETICLE OFFSET 21

$$h^*_{ij} = \begin{bmatrix}\cos\gamma & -\sin\gamma & 0\\ \sin\gamma & \cos\gamma & 0\\ 0 & 0 & 1\end{bmatrix}$$

IF:	THEN:
RETICLE AT REF. SETTING	$\gamma = 0$
RETICLE NOT AT REF. SETTING	γ SPECIFIED BY DIAL ROTATION

TRANSFORMATION FROM RETICLE AXES TO IMU AXES 22

WHEN X_T MARK ACTIVATED COMPUTE:

$$(u_{ij})_{X_T} = (d'^T_{ik})_{X_T} (h^T_{k\ell})_{\pi} h^*_{\ell j}$$

WHEN Y_T MARK ACTIVATED COMPUTE:

$$(u_{ij})_{Y_T} = (d'^T_{ik})_{Y_T} (h^T_{k\ell})_{\pi} h^*_{\ell j}$$

VECTOR DIRECTIONS NORMAL TO STAR VECTOR MEASURED IN PLATFORM COORDINATES 23

WHEN:	THEN COMPUTE A VECTOR, MEASURED IN PLATFORM COORDINATES, NORMAL TO:
X_T MARK ACTIVATED	THE X_T-Z_T PLANE: $\hat{r}^*_{P_{X_T}} = (u_{ij})_{X_T}\begin{bmatrix}0\\1\\0\end{bmatrix} = (u_{12})_{X_T}\hat{i} + (u_{22})_{X_T}\hat{j} + (u_{32})_{X_T}\hat{k}$
Y_T MARK ACTIVATED	THE Y_T-Z_T PLANE: $\hat{r}^*_{P_{Y_T}} = (u_{ij})_{Y_T}\begin{bmatrix}1\\0\\0\end{bmatrix} = (u_{11})_{Y_T}\hat{i} + (u_{21})_{Y_T}\hat{j} + (u_{31})_{Y_T}\hat{k}$

STAR VECTOR MEASURED IN PLATFORM COORDINATES 24

$$\hat{r}'_{P/S} = \frac{\hat{r}^*_{P_{Y_T}} \times \hat{r}^*_{P_{X_T}}}{\sin\mu_f} = a'_f\hat{i} + b'_f\hat{j} + c'_f\hat{k} \quad ; \; 0 \le \mu_f \le \pi$$
$$a'_f = \left[(u_{21})_{Y_T}(u_{32})_{X_T} - (u_{31})_{Y_T}(u_{22})_{X_T}\right]/\sin\mu^*_f$$
$$b'_f = \left[(u_{31})_{Y_T}(u_{12})_{X_T} - (u_{11})_{Y_T}(u_{32})_{X_T}\right]/\sin\mu^*_f$$
$$c'_f = \left[(u_{11})_{Y_T}(u_{22})_{X_T} - (u_{21})_{Y_T}(u_{12})_{X_T}\right]/\sin\mu^*_f$$

ANGLE BETWEEN VECTORS NORMAL TO STAR 25

$$\cos\mu^*_f = (u_{11})_{Y_T}(u_{12})_{X_T} + (u_{21})_{Y_T}(u_{22})_{X_T} + (u_{31})_{Y_T}(u_{32})_{X_T} \; ;$$

IF:	THEN:
$\mu^*_f = 0$	STAR LIES ALONG Z_T RETICLE AXIS, $\hat{r}'_{P/S} = (u_{13})_{\gamma}\hat{i} + (u_{23})_{\gamma}\hat{j} + (u_{33})_{\gamma}\hat{k}$

FIGURES

SHEET 1 OF 4

FIGURE-

IMU PLATFORM AXES

FOR CONFIGURATION SHOWN

$\theta_{IMU} = \psi_{IMU} = \phi_{IMU} = 0$

$\theta \neq \psi \neq \phi \neq 0$

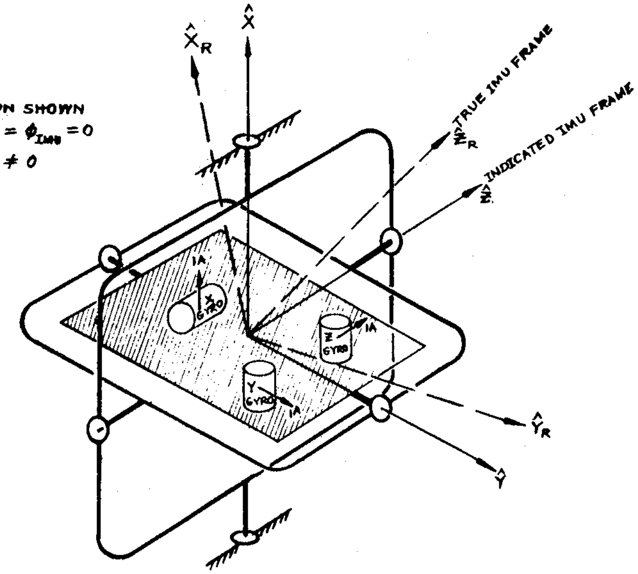

SHEET 1 OF 4

FIGURE-

LANDING SITE SELECTION SCHEMATIC

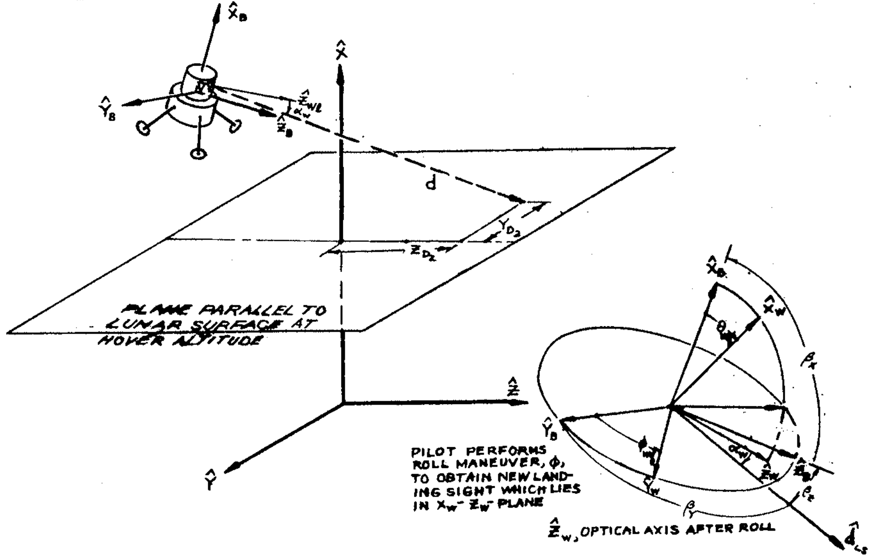

FIGURE-

LEM SEPARATION-TO-TOUCHDOWN SCHEMATIC

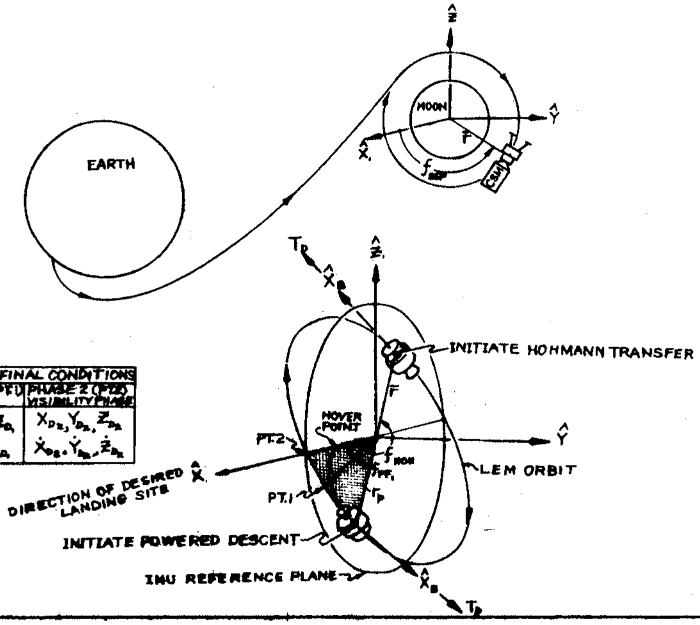

DESIRED FINAL CONDITIONS	
PHASE 1 (PF1)	PHASE 2 (PF2) VISIBILITY PHASE
$X_{D_1}, Y_{D_1}, Z_{D_1}$ $\dot{X}_{D_1}, \dot{Y}_{D_1}, \dot{Z}_{D_1}$	$X_{D_2}, Y_{D_2}, Z_{D_2}$ $\dot{X}_{D_2}, \dot{Y}_{D_2}, \dot{Z}_{D_2}$

FIGURE-

POWERED DESCENT ENGINE IGNITION CRITERIA

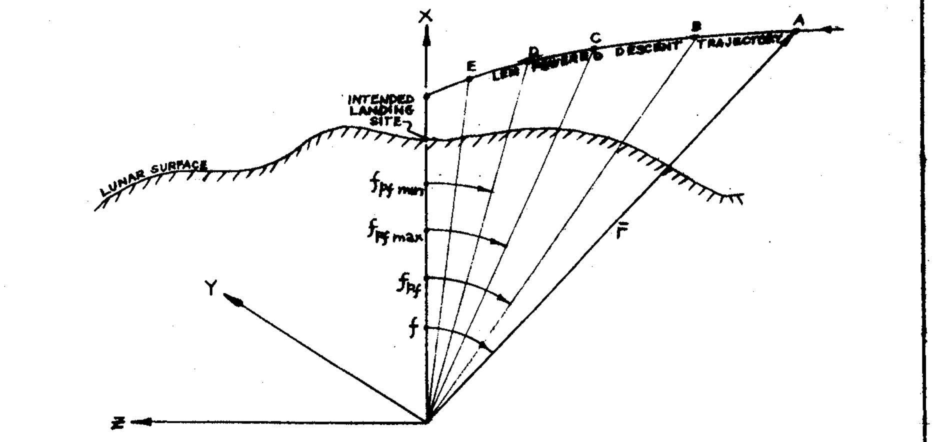

A LEM POSITION DURING POWERED DESCENT TRAJECTORY.

$\overline{BC}$ ANGULAR RANGE DURING WHICH TIME T_{GO} IS COMPUTED AND VEHICLE IS ORIENTED.

$\overline{CD}$ ANGULAR RANGE WITHIN WHICH DESCENT ENGINE SHOULD BE IGNITED.

D IF DESCENT ENGINE IS NOT IGNITED PRIOR TO THIS BOUNDARY THEN LEM CANNOT LAND AT INTENDED LANDING

E START VISIBILITY PHASE. THIS PHASE DEFINED WHEN $T_{GO} = 0$ (SPECIFIED IMPLICITLY BY DESIRED END $F_{D_E}, \dot{F}_{D_1}$).

SHEET 2 OF 4

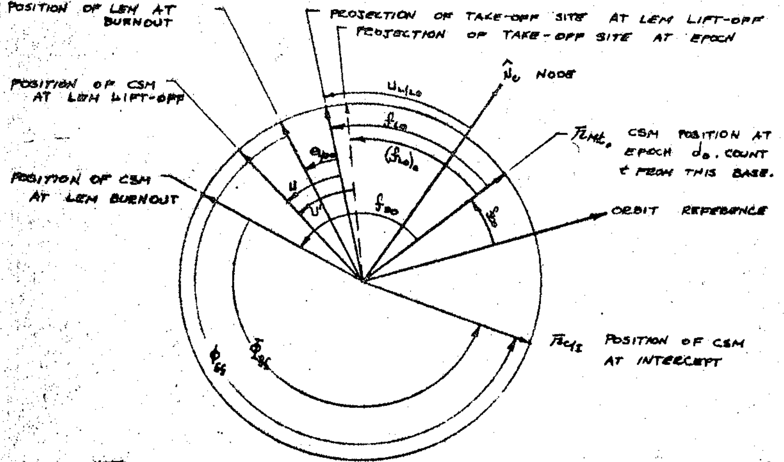

NOTE:
1. ALL ANGLES ARE MEASURED POSITIVE AS SHOWN
2. ALL ANGLES ARE MEASURED IN PLANE OF CSM WITH THE POSSIBLE EXCEPTION OF Θ_{LBO} AND ϕ_{ff}

PRE-LAUNCH SCHEMATIC

SHEET 2 OF 4

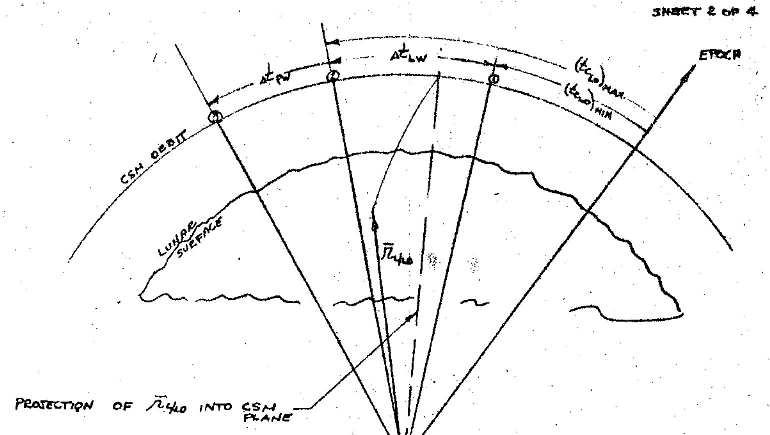

PROJECTION OF $\bar{r}_{4LO}$ INTO CSM PLANE

① FIRST OPPORTUNITY FOR DIRECT LAUNCH TO RENDEZVOUS
② LAST OPPORTUNITY FOR DIRECT LAUNCH TO RENDEZVOUS
③ LAST OPPORTUNITY FOR PARKING ORBIT

LAUNCH WINDOW SCHEMATIC

LAUNCH SCHEMATIC

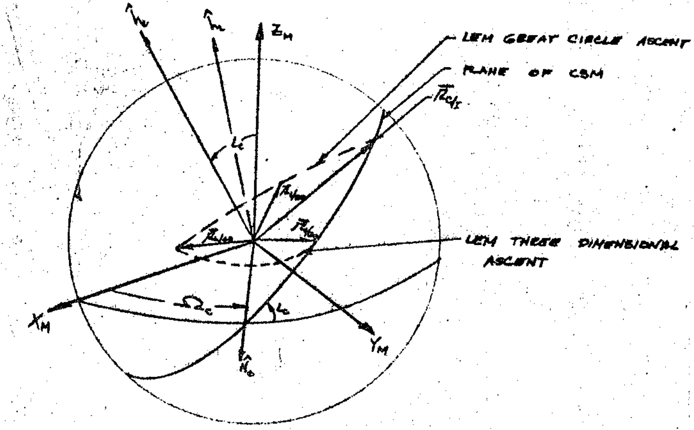

POWERED ASCENT GUIDANCE FLOW DIAGRAM

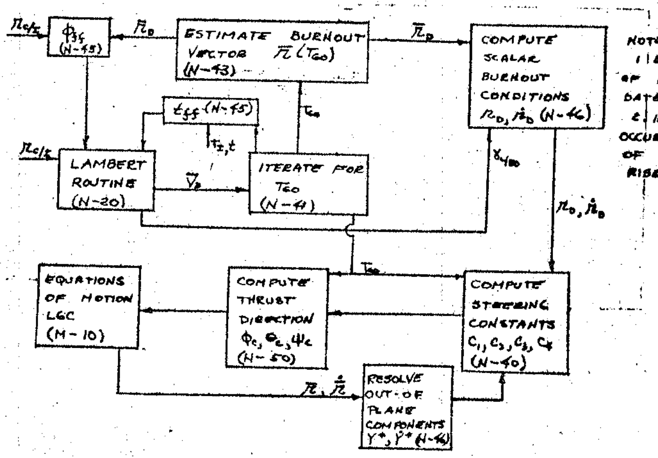

NOTE:
1 EXCEPT FOR END OF MOTION COMPUTE DATE EVERY 60 SEC
2 INITIALIZATION OCCURS AT END OF VERTICAL RISE.

FIGURES

SHEET 3 OF 4

DEFINITION OF ELEVATION AND AZIMUTH ANGLE MEASUREMENT ESTIMATES REQUIRED TO GENERATE THE $\hat{b}$ VECTOR

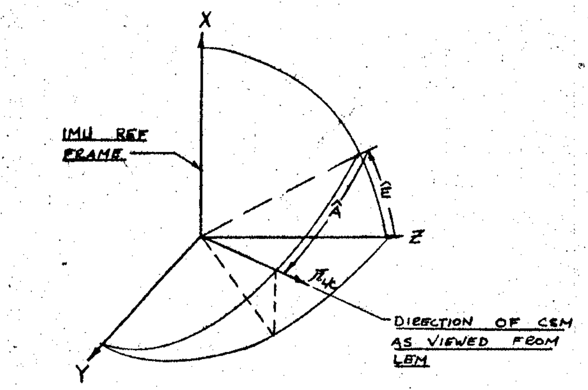

DEFINITION OF VARIOUS ORBIT PLANES

SHEET 3 OF 4

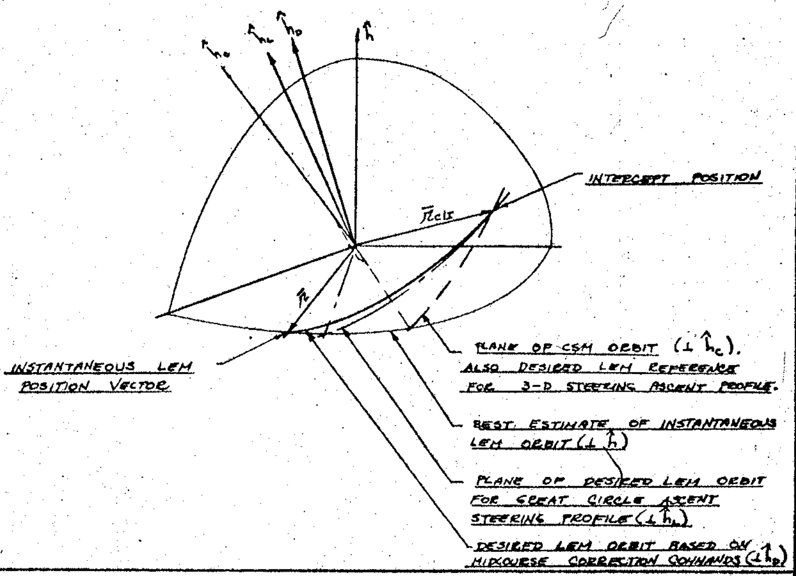

MIDCOURSE VELOCITY CORRECTION FLOW DIAGRAM

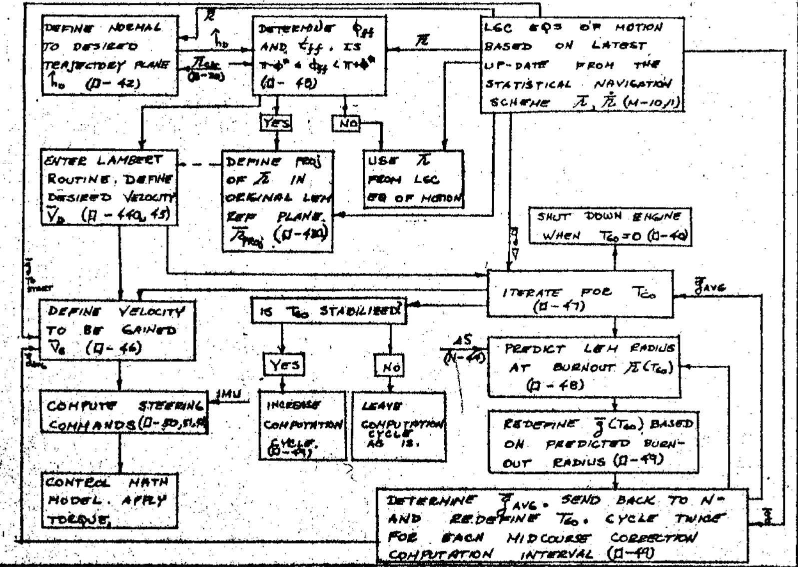

AOT COARSE ALIGN DIRECTION COSINES

γ DENOTES RETICLE ROTATION
$\gamma =$ (PILOT READING) K_R

δ DENOTES SPIRAL ROTATION
$\delta = \frac{\pi}{2}$ - (PILOT READING) K_S

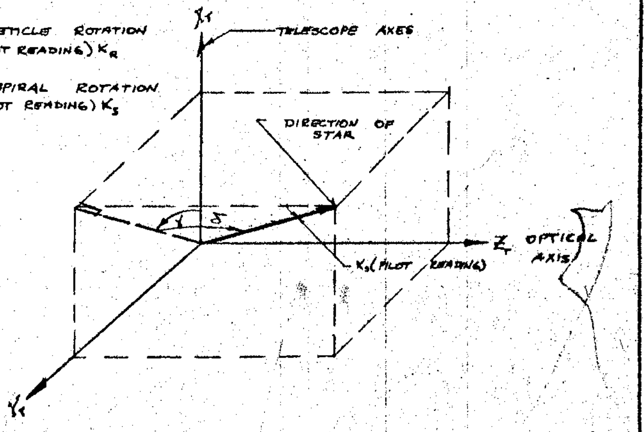

FIGURE -

COORDINATE FRAME SCHEMATIC FOR AOT

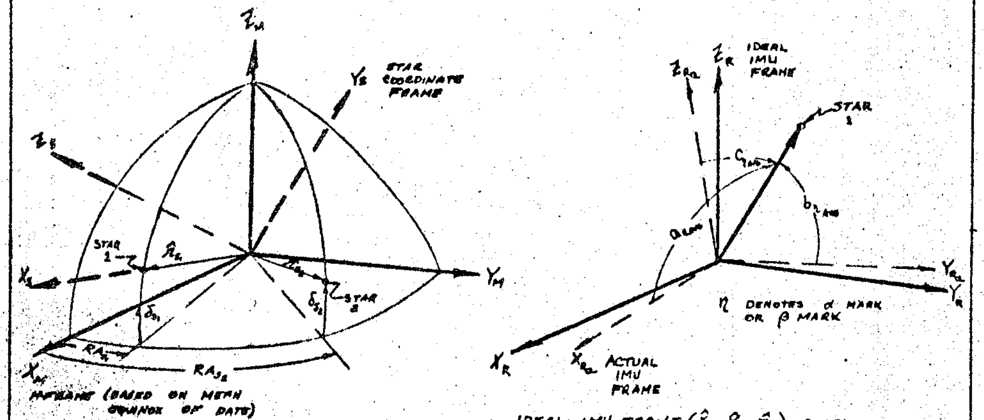

IDEAL IMU FRAME ($\hat{X}_R, \hat{Y}_R, \hat{Z}_R$) DISPLACED FROM ACTUAL IMU FRAME ($\hat{X}_{Ra}, \hat{Y}_{Ra}, \hat{Z}_{Ra}$) BY EULER ANGLES Θ_c, Ψ_c, Φ_c (ROTATE ABOUT Y_{Ra} FOLLOWED BY A ROTATION ABOUT NEW $\hat{Z}_{Ra}$ THEN $\hat{X}_{Ra}$).

FIGURE -

AOT FINE AND COARSE ALIGN SCHEMATICS

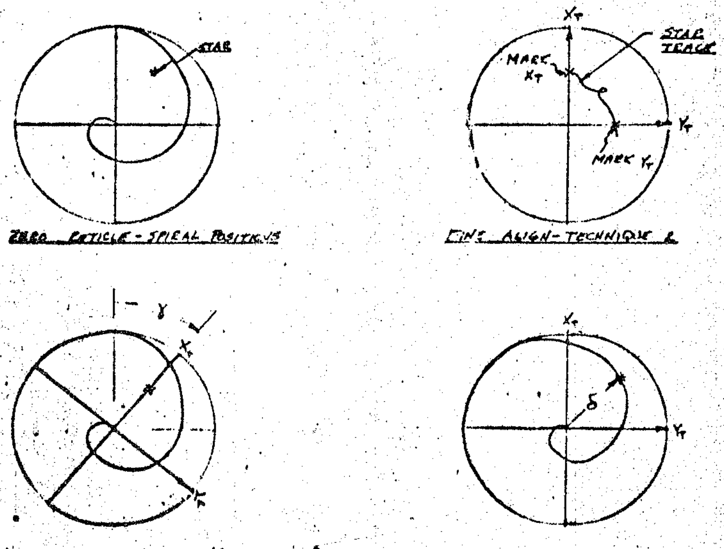

ZERO RETICLE - SPIRAL POSITIONS

FINE ALIGN - TECHNIQUE 2

ROTATE RETICLE γ DEGREES

ROTATE SPIRAL THROUGH ANGLE PROPORTIONAL TO δ DEGREES

9/66

TRUE MOTION EQUATIONS

Part II LMS Data

Section 2. Primary Guidance and Navigation

3. Equation Documentation

3. Equation Documentation

Table of Contents

I. Introduction

This is a description of the Inertial Measurement Unit (IMU) Math Model subsystem for the LEM Mission Simulator. The LEM-IMU provides a pseudo inertial reference which is used to measure changes in vehicle attitude and velocity due to non-gravity accelerations. A reference direction is maintained by fixed platform gyros. Gyro errors cause the platform to drift from the desired space fixed orientation. Periodic realignment is therefore necessary. Alignment is also required whenever the IMU is uncaged, or power is restored, or the desired reference direction is altered. These modes of operation, in addition to simplified fine and coarse align platform modes, are described herein.

Astronaut training is the prime objective of the real-time digital LEM Mission Simulator. The real time constraint requires low sampling intervals. Hence, hardware stable member gyro and accelerometer high frequency characteristic cannot be sensed. Moreover, the training requirement demands that subsystem malfunctions be faithfully included. Malfunctions can be more readily simulated by employing a functional gyro and accelerometer model than by employing an exact hardware gyro and accelerometer model. For these reasons, the explicit hardware representation of the stable member gyro and accelerometer has been neglected in the LMS-IMU math model. A gyro and accelerometer error model is included.

Detailed IMU subsystem equations are presented on "L" sheets 1 and 2 (termed Set L). Set L contains 4 subsets where:

1. Subset L-01 denotes constants and initial conditions.
2. Subset L-10 to L-17 denotes the equations required to define indicated platform gimbal angles.
3. Subset L-20 to L-26 denotes gyro drift and accelerometer output equations.
4. Subset L-30, L-31 denotes the AOT coarse and dine align modes.

Each item is discussed in Section II.

Equations, given in Section II, that are designated by a capital L followed by a number can be found on the L sheets. These equations do not necessarily follow a sequential order in the text since the flow diagrams were generated prior to documentation. Section II equations designated by a small l are used either as intermediaries to derive a subset equation or to present an alternate approach not listed on the L sheets.

II. Category 2 Equations - Primary Guidance and Navigation (Sheet L and Q only)

A. IMU Subsystem Equations

1. Indicated IMU Gimbal Angles

a. Normal Operation.-LEM Euler angles are sensed by gimbal axes mounted resolvers. Each resolver reflects angular vehicle motions relative to the stable member. In order to define the spacecraft orientation, the stable member directions relative to a known, inertial reference direction must first be ascertained. Let this known reference be the mean equinox, mean equator of date, M or E - frame, $\hat{r}_n$ (see sheet K, sheet 1). Furthermore, at any instant let the LEM platform $(\hat{r}_p)$ orientation relative to the mean equinox, mean equator of date reference system be defined by angles θ, ψ, ϕ where:

1. θ represents a rotation about the Y_n axis.
2. ψ represents a rotation about the new Z_n axis so formed.
3. ϕ represents a rotation about the new X_n axis so formed to locate the physical stable member set $\hat{r}_p$.

The foregoing rotations are combined to form the transformation N_{ij} between $\hat{r}_p$ and $\hat{r}_n$:

$$\hat{r}_p = N_{ij}\hat{r}_n. \qquad (1\text{-}11)$$

The true rotational equations of motion, are solved to generate the time dependency between the LEM body axes and the inertial M or E frame:

$$\hat{r}_B = g_{ij}\,\hat{r}_n. \qquad (D\text{-}40)$$

The relationship between the actual platform and reference platform attitude is given by

$$\hat{r}_p = Q_{ij}\,\hat{r}_n \qquad (L\text{-}11)$$

1261

Substituting equation (1-11) and (L-11) into (D-40) provides the sought for time dependent relationship between the LEM platform axes and the LEM body axes:

$$\hat{r}_B = g_{ij} C^T_{kj} Q^T_{lk} \hat{r}_p$$

whereupon:

$$d'_{ij} = g_{ij} C^T_{jk} Q^T_{kl} \qquad \text{(L-17)}$$

Gimbal angle resolver readouts are generated from matrix d'_{ij}. These angles are defined by equations (L-10). Gimbal lock logic is not provided because, in practice, the platform is caged whenever the middle angle ψ_{IMU} approaches about ± 70 degrees. Gyro or platform caging is simulated by setting the direction cosine matrix d'_{ij} equal to the unity matrix. Thus, $\theta_{IMU} = \psi_{IMU} = \phi_{IMU} = 0$.

b. Cage - Uncage Mode.- As mentioned above, when the gyros are caged the platform and gimbals are essentially locked to the body. When the gyros are uncaged, therefore, matrix Q_{ij} must be reinitialized. Since the body axes orientation is always known relative to the M or E - frame and since $d'_{ij} = (I)$, then from (L-17):

$$Q_{ij_{uncage}} = d^T_{ij} g_{jh} C^T_{lk} = g_{ik} C^T_{lk} \qquad \text{(L-14)}$$

Each time Q_{ij} is reinitialized the angles θ_{do}, ψ_{do}, and ϕ_{do} (L-14a) must also be reinitialized. This requirement stems from the necessity to establish an angular reference from which gyro drift excursions are measured. Thus, during the cage mode, drift loops L-11, L-17, L-10 and L-10a are deactivated.

c. Power-Off, Power-On Mode.-During the power-off mode matrix d_{ij} (and Q_{ij}) may be computed by inserting arbitrary time dependent elements $\theta(t)$, $\psi(t)$, $\phi(t)$ into equation L-13 at the instant the malfunction is inserted. This enables displaying the platform change relative to the body in the FDAI. The power malfunction should continue to be inserted until the gimbal angles have been rotated to prescribed angles.

At the time of power turn on, the IMU should exit into the cage mode which is followed by the alignment procedure.

d. Alter Desired Reference Frame.- The desired platform reference direction $\hat{r}_r$ can be altered during the course of a run by reinitializing the appropriate constants specified by subset equations D-20 or D-30. This computation actually represents an LGC function and has no effect on the platform gimbal angles prior to platform realignment. When the platform is realigned matrix Q_{ij} is forced to change by coarse and fine align angle inputs (L-30, L-31).

2. Gyro Drift and Accelerometer Outputs

a. Platform Drift.- Gyro drift rates preclude the LEM platform from maintaining a desired space fixed orientation (see set R sheet I figure entitled IMU Platform Axes). Matrix Q_{ij} must reflect platform drift. Gyro drift velocities ($\bar{\omega}_d$) act along the LEM platform directions, hence, platform Euler angle rates relative to the desired platform reference frame can be described as:

$$\dot{\theta} = (\cos\psi_d)^{-1}\left[\omega_{Yd}\cos\phi_d - \omega_{zd}\sin\phi_d\right]$$

$$\psi_d = \omega_{zd}\cos\phi_d + \omega_{Yd}\sin\phi_d$$

$$\dot{\phi}_d = \omega_{Xd} - \tan\psi_d\left[\omega_{Yd}\cos\phi - \omega_{zd}\sin\phi_d\right] \tag{L-13}$$

In practice, the drift rates will be small (on the order of a degree per hour) and arbitrary. For the purpose of astronaut training, therefore, no generality is lost by simplifying the Euler rate computations such that equations (L-13) are replaced by:

$$\dot{\theta}_d = \omega_{Yd}$$

$$\dot{\psi}_d = \omega_{zd}$$

$$\dot{\phi}_d = \omega_{Xd} \tag{1-1}$$

Gyro drift rate errors result from a varietyof sources. The most important error contributions are provided in the following drift model:

1863

$$\omega_i = R_i + U_s A_i - U_i A_s + (S_{ss} - S_{ii}) A_s A_i + S_{si} A_i^2 - S_{is} A_s^2$$

Accelerations A_i and A_s correspond to non-gravity acceleration components along the input and spin axes, respectively. Coefficients R, U and S are defined as:

1. R - Fixed gyro drift rate about the input axis.
2. U - Mass unbalance coefficients along the spin and input axes.
3. S - Anisoelastic coefficients associated with a compliance in a given direction due to an external acceleration in an orthogonal direction.

The bias coefficients, R, could be altered during the course of a run to reflect a gyro malfunction or even temperature variations. Furthermore, spurious drift due to noise may also be included if desired.

b. Resolution of Indicated Accelerations to Platform Axes.- Total external accelerations (F_B/m_L) acting at the composite LEM-CG are not sensed by the platform aligned accelerometers since the IMU package is not located at the LEM-CG. Instead, the sensed acceleration is:

$$\bar{A}_B = \frac{\bar{F}_B}{m_L} + \Delta \bar{A}_B \qquad \text{(L-24)}$$

Incremental accelerations, $\Delta \bar{A}_B$, are induced by accelerometers displaced a distance $\bar{d}$ from the LEM rotation vector $(\bar{\omega})$ and are given by:

$$\Delta \bar{A}_B = -\bar{\omega} \times (\bar{\omega} \times \bar{d}) - \dot{\bar{\omega}} \times \bar{d}, \qquad \text{(1-2)}$$

where

$$\bar{\omega} = p_B \hat{i}_B + q_B \hat{j}_B + r_B \hat{k}_B, \qquad \text{(C-11)}$$

and where

$$d = \bar{\alpha}_{IMU} \hat{i}_B + \bar{\beta}_{IMU} \hat{j}_B + \bar{\gamma}_{IMU} \hat{k}_B. \qquad \text{(L-25)}$$

During an emergency situation, the pitch rate can be as large as 20 deg/sec. This results is an incremental centrifugal acceleration error of approximately 0.5 ft/sec^2. Both r_B and p_B, however, would remain small. Moreover, lateral IMU-CG displacements $(\bar{\beta}, \bar{\gamma})_{IMU}$ as well as angular accelerations $(\dot{p}, \dot{q}, \dot{r})_B$ are always small. On these bases, it is recommended that equation (L-24) be simplified by neglecting higher order terms. Expanding and simplifying (L-24) yields:

$$\begin{aligned} A_{X/B} &= \frac{F_{X/B}}{m_L} - \bar{\alpha}_{IMU} q_B^2 \\ A_{Y/B} &= \frac{F_{Y/B}}{m_L} - \bar{\alpha}_{IMU} p_B q_B \qquad \text{(1-3)} \\ A_{Z/B} &= \frac{F_{Z/B}}{m_L} + \bar{\gamma}_{IMU} q_B^2 \end{aligned}$$

1864

External accelerations A_B are measured relative to the LEM body axes. The accelerometers, however, are fixed to the platform and measure non-gravity accelerations, along LEM platform directions. Transforming from body axes to platform axes gives:

$$\bar{A}_{IMU} = d'^{T}_{ij} \ \bar{A}_{B} \qquad (L\text{-}23)$$

Each accelerometer senses the applied acceleration ($\bar{A}_{IMU}$) and issues an output that includes internal accelerometer errors. An error model follows.

c. Accelerometer Outputs.- The accelerometer error model is defined by equations L-22. This model includes a bias error C_i a linear scale factor error C_{ii}, a non-linear scale factor error C_{2i}, bias sensitivity to cross acceleration errors $C4_i$, and an error due to termperature above nominal. Accelerometer malfunctions can be synthesized by altering the appropriate error model coefficients(L-22).

Accelerometer outputs $\bar{A}_{ACC}$ include the sensed accelerations plus instrument errors. These accelerations are defined by equation (L-20) and are used in all LGC calculations. Non-gravity accelerometer velocity outputs are generated by integrating (L-20):

$$\bar{V}_{ACC_L} = \left[\int_{i-1}^{i} \bar{A}_{Acc}\, dt + \Delta V_{XE} \right]_{i-1}^{i} + \left(\bar{V}_{ACC}\right)_0 + \left(V_{ACC}\right)_{i-1} \qquad (L\text{-}21)$$

Velocity outputs, (L-21) should be re-initialized at the termination of each powered maneuver.

3. Platform Alignment Modes

a. Coarse Align. - Platform coarse alignments must be performed prior to LEM-CSM separation, prior to lunar lift-off and during coast maneuvers if the platform is uncaged, power is restored or the desired reference frame is altered. AOT coarse align equations are given on Q sheets 1 and 2. The outputs of these equations are the three coarse align Euler angles θ_{e_c}, ψ_{e_c}, ϕ_{e_c} which describe the orientation of the desired reference relative to the misaligned LEM platform reference.

On pilot command, the IMU gimbals are slewed to negate the coarse align Euler angles. For the purpose of LMS simulation, gimbal motor transients are neglected. Accordingly, it is proposed to slew the gimbals sequentially at constant velocities $(\dot{\theta}, \dot{\psi}, \dot{\phi})_{e_c}$ until the errors reduce to some limiting value. The IMU coarse align technique is outlined in (L-30).

1265

b. Fine Align.- The fine align mode is normally activated after each coarse alignment is made. This mode is also activated periodically, during coasting flight, for the purpose of minimizing platform drift. Fine align errors are computed in Q sheets 1, 2, 3,. On command the platform gimbals are slewed to negate fine align errors with $\dot{\theta}_{ef}$, $\dot{\psi}_{ef}$, $\dot{\phi}_{ef}$.

Rates $(\dot{\theta}, \dot{\psi}, \dot{\phi})_{ef}$ are sequenced until the fine align errors are reduced to some prespecified level (L-31).

1266

B. Power Servo Assembly (PSA)

1. Introduction

The PSA hardware is a support item used in all real system operations of the IMU and LGC. It consists of six amplifiers (gimbal servo and coarse align amplifier), relays for IMU moding, power supply electronics for generating various power sources, and a Failure Indicating Module (FIM). The function of the FIM is to detect errors in the IMU servo errors or the loss of either or both of gyro spin supply and the 3.2 KC supply.

An independent model for PSA does not exist for LMS; however, the equivalent of PSA modeling for the LMS is implicitly included in the analytical IMU mode, sheets L 1 and 2.

2. LMS Simulation

a. Power Supply Simulation.- Modeling of the power supply section is accomplished by assigning booleans to the various input and output power sources which are then included with particular variables in the quations on sheets L. The variable or variables to which the boolean is attached must of course be dependent in actual system operation; thus by the assignment of an "0" or "1" (as the case may be) to the boolean, the effect of the power supply operation or the IMU variable may be simulated.

The booleans assigned to power sources are listed in the LMS Symbol Definition Tables. The real world assignment of booleans to the power sources was made with the aid of overall PSA DWG LDW-370-21001 sheet 5.00 (see Part I Section 3 - level 3 dwgs). A simplified reference block diagram (figure II-2-3-1) showing the power supply with assigned booleans and power supply destinations is also provided in this section.

1267

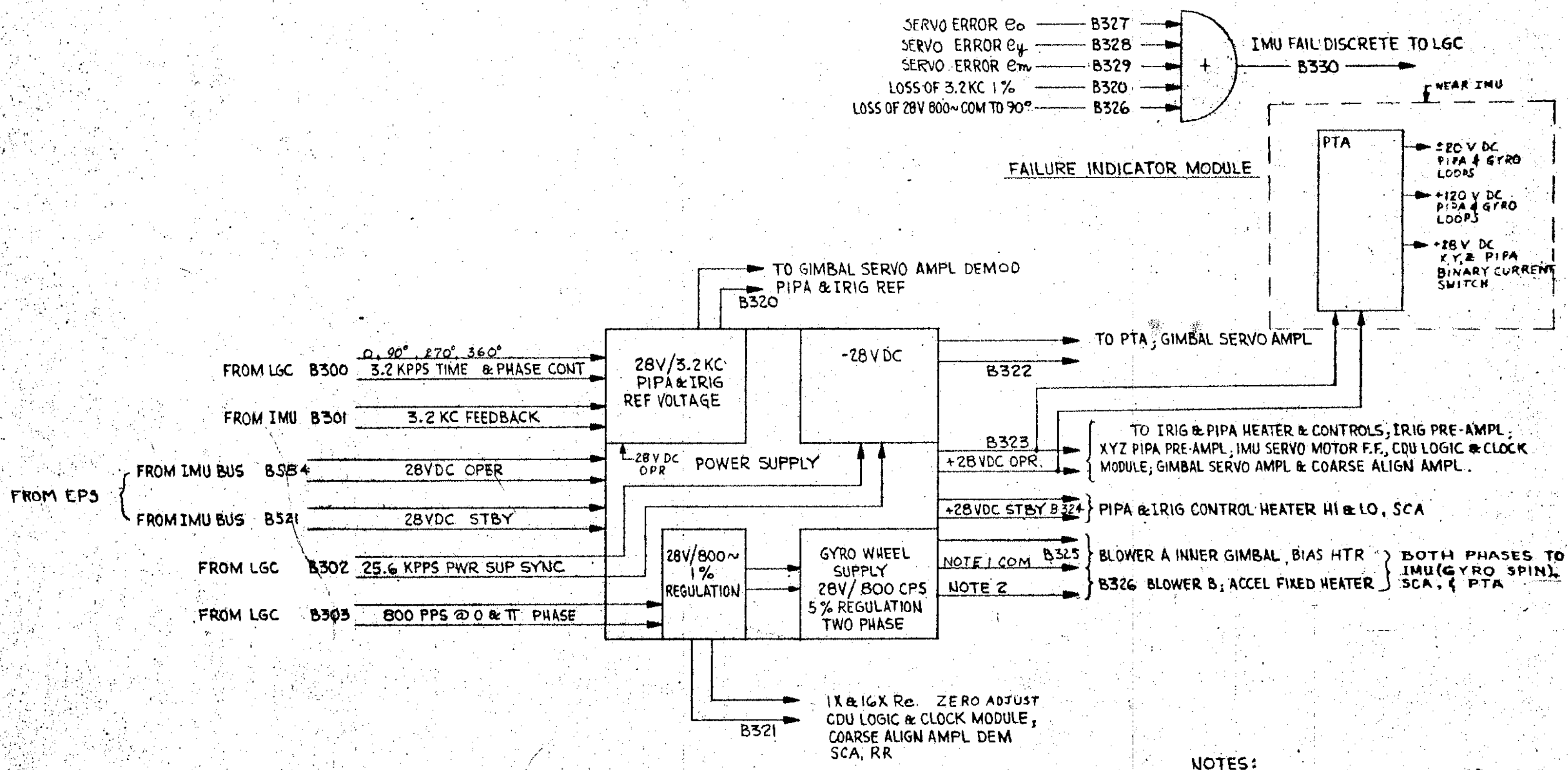

NOTES:

1. PHASE A: 0° PHASE
2. PHASE B: -90° PHASE

F.F. = FIXED FIELD

ABBREV:

PTA: PULSE TORQUING AMP
SCA: SIG COND ASS'Y
RR: RENDEZVOUS RADAR

FIGURE II-4-1
POWER AND SERVO AMPLIFIER SUPPLY

Figure II-2-3-1. Power & Servo Amplifier Power Supply - PG&N Less Radar

GRUMMAN AIRCRAFT ENGRG CORP. BETHPAGE, L.I. NEW YORK

SIZE	CODE IDENT NO.		
D	26512	LED-440-3 LMS MATH MODEL	A

11/65 1 1864

b. Failure Indicating Module Simulation.- Simulation of the Failure Indicating Module is shown in block L-10a. It is a logic "or" expression which shows that a descrete is generated (B330) if anyone or any combination of the following malfunctions occur:

$e_Y \geq$ 5.5 vrms

$e_m \geq$ 5.5 vrms

$e_o \geq$ 5.5 vrms

Loss of Gyro Spin Supply

Loss of 3.2 KC Supply $(\bar{B}_{320})$

c. Gimbal Servo and Coarse Align Amplifier Simulation.- Modeling of the Gimbal Servo and Coarse Align Amplifiers are inherent in the equations given in boxes L-12 and L-13.

In actual system operation the Coarse Align Amplifiers are used in the IMU Cage and Coarse Alignment. The modeled coarse align amplifiers are given by the quantities $\int \dot{\theta}ecdt$, $\int \dot{\psi}ecdt$, and $\int \dot{\phi}ecdt$ in block L-12. In the cage operation, the coarse align amplifiers are modeled by the unity matrix d'_{ij}.

The Gimbal and Coarse Align amplifiers in the PSA are shown in Ref. DWG LDW-370-21001 Sheet 5 in Part I, Section 3 (level 3 dwg). The power sources required for operation of these amplifiers are shown in this reference drawing and in figure II-2-3-2.

In actual system operation the gimbal servo amplifiers are used for IMU fine alignment and during inertial mode operation. The modeled servo amplifiers in the fine align mode are given by the expressions $\int \dot{\theta}_{ef}$, $\int \dot{\psi}_{ef}$, $\int \dot{\phi}_{ef}$ in block L-12. During inertial operation the modeled servo amplifiers are given by the expression below shown in block L-12.

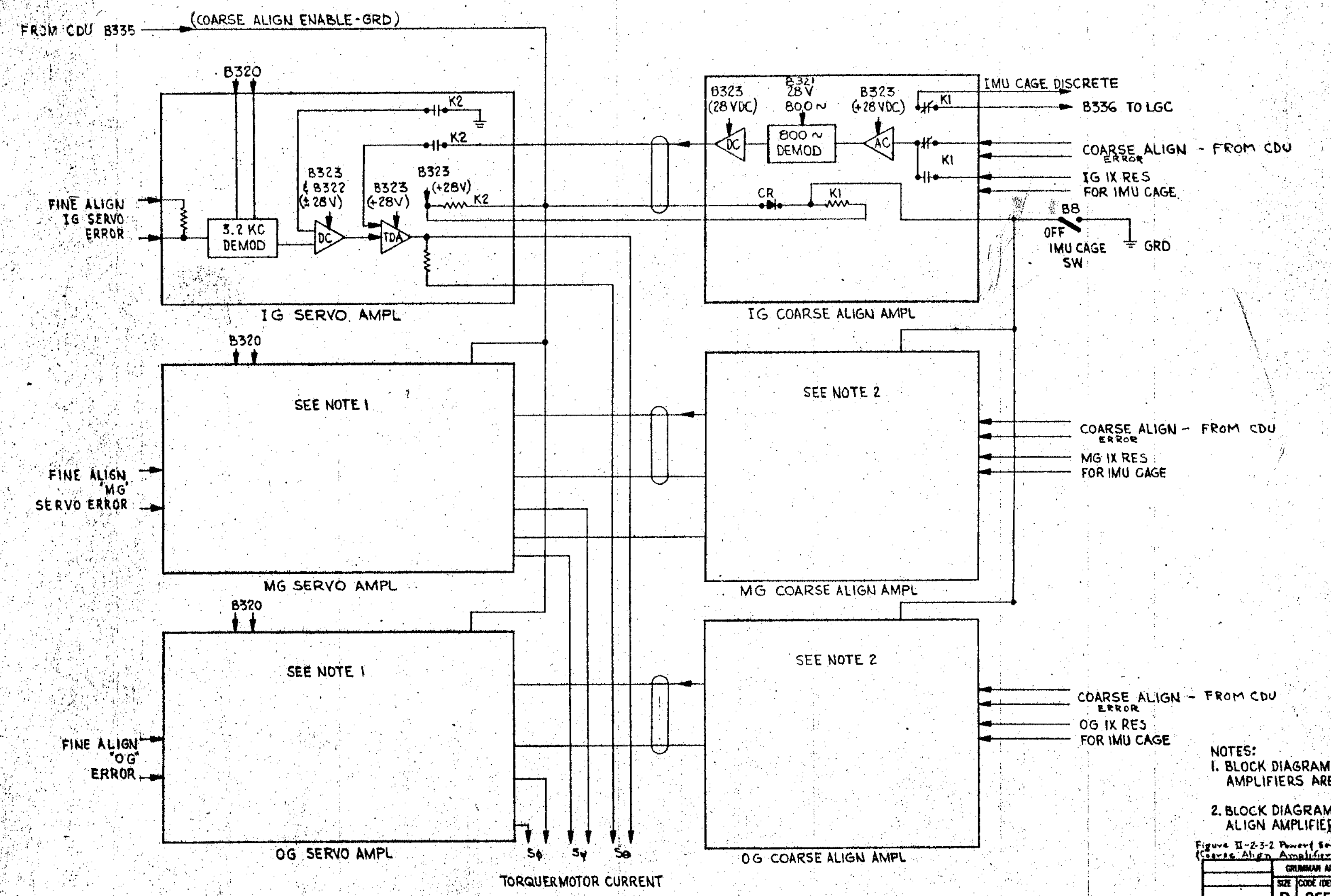

FIGURE II-4-2 - POWER & SERVO AMPLIFIER - GIMBAL SERVO AMPLIFIERS & COARSE ALIGN AMPLIFIERS

NOTES:
1. BLOCK DIAGRAM FOR IG, MG & OG SERVO AMPLIFIERS ARE THE SAME.

2. BLOCK DIAGRAM FOR IG, MG & OG COARSE ALIGN AMPLIFIERS ARE THE SAME.

Figure II-2-3-2 Power Servo Amplifier - Gimbal Servo Amplifiers (Coarse Align Amplifiers - PGN Less Radar

MANUFACTURING OPERATIONS
UNLESS OTHERWISE SPECIFIED
NOTES CHECKED ✓ APPLY TO THIS DWG.

PART NUMBER
AND ALL OTHER MARKINGS
IN REGION MARKED
USE BOTH SIDES IF NECESSARY.

FILLET AND INSIDE CORNER
RADII TOLERANCES
.0158 TO .0629 ± .008
.0630 TO .2500 ± .015
OVER .2500 ± .030

DEPTH SHOWN FOR TAPPED
HOLES IS FULL THDS 1-1 IMP. THDS
BEYOND PERMISSIBLE

EXTERNAL THREAD LENGTH
SHOWN INCLUDES
2 IMPERFECT THREADS MAX.

DO NOT CADMIUM PLATE & PAINT
HOLES OR SURFACES MARKED
WITH DOUBLE ASTERISK

MISMATCH STEP OF ± .005
PERMISSIBLE DUE TO CHANGE
OF CUTTERS AT INSIDE
INTERSECTING SURFACES

DIAMETERS MARKED
MUST BE CONCENTRIC WITHIN
FULL INDICATOR
READING

HOLES MUST BE KEPT FREE OF
CHROME PLATING SOLUTION

ALL DIMENSIONS SHOWN TO BE MET
AFTER CADMIUM PLATING
THICKNESS OF PLATE .0003 MIN
TO .0005 MAX. MIN THICKNESS TO
BE .0002 ON THREADED AREAS.
NO ALLOWANCES FOR PLATING IN
HOLES

125 SURFACE ROUGHNESS
INCLUDING REAMED HOLES
PER MIL-STD-10

200 FOR ALL DRILLED HOLES

REMOVE ALL BURRS
BREAK ALL EDGES .015-.030

INSPECTION INFORMATION
MINIMUM PERMISSIBLE
AVERAGE EDGE DISTANCE
MARKED IS

SYMBOL ✓ DENOTES SURFACE
TO BE MACHINED

UNLESS OTHERWISE SPECIFIED
TOLERANCE ON FLANGES IS ± 1/32

LENGTHS OF AN, NAS & MS AL ALY
RIVETS SHORTER THAN 1 INCH ARE
NOT SPECIFIED

TOLERANCE ON LOFTED
DELINEATIONS IS

GRUMMAN AIRCRAFT ENGRG CORP. BETHPAGE, L. I., NEW YORK

SIZE	CODE IDENT NO.		
D	26512	LED-440-3 LM3 MATH MODEL	A

MODEL OR END ITEM | SCALE | SHEET 1

11/65 1 1866

During inertial operation the modeled servo amplifiers are given by the expression below shown in block L-12.

$$\theta_d = \theta_{do} + B_{320} \int \dot{\theta}_d dt$$

$$\psi_d = \psi_{do} + B_{320} \int \dot{\psi}_d dt$$

$$\phi_d = \phi_{do} + B_{320} \int \dot{\phi}_d dt$$

In order to provide servo errors required for telemetry and for inputing to the Failure Indicator Module, the servo error in actual IMU coordinates must be computed. This computation is shown in block L-10a. The constants K_y, K_m, and K_o are simplified servo motor transfer functions relating IMU gimbal rates to servo amplifier output. Servo motor legs have been neglected.

d. Moding. - In the simulation, system (PGNCS) moding is accomplished by the terms in the equations shown in box L-12. These modes are defined in LSP 470-2A "Master End-Item Specification for LEM", page 99.

C. Coupling Data Units (CDU)

1. Introduction

The CDU's transmit three IMU gimbal angles to the LGC. In addition, during certain align modes (coarse align, cage), the CDU's act in a reverse fashion and slew the gimbals to a new orientation. For LMS purposes, the CDU role of A-D conversion is not required since the models (IMU, LGC) are in digital form. For example, the CDU angles are in digital format in Block L-10. The inclusion of the CDU function in the IMU analytical model during align and display modes is discussed next.

2. LMS Simulation

As previously discussed, the major CDU role of A-D Conversion of IMU gimbal angles and subsequent transmission to LGC is not required in the LMS simulation. The gimbal angles are available in digital format in block L-10. The CDU role in IMU CAGE, COARSE ALIGN, FINE ALIGN and "Inertial" modes is considered next.

a. IMU Cage.- During this mode the IMU stable member axes are aligned with the body axes. This is accomplished by forcing the d_{ij} matrix (block L-17) to a unity value. The gimbal angles, θ_{IMU}, ψ_{IMU}, and ϕ_{IMU}, assume a reading of zero degrees. Since the d_{ij} matrix is held at unity, the body can still be in motion during cage (g_{ij} matrix Block L-17). Therefore the Q_{ij} matrix (block L-11) must be re-initialized when coming out of the cage mode to preclude false astronaut cues on the "8" ball. This is accomplished by blocks L-14 and L-14a.

b. Coarse Align.- The CDU function here is to command the IMU gimbals to a new orientation. The commands are either derived from star shots (Q series) or astronaut entered DSKY input. Block L-30, in the IMU model, contains the equations for coarse align.

c. Fine Align.- In this spacecraft mode the CDU acts to repeat gimbal angles to the LGC. The CDU is not conditioned to operate in this spacecraft mode. For example, the CDU must receive conditioning signals to operate in coarse align and IMU cage. The fine align signals are generated in the "Q" series and applied to block L-31 in the IMU model.

d. Inertial.- The CDU operates in this mode the same way as described under Fine Align. The gimbal angles appear in block L-10 of the IMU model. In addition, the CDU is utilized to display steering errors on the error needles of the "8" ball. Steering errors are generated in equation 13 of the Digital Autopilot (DAP) math model. An ERROR COUNTER ENABLE conditions the CDU, under LGC program control, to allow this display. LGC program information is not available at this time.

D. Alignment Optical Telescope (AOT) - Sheet Q

1. Introduction

The AOT is a unity power telescope, mounted on the navigation base, which is used to align the IMU during free-fall and prior to launch from the lunar surface. Platform alignment is achieved by using optical sightings of at least two stars to determine the IMU orientation with respect to an inertial frame. Optical sightings are performed by the astronaut. Optical readings are marked into the LGC where computations are made to determine misalignment angles between the actual and desired platform orientation. The simulation equations that define the misalignment between the desired and actual platform orientation, based on both fine and coarse alignment modes of operation, are described in this section.

Detailed AOT subsystem equations are presented in Sheets Q-1 and Q-2. Set Q contains 4 subsets where:

a. Subset Q-01 denotes constants and the star catalogue.

b. Subset Q-10 to Q-12 presents the equations required to establish a star coordinate frame relative to the desired platform orientation (Sec. 2).

c. Subset Q-20 to Q-25 presents the fine align mode equations and the equations required to define a star's direction based on AOT reticle readings. (Sections 3, 4 and 6).

d. Subset Q-30 to Q-35 presents the coarse align mode equations and the actual platform misalignment errors (Section 5, 7).

Equations, given in the following Sections, that are designated by a capital Q followed by a number can be found on sheets Q-1 and Q-2. These equations do not follow a sequential order in the text since the flow diagrams were generated prior to documentation. Test equations designated by a small q followed by a number are used as intermediaries to derive a subset equation and, as such, cannot be found on sheets Q-1 and 2 flow diagrams. Equations not defined by either a small q or a capital Q can be found in references 2, 3 or 4.

Equations derived in Sections 2 through 7 were based on a description of the AOT given in reference 1. Each symbol given on sheets Q1 and Q2 are defined in the Symbol List.

2. Star Frame In Desired Platform Coordinates

Fifty-four stars are used for navigation and alignment purposes. Each star is catalogued in the LGC and specified in terms of a right ascension (RA_s) and declination (δ_s) relative to the mean equinox, mean equator of date reference system. It is assumed that the star catalogue is consistent with observational data that can be obtained from AOT sightings. Accordingly, corrections for proper motion, orbital motion and aberration need not be computed. Whenever the astronaut selects a star, the direction of the star in the mean equinox system is therefore known:

$$\begin{aligned} \hat{r}_{sk} &= \cos\delta_{sk} \cos RA_{sk}\, \hat{i}_s \\ &\quad + \cos\delta_{sk} \sin RA_{sk}\, \hat{j}_s + \sin\delta_{sk}\, \hat{k}_s \end{aligned} \qquad \text{(q-1)}$$

Subscript k denotes either star 1 or 2. At least two stars are required to align the platform.

In order to define platform orientation errors, it is necessary to compute star directions in desired platform coordinates. The desired platform coordinates, relative to the mean equinox system, have been computed in reference 2 for either Earth (E) or Moon (M) mission exercises:

$$\hat{r}_R = (C_{ij})_n\, \hat{r}_n \qquad n = E \text{ or } M \qquad \text{(D-20, 30)}$$

Accordingly, the direction of any star can be transformed from the M or E frame to the desired platform frame by substituting equation (q-1) into (D-20, 30):

$$\hat{r}_{R/S_k} = (C_{ij})_n \hat{r}_{sk} \qquad \text{(Q-12)}$$

Hence, for stars 1 and 2:

$$\hat{r}_{R/S1} = V_{x_1} \hat{i}_R + V_{y1} \hat{j}_R + V_{z1} \hat{k}_R$$

$$\hat{r}_{R/S2} = V_{x2} \hat{i}_R + V_{y2} \hat{j}_R + V_{z2} \hat{k}_R \qquad \text{(Q-12)}$$

Equations (Q-12) form the basis to develop a star coordinate system $\hat{r}_s$. Let coordinate axis $\hat{X}_s$ be arbitrarily directed toward the first star sighted. Then:

$$\hat{X}_s = V_{x1} \hat{i}_R + V_{y1} \hat{j}_R + V_{z1} \hat{k}_R \qquad \text{(q-2)}$$

Next, construct axis $\hat{Y}_s$ normal to the plane defined by the lines of sight to star 1 and star 2:

$$\hat{Y}_s = \frac{\hat{r}_{R/S1} \times \hat{r}_{R/S2}}{\sin \mu s} \qquad \text{(q-3)}$$

Finally $\hat{Z}_s$ completes the star frame triad:

$$\hat{Z}_s = \hat{X}_s \times \hat{Y}_s \qquad \text{(q-4)}$$

Angle μs, given above, denotes the central angle between the two measured stars. Ideally, this angle should be 90°, since, as μs approaches zero, measurement errors are magnified. Angle μs is given by:

$$\cos \mu s = \hat{r}_{R/S1} \cdot \hat{r}_{R/S2}$$

$$0 \leq \mu s \leq \pi \qquad \text{(Q-11)}$$

1273

Combining equations q-2, q-3 and q-4 gives the sought for transformation between the star frame and the platform frame:

$$\hat{r}_s = S_{ij} \hat{r}_R \tag{Q-10}$$

The LGC compares the star coordinates relative to the desired platform orientation (Q-10) with the same star coordinates relative to the actual platform orientation (S^*_{ijv}). The difference in orientation between the two frames is used to generate error signals that drive the actual platform to the desired orientation. Astronaut measurement techniques required to define the star coordinate frame (S^*_{ijv}) in actual platform coordinates are described below following a brief discussion of the telescope optical axes and telescope reticle pattern.

3. Orientation of LEM AOT Axes ($\hat{r}_{Tq}$) Relative to LEM Body Axes ($\hat{r}_B$)

The AOT has three fixed viewing positions relative to the LEM body axes. These positions are provided to ensure that the sun will not be in the field of view when star sightings are made on the lunar surface. By means of a pinion knob, the astronaut can detent the telescope in either position left (1) or above (a) or right (r), (see reference 1).

Consider the left telescope position. Three independent rotations are required to define this telescope orientation relative to the LEM body axis. First rotate about body axis X_B through positive angle ϕ_{T1}. Follow this by a rotation θ_{T1} about the new Y'_B axis so formed. Last, rotate about the optical line-of-sight Z''_B through angle $-\psi_{T1}$ to generate the left telescope coordinate axes $\hat{r}_{T1}$. The last rotation ($-\psi_{T1}$) about the line-of-sight is necessary to simulate prism rotation that occurs whenever the AOT is detented in either the left or right positions. This results because the AOT optics do not have a derotation mechanism. Hence, the astronaut sees the true star field rotated about his line of sight axis ($\hat{Z}_{Tl, r}$).

Right telescope ordered rotations are given by $-\phi_{Tr}$, $+\theta_{Tr}$, and $+\psi_{Tr}$. Only a single rotation ($+\theta_{Ta}$) about the Y_B axis is required to locate the above or center telescope coordinate axes. The foregoing rotations lead to the following operator between the body and telescope systems (reference 2):

$$\hat{r}_{Tg} = (h_{ij})T_q \hat{r}_B \tag{D-70}$$

where, q=1 or r or a.

Prior to any alignment, the astronaut must enter the telescope position into the LGC.

4. AOT Reticle Pattern

The AOT reticle pattern (Figure II-D-4-1) consists of two straight lines (cross hairs) and a spiral which are used to compute the direction cosines of any star in telescope coordinates. For example, let the astronaut rotate the reticle pattern until the X_T cross hair coincides with a predetermined star. The reticle rotation γ is read, entered into the LGC, and marked. Rotation γ corresponds to the angle measured between the X_T axis and the projection of the star's direction into the X_T - Y_T plane.

Once γ has been ascertained, the reticle is further rotated until the spiral coincides with the star. This rotation (θ_s) is also read and marked into the LGC. Angles θ_s and γ define the sought for central angle δ measured between the $\hat{Z}_{Tq}$ optical axis and the star direction, (see sheet Q-1). Angle δ computations follow.

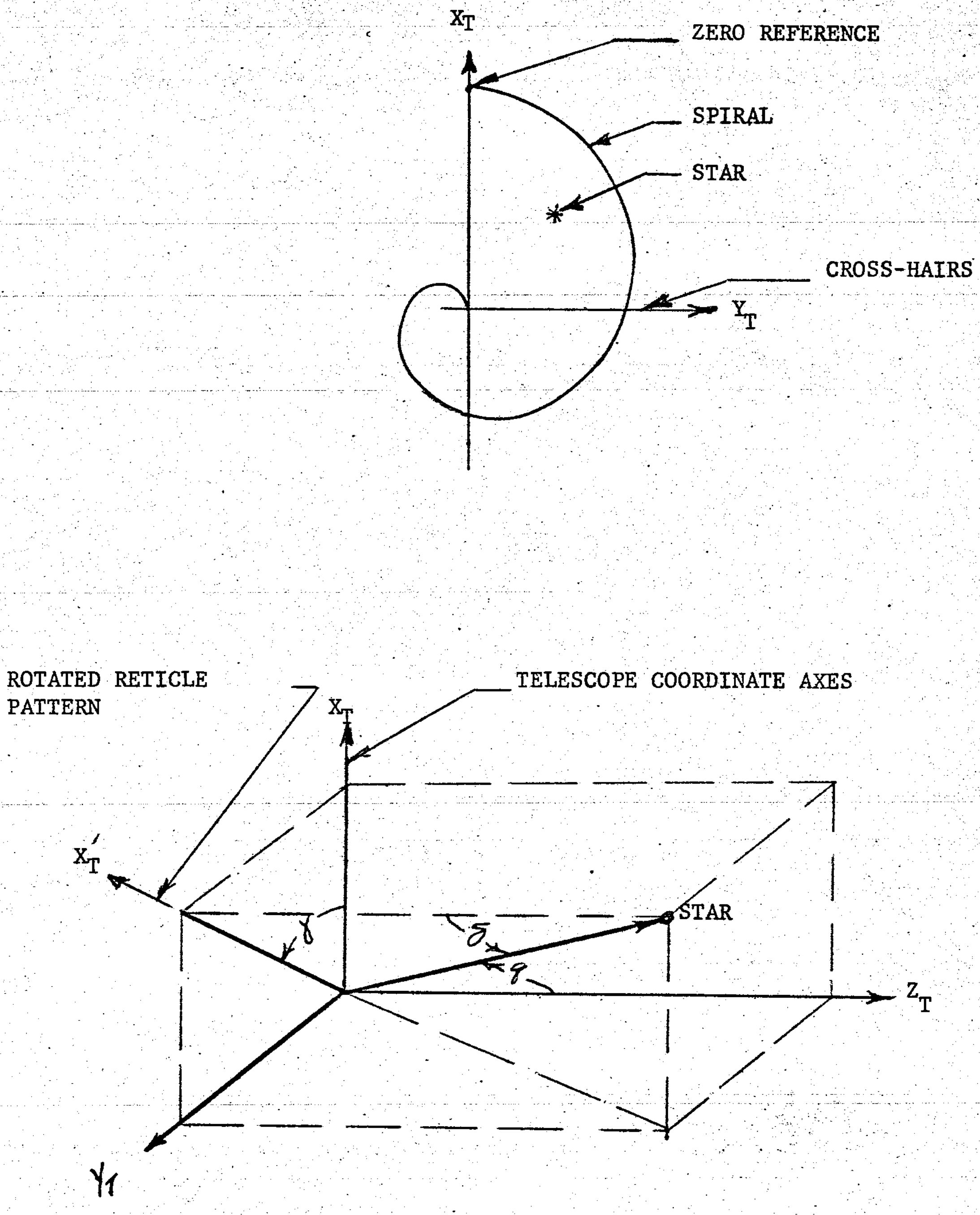

Figure II-D-4-1. AOT Reticle Pattern and Star Direction Cosines

As the spiral is rotated, any point on the spiral departs radially from the center (ρs) as a linear function of rotation. In terms of the fixed telescope, $\hat{r}_{Tq}$ coordinate system;

$$\rho_s = K_s^* \theta_s^* \qquad \text{(q-5)}$$

where, θ_s^* (see Figure II-D-4-2) is the angle measured from the zero X_T direction, counter clockwise to any point on the spiral. Since the distance between the design eye and reticle is fixed (see sketch), angle δ becomes:

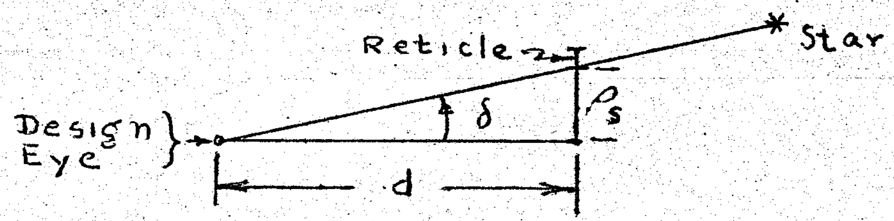

$$\delta = \tan^{-1} \frac{\rho s}{d} = \tan^{-1} K_s \theta_s^*; \quad K_s = \frac{K_s^*}{d} \qquad \text{(Q-20b)}$$

It remains to determine θ_s^*.

Refer to Figure II-D-4-2. Note that all reticle rotations are counted positive in a clockwise direction. On this basis, angle θ_s^* is given by the following logic table.

IF :	THEN :
$(\theta_s - \gamma) > 0$	$\theta_s^* = (\theta_s - \gamma)$
$(\theta_s - \gamma) < 0$	$\theta_s^* = 2\pi - (\theta_s - \gamma)$

(Q-20a)

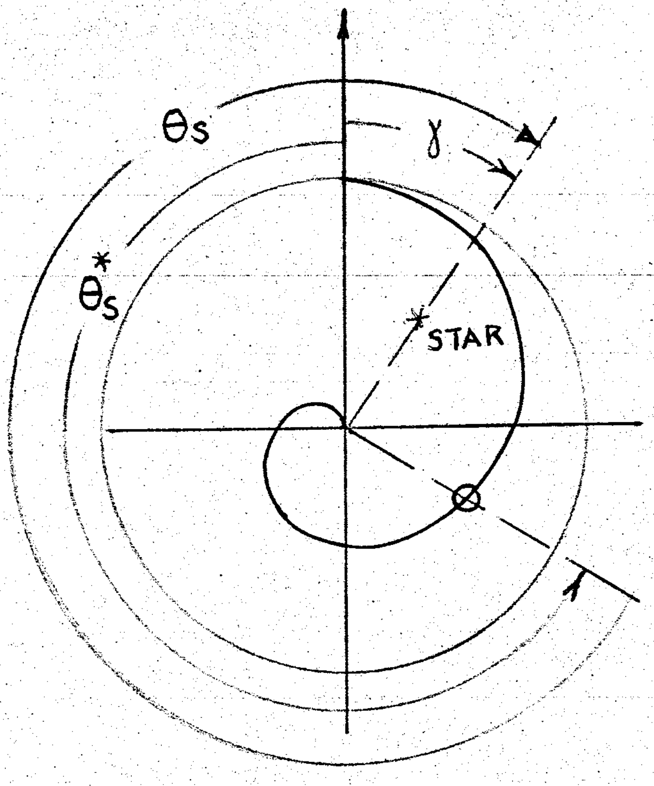

1. Rotate Reticle until X_T cross hair with star. Read γ and mark.
2. Continue to rotate reticle until spiral (point A) coincides with star. Read θ_s and mark.

Note: Rotations shown are positive.

$$(\theta_s - \gamma) \geq 0$$

Spiral angle counted from origin i:

$$\theta_s^* = \theta_s - \delta$$

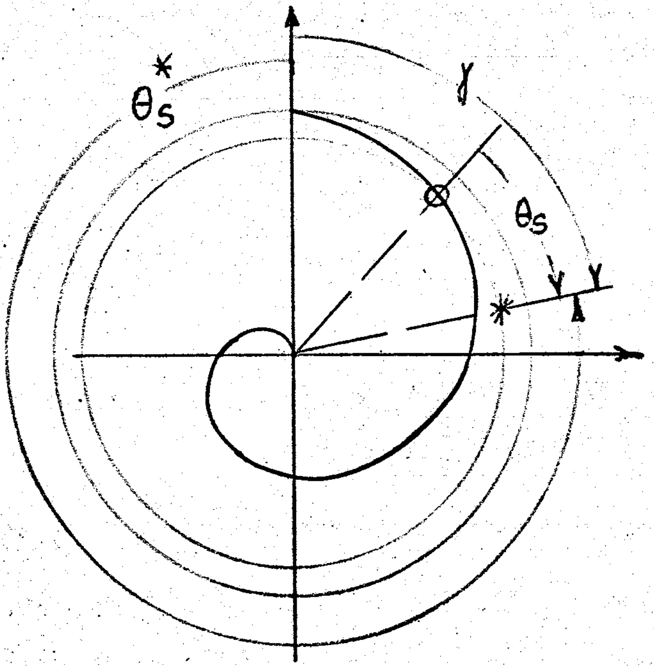

See 1 and 2 above.

$$(\theta_s - \gamma) < 0$$

Spiral Angle counted from Origin is:

$$\theta_s^* = 2\pi - (\theta_s - \gamma)$$

Figure II-D-4-2. Lunar Surface Alignment

5. Coarse Align Mode

a. General.- A coarse align mode is manually initiated whenever the LEM platform deviates from the desired direction by more than one degree. This occurs:

1. On the lunar surface prior to lift-off
2. During free fall following gimbal lock, or a momentary power failure, or excessive platform drift.
3. Prior to LEM-CSM separation.

Each item is discussed below:

b. Coarse Align - Lunar Surface.- On the lunar surface, both coarse and fine align sighting procedures are identical. First, the astronaut selects a telescope viewing position and a navigation star. These data are entered into the LGC. Next, the astronaut rotates the reticle until the cross hair and spiral sequentially coincide with the star. At each crossing, the computer is marked. This enables the computation of angles γ and δ. Thus, the star's direction relative to the telescope axes is ascertained:

$$\hat{r}_{Tq/s} = \cos\delta\cos\gamma\,\hat{i}_{Tq} + \cos\delta\ \sin\gamma\ \hat{j}_{Tq} + \sin\delta\,\hat{k}_{Tq} \qquad (q\text{-}6)$$

The star's direction in body axes coordinates can be found by substituting equation (q-6) into equation (D-70):

$$\hat{r}_{B/s} = (h_{ij}^{T})_{Tq}\ \hat{r}_{Tq/s} \qquad (q\text{-}7)$$

1279

It is assumed that the IMU has been energized; consequently, the direction cosine matrix that relates the platform orientation to the body axes is known at any instant of time (reference 2, 3):

$$\hat{r}_B = d'_{ij}\hat{r} \qquad (L-17)$$

Equations (L-17) and (q-7) define the star's direction measured in platform coordinates:

$$\hat{r}_{P/S} = (d'_{ij})^T (h_{jK})^T_{Tq}\, \hat{r}_{Tq/S} \qquad (Q-31)$$

The above procedure is repeated for a second star. Accordingly, for star 1:

$$\hat{r}'_{P/S} = a'_v \hat{i}_P + b'_v \hat{j}_P + c'_v \hat{k}_P \qquad (Q-31)$$

and for star 2:

$$\hat{r}''_{P/S} = a''_v \hat{i}_P + b''_v \hat{j}_P + c''_v \hat{k}_P$$

Subscript v refers to either the coarse (v = c) or fine (v = f) align mode. Repeated sightings on each of the two navigation stars could be made to increase the accuracy of vectors (Q-31).

Vectors $\hat{r}'_{P/S}$ and $\hat{r}''_{P/S}$ are used to generate a star coordinate system ($\hat{r}_S$) relative to the actual platform orientation. Following the procedure outlined in Section 2, the star coordinate frame is:

$$\hat{X}_S = a'_v \hat{i}_P + b'_v \hat{j}_P + c'_v \hat{k}_P \qquad (q-8)$$

$$\hat{Y}_S = \frac{\hat{r}'_{P/S} \times \hat{r}''_{P/S}}{\sin \mu_{Sv}}$$

$$\hat{Z}_S = \hat{X}_S \times \hat{Y}_S$$

where,

$$\cos \mu_{Sv} = \hat{r}'_{S/P} \cdot \hat{r}''_{S/P} \qquad (Q-32)$$

Equations (q-8) establishes the operator S^*_{ijv}:

$$\hat{r}_S = S^*_{ijv}\, \hat{r}_P \qquad (Q-33)$$

c. Coarse Align - Free Fall. - It is assumed that the platform is energized and stabilized. After the navigation stars have been selected and marked, the astronaut maneuvers the LEM until the desired star is located at the intersection of the cross hairs ($\gamma = \delta = 0$). When the mark buttons are pressed, the direction cosine matrix (d'_{ij}) is recorded and stored. Since γ and δ are both known, vector $\hat{\lambda}'_{P/S}$ (Q-31) is also known. Repeating this procedure for a second star gives $\hat{\lambda}''_{P/S}$. Matrix S^*_{ijc} is therefore defined.

Additional techniques could be used for coarse align. For example, the astronaut could attempt to maintain a fixed LEM attitude and sight a star by rotating the cross hair and spiral. Furthermore, the free-fall fine align technique, discussed in Section 6, could also be used for coarse align.

d. Coarse Align - LEM-CSM Mated. - Prior to separation, when the LEM and CSM are mated, the LEM platform can be coarse aligned by star sightings or more appropriately by duplicating the alignment present in the CSM-IMU. The latter technique is preferred.

6. Fine Align Mode

a. General. - Fine alignments are generally made prior to Hohmann insertion, prior to powered descent and prior to ascent. On the lunar surface, fine and coarse align procedures are identical. During free-fall, only the reticle pattern cross hairs are used to fine align (Figure II-D-6-1). The cross hairs may be at any aribtrary reference angle γ . Once a star has been selected, the telescope position fixed (l, r or a) and γ reference noted, the vehicle is put into the fine attitude hold mode. As the vehicle limit cycles, the astronaut marks the computer each time the star alternately crosses the X'_T and Y'_T axes (see Figure II-D-6-1). Whenever the LGC receives a mark command, the IMU gimbal angles are noted and used to compute the direction cosine matrix (d'_{ij}). Any two consecutive marks (X'_T, Y'_T star crossings) are sufficient to generate the star - platform transformation matrix S^*_{ijf}.

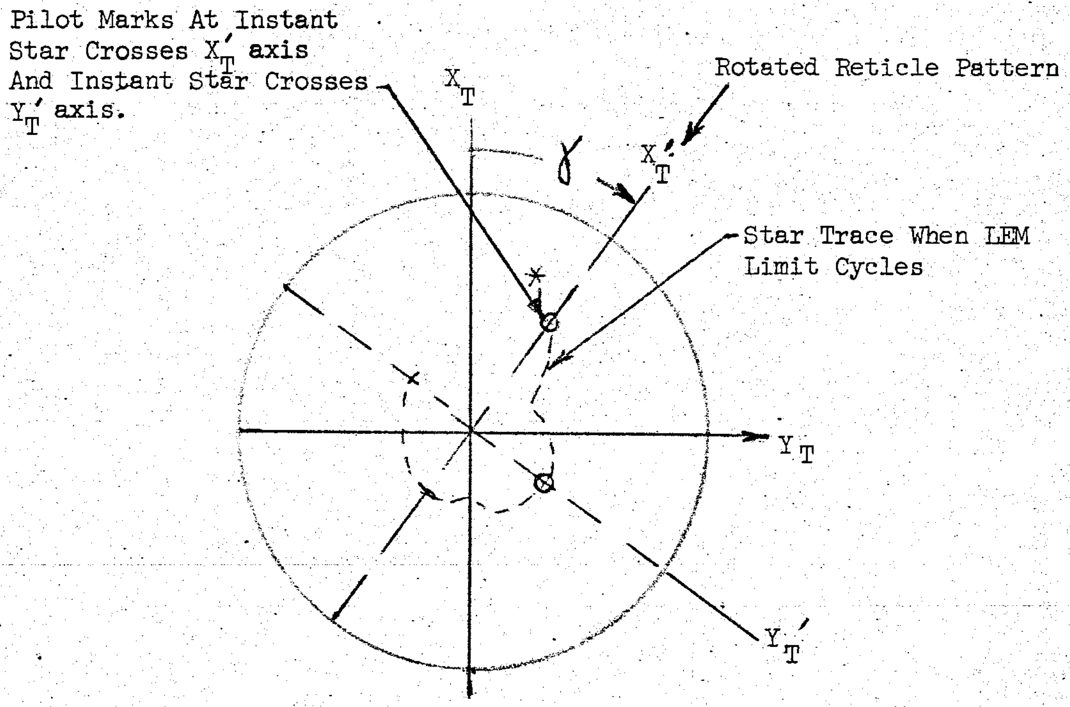

Figure II-D-6-1. Free Fall Fine Alignment

1282

b. Fine Align - Free Fall.- As mentioned above, the reticle cross hairs may be in any known arbitrary position. For this configuration, a transformation is required to relate the rotated reticle position to the original $\hat{r}_{Tq}$ telescope axes. A rotation about $\hat{Z}_{Tq}$ gives:

$$\hat{r}_{Tq} = h^{*}_{ij} \; r'_{Tq} \qquad \text{(Q-21)}$$

where:

$$h^{*}_{ij} = \begin{bmatrix} \cos\gamma & -\sin\gamma & 0 \\ \sin\gamma & \cos\gamma & 0 \\ 0 & 0 & 1 \end{bmatrix}$$

Equation (Q-21), substituted into equation (Q-31) yields the operator between the rotated reticle axes and the platform axes. For the X_T mark:

$$\hat{r}_{Tq} = (u_{ij})_{XT} \, \hat{r}_{Tq} \qquad \text{(Q-22)}$$

For the y_T mark:

$$\hat{r}_{p} = (u_{ij})_{YT} \; \hat{r}'_{Tq} \qquad \text{(Q-22)}$$

where:

$$u_{ij} = (d'^{T}_{ik})(h^{T}_{kl})_{Tq} \; h^{*}_{lj} \qquad \text{(Q-22)}$$

Subscripts X_T and Y_T denote the values of the direction cosine matrix (d'^{T}_{ik}) when the star crosses the rotated X'_T cross hair (X_T mark) and the Y'_T cross hair (Y_T mark), respectively.

Each time the star coincides with a cross hair, the plane containing the star is known. Consider the X'_T crossing. At this instant the star lies in the reticle X'_T - Z'_T plane; consequently, a vector normal to the star can be constructed. Call this vector $\hat{r}'_{Tq}$ where:

$$\hat{r}'_{Tq} = j_{T}{q}' \qquad (q\text{-}9)$$

Substituting (q-9) into (Q-22) relates the direction normal to the star into platform coordinates. Thus:

$$\hat{r}^{*}_{P_{X_T}} = (\mu_{ij})_{X_T} \begin{pmatrix} 0 \\ 1 \\ 0 \end{pmatrix} = (\mu_{12})_{X_T} \hat{i}_p + (\mu_{22})_{X_T} \hat{j}_p + (\mu_{32})_{X_T} \hat{k}_p \qquad \text{(Q-23)}$$

Repeating this procedure for the y_T' crossing produces a second vector, measured in platform coordinates, that is also normal to the star direction:

$$\hat{r}^{*}_{P_{Y_T}} = (\mu_{11})_{Y_T} \hat{i}_p + (\mu_{21})_{Y_T} \hat{j}_p + (\mu_{31})_{Y_T} \hat{k}_p \qquad \text{(Q-23)}$$

Since $\hat{r}^{*}_{P_{X_T}}$ and $\hat{r}^{*}_{P_{X_T}}$ are both normal to the same star, it follows, therefore, that the star direction is specified by the vector cross product; hence:

$$\hat{r}'_{P/S} = \frac{\hat{r}^{*}_{P_{Y_T}} \times \hat{r}^{*}_{P_{X_T}}}{\sin \mu^{*}_{f}} = a'_{f}\hat{i}_{P} + b'_{f}\hat{j}_{P} + c'_{f}\hat{k}_{P} \qquad (Q\text{-}24)$$

Angle μ^{*}_{f} is:

$$\cos \mu^{*}_{f} = \hat{r}^{*}_{P_{Y_T}} \cdot \hat{r}^{*}_{P_{X_T}}$$

A second navigation star is selected and the entire process is repeated. This gives the direction to the second star:

$$\hat{r}''_{P/S} = a''_{f}\hat{i}_{p} + b''_{f}\hat{j}_{p} + c''_{f}\hat{k}_{p} \qquad (Q\text{-}24)$$

Coefficients a, b, and c are employed in equation (Q-33) to define the star coordinate transformation matrix S^{*}_{ijf}

7. Platform Misalignment

A star coordinate system relative to a desired platform orientation has been obtained:

$$\hat{r}_{s} = S_{ij}\,\hat{r}_{R} \qquad (Q\text{-}10)$$

The same star coordinate system has been found relative to the actual platform orientation.

$$\hat{r}_{s} = S^{*}_{ijv}\,\hat{r}_{p}$$

It follows from (Q-10) and (Q-33), therefore, that the orientation between the actual platform and the desired platform is:

$$\hat{r}_{R} = (S_{ij}^{T})(S^{*}_{ijv})\hat{r}_{p} = S^{**}_{ijv}\,\hat{r}_{p}$$

The orientation error between the actual platform and the desired platform is given in terms of Euler angles θ_{ev}, ψ_{ev}, and ϕ_{ev}, where:

a. θ_{ev} represents a rotation about the Y_p platform axis.
b. ψ_{ev} represents a rotation about the new Z_p' axis so formed.
c. ϕ_{ev} represents rotation about the new X_p'' axis to give the desired platform axes $\hat{r}_{R}$.

The alignment error angles are defined by matric (Q-34):

$$\tan\theta_{ev} = \frac{-S^{**}_{13v}}{S^{**}_{11v}}$$

$$\tan\psi_{ev} = \frac{S^{**}_{12}}{S^{**}_{11v}\cos\theta_{ev} - S^{**}_{13v}\sin\theta_{ev}} \qquad (Q\text{-}35)$$

$$\tan\phi_{ev} = \frac{-S^{**}_{32v}}{S^{**}_{22v}}$$

1882

Error angles (Q-35) are sent to the IMU. On command, the platform or gimbals are slewed sequentially and the error angles are reduced to some limiting value.

8. References:

1. Trageser, M.B.; Woodbury, R.B.: "Apollo Primary G & N System Lunar Orbit Operations" MIT Instrument Laboratory, R-446 Volume I of II, April 1964 (confidential)
2. Shapiro, M.; Murra, F.: "LMS Math Model Equations of Motion, Subsystem Interfaces and Visual Display Drive Equations,"LED-500-5, 22 April 1965.
3. Shapiro, M.: "LEM Mission Simulator-IMU Subsystem Math Model, " LMO-500-284 (A), July 6, 1965.
4. GAEC: "Mathematical Model for LEM Mission Simulator", LED-440-3, May 1965.

TRUE MOTION EQUATION

Part II LMS Data

Section 2. Primary Guidance and Navigation

4. Intersystem Requirements

See Page 1130